2009

Impact of co-contaminant chelating agents on the speciation, sorption and migration of actinides

May, Colin Charles

The impact of co-contaminant chelating agents on the speciation, sorption and migration of actinides

by

Colin Charles May

A thesis submitted to the University of Plymouth in partial fulfilment for the degree of

Doctor of Philosophy

School of Earth, Ocean and Environmental Sciences

Faculty of Science

September 2009

Signed: C. May.....

Date: 10/12/09.....

Author's Declaration

At no time during the registration for the degree of Doctor of Philosophy has the author been registered for any other University award without prior agreement of the Graduate Committee.

This study was financed with the aid of a studentship from the Natural Environment Research Council (Studentship number; NER/S/A/2005/13371).

Relevant scientific seminars and conferences were regularly attended at which work was often presented; external institutions were visited for consultation purposes and papers were prepared for publication.

The work presented in this thesis is primarily the work of the author except where specified.

Word count of main body of thesis:
23,360 words

Signed:.....C. May.....

Date:.....10/12/09.....

Abstract

The impact of co-contaminant chelating agents on the speciation, sorption and migration of actinides

Colin Charles May

Actinide elements are a major long term hazard in wastes arising from nuclear industries. Anthropogenic chelating agents used in nuclear site clean-up operations (*e.g.* EDTA and NTA) and cellulose degradation products (*e.g.* ISA) are found in mixed wastes, and the impact of these ligands on actinide sorption and migration is relatively poorly understood. Knowledge of actinide speciation is fundamental for elucidating sorption processes affecting the migration of actinides in the terrestrial environment. This project has used Th(IV) and UO_2^{2+} as model actinides in key oxidation states to investigate the impact of EDTA, NTA and ISA on actinide speciation, sorption and migration.

Electrospray ionisation-mass spectrometry analysis provided direct observation of aqueous radionuclide-ligand species. Results showed speciation changes as a function of increased pH, and ligand concentrations. Novel species not currently included in thermodynamic databases were identified, such as $[ThNTA_2]^{2-}$ and $[ThNTAEDTA]^{3-}$. This technique also provided supporting data to elucidate the mechanisms occurring in the aqueous ternary Th-EDTA-Fe system, to assess competition for the ligand from a model environmental metal. Quantitative data established that Fe precipitated when added to solutions of Th-EDTA, and there was a subsequent loss of soluble Th due to sorption to the Fe precipitate. After 7 days the concentration of soluble Fe increased while Th decreased, with ESI-MS showing this to be due to the formation of FeEDTA species at the expense of ThEDTA, suggesting a surface exchange mechanism. The magnitude and rate of change was dependent on the concentration of Fe.

The influence of the ligands on sorption of Th(IV) and UO_2^{2+} to sand was investigated over a range of concentrations and various ligand : radionuclide ratios. EDTA and NTA significantly affected Th sorption. With a high Th concentration (500 μM) sorption to the solid was decreased, while at lower Th concentrations (5 and 50 μM) sorption was increased over the timescale of the experiments (7 d). The key processes were identified, and highlighted the importance of competition from matrix cations interacting with the complexing agents, and the sorption sites created as matrix metals were solubilised. There was no influence of the ligands on UO_2^{2+} sorption, suggesting carbonate species played a greater role in influencing UO_2^{2+} sorption

In column migration experiments, EDTA and NTA both enhanced the migration of Th through sand. No Th was eluted in the absence of either ligand, while equi-molar EDTA resulted in elution of 19 % of the Th injected, and with a 10-fold excess of EDTA or NTA, 35 and 11 % of the Th was eluted respectively. From the elution profiles and model simulations it was shown that Th-EDTA did not migrate as a simple chemical species, and in EDTA mediated transport colloidal Th played an important role. Th-NTA migration was governed by a simple equilibrium speciation mechanism.

Acknowledgements

Firstly a big thank-you to my supervisors for helping me to reach this point; to Miranda and Paul, for constantly hammering the simple messages home, and for keeping me on the straight and narrow of the scientific process; to Nick in Manchester for your help in planning the column experiments and modelling the results.

Thanks also to all the BEACh group academics who've helped greatly over the years, in particular to Maeve for her annual interrogation and constructive criticism, also thanks to guys like Mike, Mark, Andy T for gainful employment shepherding the undergrads, and Geoff for his support in the Corif lab.

Thanks to all the Davy guys for the technical support over the years: Roger, Andy A, Andrew, Andy F, Rob H, Rob C and Ian; to Gordon for actually staying in working condition for long enough to analyse my samples; especially to A.C. for your help with the ESI-MS, and Steph and Estela for help in the lab; thanks to all of the office girls, especially Debbie and Annie for keeping me on top of the paperwork!

Also thanks to all the members of the BEACh group past and present, who made Plymouth such a friendly and welcoming environment to study; the old faces now long gone: Omaka, Angie, Cath, Utra, A.C., Laura; the current incumbents: Marie, Estela – I'm going to miss you, Jinbo, Rachel, Gerald, Steph, Alison, Jane, Neil; good friends in the SEA and PEG groups, and even some biologists – that's you Canty! – the Nowhere group; and all the guys who've visited the BEACh group over the years, adding such a lovely international flavour to the social side of life. To other friends: Antonio, you're a legend sorely missed, Fay and Frank, Ahmed, Yaad, Sophie, Gary, Cecile for your wonderful hospitality – and even your tea!, Pip – I'll carry on painting, Phillipe for

showing the delights of an arctic Newquay harbour and what can be done on a surfboard, McGillie for Mad Dog and great music, Pritesh and the Seymour crew for letting me continue to collect cricket ducks after a 20 year hiatus, and Yaswant – I'm still not sure I believe anything. Thanks to all the guys who've recently given me a bed, or at least somewhere dry to sleep, particularly Rachel, Ahmed and Mole! Si, what can I say? Pleasure to have shared some of the important things in life with you: great surf, Doom Bar, good rum and shaky philosophy. Just stock up on those points for Bermuda!

Thanks to Marie, for everything, for the good times, for being there when things were tough, you're an inspiration.

A big thank-you to my parents, sister and Duncan for all of your support, particularly financial that you could ill afford; and giving me somewhere to live with (almost) never a grumble while I was writing up. And to Ken Grubb, who planted seeds.

Finally, thanks to NERC for funding this studentship (NER/S/A/2005/13371).

Presentations

Posters

May, C. C., Worsfold, P.J., & Keith-Roach, M. J., 2008. Impact of organic co-contaminant complexation on Th sorption to sand. Goldschmidt 2008, from Sea to Sky, Vancouver, Canada, 13th – 18th July 2008.

May, C. C., Reinoso-Maset, E., Worsfold, P. J., & Keith-Roach, M. J., 2008. Impact of co-contaminant complex speciation on radionuclide sorption to sand. 2nd International Nuclear Chemistry Congress, Cancun, Mexico, 13th – 18th April 2008.

May, C. C., Cartwright, A. J., Worsfold, P. J., & Keith-Roach, M. J., 2007. Electrospray ionisation mass spectrometry as a technique for the direct speciation analysis of actinides. Analytical Research Forum, University of Strathclyde, U.K. 16th – 18th July 2007.

Oral

May, C. C., Cartwright, A. J., Worsfold, P. J., & Keith-Roach, M. J., 2007. Speciation analysis of aqueous Th complexes using electrospray ionisation mass spectrometry. Co-ordinating Group on Environmental Radioactivity in the U.K. Annual Meeting. University of Loughborough, U.K. 17th – 19th April 2007.

May, C. C., Cartwright, A. J., Worsfold, P. J., & Keith-Roach, M. J., 2007. Speciation analysis of aqueous Th complexes using electrospray ionisation mass spectrometry. Nexia Underpinning Sciences Symposia. Sellafield, U.K. 8th – 9th February 2007

May, C. C., Worsfold, P. J., & Keith-Roach, M. J., 2006. Impact of co-contaminants on the mobility of anthropogenic radionuclide contamination. Co-ordinating Group on Environmental Radioactivity in the U.K. Annual Meeting. Sellafield, U.K. 3rd – 6th April 2006

Publications

May, C. C., Worsfold, P. J., & Keith-Roach, M. J., 2008. Analytical techniques for speciation analysis of aqueous long-lived radionuclides in environmental matrices. *Trends in Analytical Chemistry* (*TrAC*), **27** (2), 160 - 168

Cartwright, A. J., May, C. C., Worsfold, P. J., & Keith-Roach, M. J., 2007. Characterisation of thorium-ethylenediaminetetraacetic acid and thorium- nitrilotriacetic acid species by electrospray ionisation mass spectrometry. *Analytica Chimica Acta*, **590**, 125-131

Contents

List of Figures **Page**

List of Tables **Page**

Chapter 1

Introduction

1.1 General background

The development and use of nuclear reactors for military purposes and power generation in the U.K. over the past 60 years has left a legacy of nuclear wastes that require safe long term storage and disposal. The Nuclear Decommissioning Authority (NDA) is responsible for decommissioning civil nuclear sites, and licences companies to operate and decommission civil nuclear sites. There are 20 sites under its remit, and with the current generation nuclear reactors approaching the end of their working lifetimes, the majority are scheduled for de-commissioning by the year 2035 (www.nda.gov.uk). However, in the current economic, political and environmental climate, the security of energy supply from traditional fossil fuels is in question and there is a drive towards technologies with lower CO_2 emissions. The U.K. Government recently published a white paper to address the viability of new build nuclear power stations to address these concerns, and concluded "that it would be in the public interest to give energy companies the option" to invest in nuclear power in this context (DBERR, 2008). Therefore, with the likelihood of a new generation of nuclear fuelled power stations, the safe management and disposal of nuclear wastes is a pressing issue that must be addressed, with full consideration of the potential environmental impact.

1.2 Nuclear waste management

Wastes are classified as high level wastes (HLW), intermediate level wastes (ILW) and low level wastes (LLW) depending on the specific activity, and their propensity to generate heat through radioactive decay. HLW and ILW typically arise from nuclear power generation, while LLW can also be generated from universities, hospitals and research facilities. In the U.K. HLW and ILW wastes are often stored on the site of generation (*e.g.* Sellafield), which prevents the need for unnecessary transport of dangerous material and allows the dissipation of radioactivity over time through decay

of short-lived radioisotopes. LLW is currently disposed of at the nuclear waste storage facility near the village of Drigg in Cumbria (www.environment-agency.gov.uk). The interim storage of wastes at surface facilities has been fallible in terms of storage integrity in the U.K. and worldwide, resulting in radioactive contaminated land. Historical leaks at the Sellafield site were recently reported by Reeve and Eilbeck (2007). In the U.S.A., groundwater has become contaminated with transuranic elements from unlined disposal trenches at the Oak Ridge National Laboratory site (McCarthy *et al.*, 1998), surface soils have been contaminated with ^{239,240}Pu and ^{241}Am that leaked from storage drums at the Rocky Flats Environmental Technology site (Santschi *et al.*, 2002) and ^{90}Sr from leaking waste storage tanks has contaminated sub-surface soils at Hanford (Pace *et al.*, 2007).

A number of countries (*e.g.* Sweden, France, Lithuania, U.S.A.) have begun to investigate the option of a deep geologic repository for the safe and secure long term disposal of nuclear waste (Figure 1.1), and the U.K. is also likely to develop such a repository (www.nda.gov.uk). This would incorporate a multi-barrier approach, with various disposal concepts being considered where solidified compacted wastes are encased in concrete in steel drums, with a bentonite or cement backfill, with the host geologic formation providing the final barrier to contaminant migration off-site (Baldwin *et al.*, 2008). Over geological timescales there is a risk of groundwater intrusion, and corrosion of waste containing vessels, with subsequent leaching of radioactive material into the environment. Hence there is a pressing need for research in deep repository performance assessment (*e.g.* Smith *et al.*, 2001) and related studies of the environmental impact of radionuclide contamination from surface storage sites.

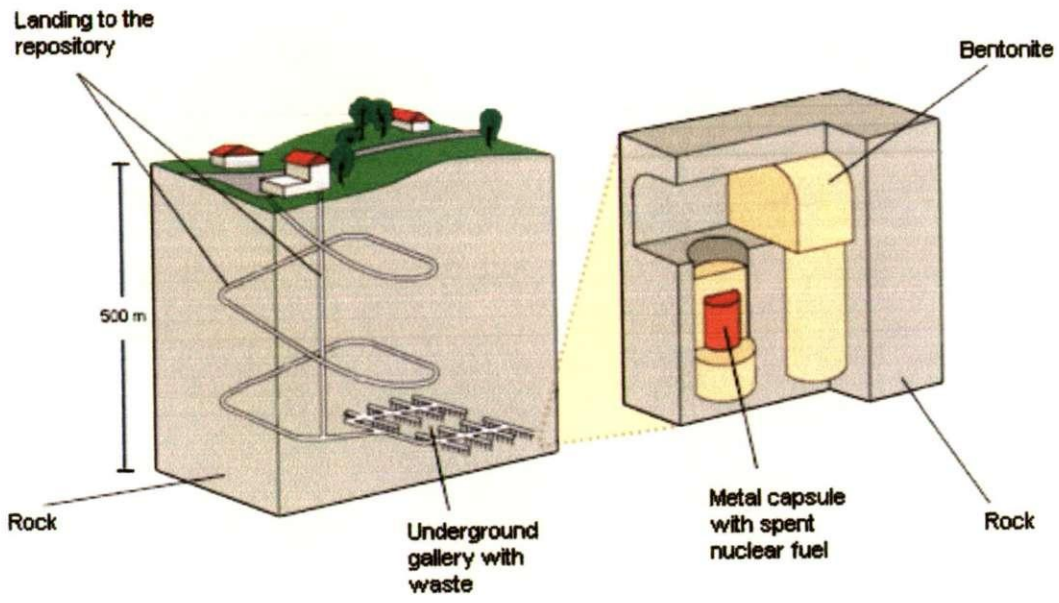

Figure 1.1 Schematic of the proposed Lithuanian deep geological repository (http://www.vae.lt)

Table 1.1 lists long-lived radionuclides present in nuclear industrial waste (adapted from Milnes, 1985), and shows that actinides are of particular importance in disposed wastes due to their high abundance in irradiated nuclear fuel and long half lives. They therefore comprise a long term contribution to the hazardous inventory of any waste repository (Denecke, 2006). The study of U(VI) and Th(IV) is therefore important as representative long-lived actinides in two key oxidation states.

Anthropogenic chelating agents have been extensively used in the clean-up of nuclear facilities due to their ability to complex radionuclides and are therefore present in mixed wastes (Toste *et al.*, 1988). For example, high concentrations of aminopolycarboxylate organic complexing agents; 31.4 mM ethylenediaminetetraacetic acid (EDTA) and 7.3 mM nitrilotriacetic acid (NTA) (Toste *et al.*, 1995) were measured in mixed wastes from the Hanford site (U.S.A.). Cellulose is also present in large amounts in low and

intermediate level wastes from materials such as clothing and tissues and the cellulose degradation product iso-saccharinic acid (ISA) is therefore an important ligand in low level wastes (Glaus *et al.*, 1999; Askarieh *et al.*, 2000).

Table 1.1 Long-lived radionuclides in spent nuclear fuel[adapted from Milnes, 1985]

Radioisotope	$t^{1/2}$ (y)	% weight in spent fuel
^{93}Zr	1.5×10^{6}	-
^{99}Tc	2.1×10^{5}	-
^{107}Pd	6.5×10^{6}	-
^{129}I	1.6×10^{7}	-
^{226}Ra	1.6×10^{3}	-
^{229}Th	7.3×10^{3}	-
^{230}Th	7.5×10^{4}	-
^{234}U	2.5×10^{5}	-
^{235}U	7.1×10^{8}	0.76
^{236}U	2.4×10^{7}	0.46
^{238}U	4.5×10^{9}	94.2
^{237}Np	2.1×10^{6}	0.05
^{239}Pu	2.4×10^{4}	0.53
^{240}Pu	6.6×10^{3}	0.22
^{242}Pu	3.8×10^{5}	0.04
^{243}Am	7.7×10^{3}	0.02
^{245}Cm	9.3×10^{3}	-

1.3 Uranium and thorium chemistry

Uranium and thorium are both naturally occurring radionuclides that are principally found in the mineral phases pitchblende and monazite respectively. Uranium is predominantly present in two oxidation states: the reduced form U(IV) which is highly insoluble under typical environmental conditions, and the oxidised form U(VI), which exists as the uranyl ion (UO_2^{2+}). Tri- and penta- valent oxidation states of uranium are also known, however U(III) readily oxidises to U(IV); and U(V) disproportionates to U(IV) and U(VI) species in aqueous solution (Cotton, 2006; Katz and Seaborg, 1957).

Thorium is only stable in the tetra-valent oxidation state. It has a long half-life (^{232}Th $t^1/_2 = 1.41 \times 10^{10}$ y, Cotton, 2006) and hence a low specific activity, properties that

make it a useful chemical analogue for more radiotoxic elements such as Pu(IV). Th(IV) is known to undergo extensive hydrolysis in aqueous solution, with a number of proposed hydrolysed species that limit Th solubility through the formation of polymerised and amorphous solid phases according to the pH (*e.g.* Ekberg *et al.*, 2000; Milic and Sumaji, 1982).

Tetravalent actinides that have a tendency to hydrolyse, such as Pu(IV) and Th(IV), can form colloids when concentrations are greater than the solubility limit (Walther *et al.*, 2009; Yun *et al.*, 2006). Such colloids are typically 1 - 100 nm in size, and are described as intrinsic (or real) colloids, formed from aggregations of hydrolysed species (*e.g.* Bitea *et al.*, 2003). Bitea *et al.* (2003) reported that intrinsic Th colloids were stable in solution over experimental timescales (up to 400 d). Since colloids are potentially mobile in groundwater (McCarthy and Zachara, 1989), they are likely to be important when considering radionuclide mobility.

Actinide solution chemistry has been widely discussed elsewhere (*e.g.* Cotton, 2006; Katz and Seaborg, 1957; and references therein). Both Th(IV) and U(VI) exhibit high coordination numbers in their sphere of hydration (10-12 and 6 respectively (*e.g.* Walther *et al.*, 2003; Cotton, 2006), and readily form complexes with inorganic ligands such as F^-, CO_3^{2-}, NO_3^- and Cl^- (*e.g.* Vallet *et al.*, 2006; Szabo *et al.*, 2006; Morris, 2002; Cocalia *et al.*, 2006; Altmaier *et al.*, 2005), and organic ligands such as fulvic and humic acids, bacteriogenic siderophores and anthropogenic chelating agents (*e.g.* Bryan *et al.*, 2000; Keith-Roach *et al.*, 2005; Cartwright *et al.*, 2007).

1.4 Influence of environmental conditions on radionuclide speciation and mobility

Understanding speciation is fundamental to predicting radionuclide behaviour and fate in the environment and factors affecting speciation (pH, Eh and ligand availability) ultimately control radionuclide solubility and mobility. Speciation data are therefore required to predict the migration of radionuclides from long-term nuclear waste storage facilities and their transport through the environment. The predominant pathway for radionuclide migration is by solute transport in groundwater (Dozol *et al.*, 1993) and migration through the environment can be influenced by the presence of natural (Bryan *et al.*, 2000; Warwick *et al.*, 2000) and co-contaminant organic complexing agents. Therefore understanding the geochemical processes that affect radionuclide solubility and hence transport are vital for choosing the safest possible site (Evans and Heath, 2004). Environmental chemical factors that influence radionuclide speciation are illustrated in Figure 1.2 using uranium as an example.

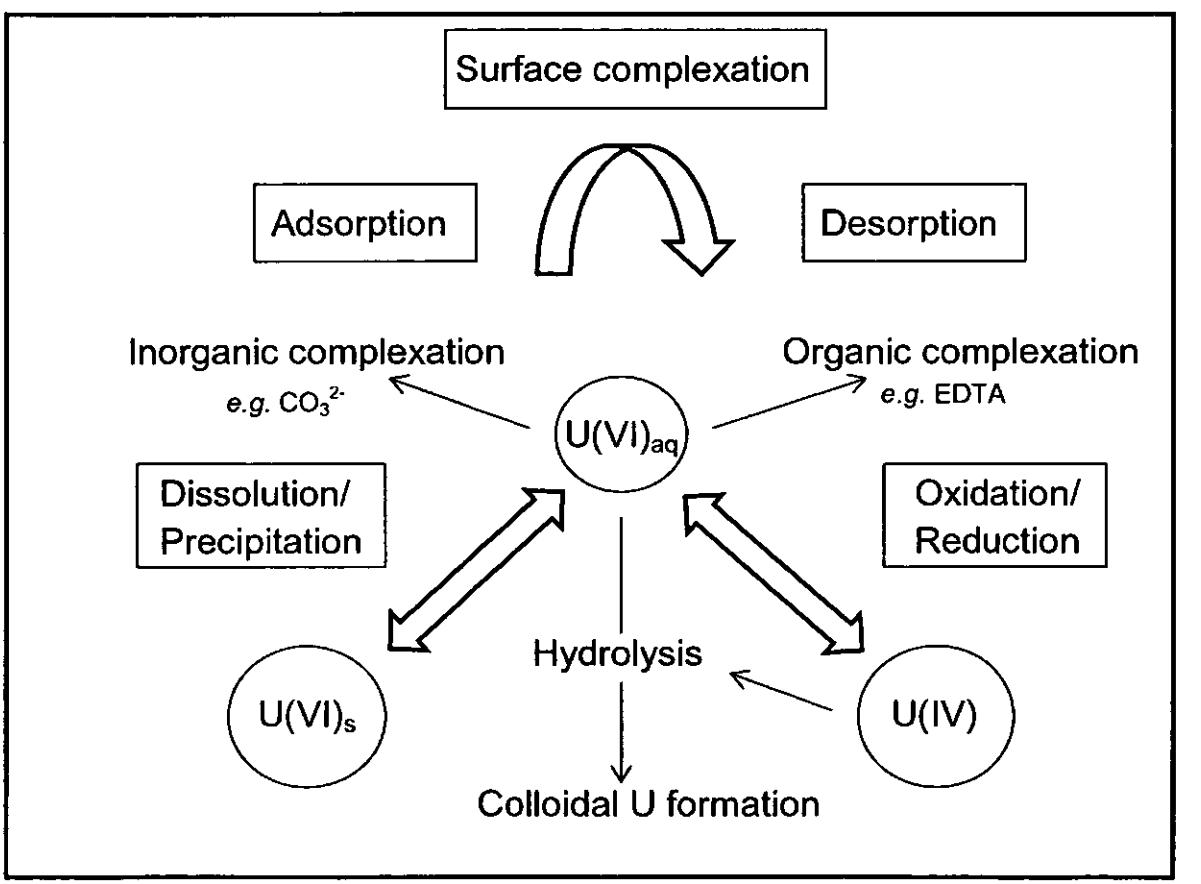

Figure 1.2. Chemical factors affecting radionuclide speciation in the environment

Over geological timescales changes in temperature, pH and Eh will be important factors influencing radionuclide speciation when considering radionuclide release from a geological repository (Evans and Heath, 2004). It is widely accepted that organic substances affect the transport of radionuclides at contaminated sites (*e.g.* Means *et al.*, 1978; Cleveland and Rees, 1981). The roles of the anthropogenic chelates EDTA and NTA are of particular importance due to: their widespread use as decontamination agents at nuclear facilities and hence high concentrations in nuclear wastes (Toste *et al.*, 1995); their ability to chelate tri- and tetra-valent actinides and lanthanides (*e.g.* Hu in press), and; particularly in the case of EDTA, persistence in the environment (Means *et al.*, 1980; Sillanpää and Sihvonen, 1997). EDTA has also been suggested as a significant contributor to radionuclide migration at the Oak Ridge National Laboratory disposal site (Means *et al.*, 1978), and Pu mobilisation in Maxey Flat leachates (Cleveland and Rees, 1981). A full understanding of the solution chemistry of these components, and how they interact with common environmental constituents such as Fe, is required before environmental behaviour can be modelled with confidence (*e.g.* Kent *et al.*, 2002).

Where available, thermodynamic stability constants can be used to predict speciation. In multi-component systems, such as natural waters, the stability constants of all the known complexes and the concentrations of each component are used to predict the resultant species (Dimmock *et al.*, 1995). Therefore, the inclusion of all relevant species is crucial for obtaining accurate predictions, and experimental speciation data are required to underpin and independently verify these models. Carey *et al.* (1964) demonstrated the importance of $[ThNTA_2]^{2-}$ and the mixed ligand 1:1:1 Th–EDTA–NTA complex in 1964, but this information has not been integrated into stability constant measurements or databases. Similarly, Xia *et al.* (2003) demonstrated that Th

interactions with EDTA are poorly predicted by current databases, whilst De Stefano *et al.* (2006) highlighted the variation in stability constant data for UO_2^{2+} species with EDTA and NTA, emphasising the need for improved speciation analysis.

1.5 Radionuclide sorption to solid phase matrices

Sorption of contaminants to environmental solid surfaces is a fundamental factor in determining radionuclide mobility and radionuclide sorption has been shown to be sensitive to environmental chemical factors, particularly pH, Eh and the presence of ligands. For example, sorption of UO_2^{2+} to alumino silicate surfaces typically follows the trend of increased sorption from low pH to neutral pH, and a decrease in sorption at pH > 8 through solubilisation of the radionuclide due to the formation of aqueous carbonate species (*e.g.* Arai *et al.*, 2006). These authors proposed a change in surface binding mechanism with increasing pH to explain this behaviour, from an inner sphere uranyl complex bound to alumino groups to an outer sphere ternary UO_2-carbonate complex.

A change in the dominant binding mechanism from cation exchange at low pH (< 4), inner sphere surface complexation at pH > 5 and incorporation of the radionuclides in surface precipitates at pH > 12 pH was proposed by Rabung *et al.* (2005) to explain the pH dependent sorption of Cm and Eu to clays. Th sorption has also been shown to be sensitive to pH; Osthols (1995) reported increased sorption of Th to colloidal silica with increased pH over the range 1 – 3, and in modelling the data of Rydberg and Rydberg (1952) showed that the formation of aqueous Th hydrolysis species played an important role in decreasing sorption when pH was increased from pH 6 to 10.

In deep groundwaters where Eh conditions are likely to be reducing (Mibus, 2007), redox sensitive radionuclides will be present in reduced oxidation states, such as U(IV) and Tc(IV), which are generally less soluble than their oxidised forms, and will readily sorb to environmental solid surfaces (*e.g.* Morris *et al.*, 2008; Hu *et al.*, 2008).

Organic ligands will also play an important role in radionuclide sorption. EDTA increased UO_2^{2+} sorption to hydrous silica at pH 2.9 compared with sorption of UO_2^{2+} alone, but the influence of the ligand decreased with increasing pH, and had no effect at the highest pH studied (pH 5.6) (Pathak and Choppin, 2007a). Sorption of Th to colloidal haematite at pH 6 - 8 was reduced by ~ 90 % when humic acid was added prior to addition of Th, compared with systems where humic acid was added after pre-equilibration of Th with the solid (Reiller *et al.*, 2005). This demonstrates that humic acid was more effective in competing with the haematite surface for solution phase Th than for Th bound to the solid.

The influence of natural organic matter on Th sorption has been shown to be dependent on pH, Xu *et al.* (2007) found that humic acid increased Th sorption to Na-rectorite at low pH (< 4), but had little influence at pH > 4 compared with sorption of Th alone. This was explained by the formation of a ternary Th complex with surface bound HA at low pH. A similar trend of Th sorption to silica at low pH (< 4) was observed by Chen and Wang (2007) in the presence of humic and fulvic acids. These authors also reported a decrease in Th sorption in the presence of these organic compounds at pH > 8. The formation of ternary surface species with a bridging ligand is an important mechanism for Th sorption at low pH. Guo *et al.* (2005) proposed the formation of a ternary Th-phosphate surface species as the controlling factor in their study of Th sorption to

alumina, with increased sorption of Th in the presence of this inorganic ligand from pH 1 - 4.

There have been few studies investigating the influence of anthropogenic chelating agents on Th sorption. Vercammen *et al.* (1999, 2001) investigated the influence of ISA on sorption of 10^{-4} M Th at fixed high pH (>10) to a cation exchange resin and reported decreased sorption with increased concentrations (μM – mM) of the ligand. To the author's knowledge there have been no studies published reporting the influence of EDTA or NTA on the sorption of Th to environmental solid matrices. However, the influence of these ligands on sorption of trace metals has been widely investigated. Elliott and Denneny (1982) reported a decrease in Cd sorption to soil in the presence of EDTA and NTA relative to the metal alone, which was particularly noticeable at pH > 6. Sorption of Co(II)EDTA^{2-} to goethite was dependent on pH (Zachara *et al.*, 1995). At pH > 5 the analytes sorbed to the surface as the metal-ligand complex, however at low pH the sorption behaviour of Co and EDTA was independent. Co sorption increased with increased pH, and EDTA sorption increased with decreased pH with sharp sorption edges for both species between pH 5 - 8. The authors suggested that at pH < 5, a concomitant increase in aqueous Fe(III) concentrations implied metal exchange at the goethite surface, with dissolution of mineral Fe.

Nowack and Sigg (1996) also observed exchange of EDTA complexed metals with solid phase Fe through the formation of ternary surface species. These authors also showed that the sorption of lanthanide to goethite in the presence of EDTA proceeds via the mechanism of ternary surface complexation followed by exchange with matrix metals (Nowack and Sigg, 1997). Exchange of radionuclides with matrix cations may therefore play a key role in radionuclide sorption, and is important when considering the

environmental implications of organic co-contaminants on radionuclide contamination in mineral matrices rich in Fe and Mn (Rai *et al.*, 2008; Brooks and Carroll, 2003).

1.6 Radionuclide migration through the terrestrial environment

The role of organic chelates in enhancing radionuclide transport has been the focus of a number of studies using column experiments to simulate groundwater flow through terrestrial matrices. Mayes *et al.* (2000) determined that enhanced transport of ^{60}Co through a saprolite column was due to surface mediated oxidation of $Co(II)EDTA^{2-}$ to the highly stable $Co(III)EDTA^{-}$ complex (log k = 43.9, Brooks *et* al., 1996). Uranyl ion migration through sandstone cores was significantly enhanced when the radionuclide was co-injected with EDTA (Read *et al.*, 1998). However, when uranyl ion was injected prior to the addition of EDTA, the metal showed a strong affinity for the solid surface, and desorption of surface bound U by EDTA was kinetically slow. In contrast to this study, pre-equilibration of Sr and EDTA resulted in lower Sr mobility in a 95 % sand matrix with interbedded silt and clay compared with Sr alone, because the ligand mobilised trace metals which created additional surface binding sites (Pace *et al.*, 2007).

Radionuclide migration through the terrestrial environment is also influenced by colloids (*e.g.* Champ *et al.*, 1984; McCarthy and Zachara, 1989). Novikov *et al.* (2006) reported the iron-oxide colloid facilitated transport of Pu(IV) to the surrounding environment from a Russian nuclear facility (Mayak Production Association). Delos *et al.* (2008) found that reversible sorption of Am and Pu to montmorillonite colloids enhanced migration of these radionuclides through porous ceramic columns.

1.7 Analytical techniques for radionuclide determination

Knowledge of the aqueous chemical speciation of long-lived radionuclides in an environmental sample enables better prediction of their behaviour and fate in the sub-surface environment, with information at the molecular level being a fundamental driver to increase the reliability of geochemical models (Geckeis, 2006). The analytical challenge is to adapt current direct speciation techniques to provide sensitive analyses capable of acquiring quantitative values for radionuclide species present in a given environmental matrix, thus allowing experimental work to underpin models with relevant thermodynamic data (Cartwright *et al.*, 2007).

The main techniques applied to the determination of long-lived radionuclide species are shown in Table 1.2. This highlights the low number of analyses involving environmental matrices (*e.g.* Moulin *et al.*, 1999). Direct speciation analysis has been provided by UV-visible spectrophotometry, nuclear magnetic resonance spectroscopy (NMR), Raman spectroscopy, time resolved laser induced fluorescence (TRLIF) spectroscopy, electrospray ionisation-mass spectrometry (ESI-MS), and X-ray absorbance spectroscopy (XAS) (encompassing extended X-ray absorption fine structure spectroscopy (EXAFS)) (May *et al.*, 2008).

Figure 1.3 provides a summary of the working ranges of these techniques in moles per litre or per kilogram, compared with typical concentrations of uranium in different environments including 'natural' background, contaminated sites and nuclear process liquids.

Table 1.2 Analytical techniques for aqueous speciation analysis of long-lived radionuclides

Technique	Analyte	Concentration	Comment	Reference
CE-ICP-MS	Pu	10^{-7} M	Pu redox states determined	Ambard *et al.*, 2005
NMR	UO_2^{2+}	10^{-1} M	Complexes with iminodiacetate and oxydiacetate	Jiang *et al.*,2003
Raman	U(VI)	10^{-3}– 10^{-5} M	OH, NO_3, ClO_4 and acetate species	Quiles and Burneau, 1998
SERS	Tc	10^{-4} – 10^{-7} M	Humic/EDTA species, kinetic oxidation of Tc(IV)	Gu and Ruan, 2007
Uv-vis	Th	10^{-5} M	Organic complexation, competition	Rao *et al.*, 2000
EXAFS	U(VI)	10^{-2} M	Aquo, Cl complexation	Hennig *et* al., 2005
TRLIF	Eu	10^{-6} M	CO_3, humic species in simulated natural waters	Moulin *et* al., 1999
TRLIF	U(VI)	10^{-4}-10^{-7} M	Analysis of nuclear reprocessing liquids	Moulin *et* al., 1996
ESI-MS	U(VI)	10^{-4} M	HEDP complexation by pH and ligand ratio	Jacopin *et al.*, 2003
ESI-MS	Th	10-5 M	EDTA, NTA complexes, pH effect	Cartwright *et al.*, 2007

CE-ICP-MS = capillary electrophoresis – inductively coupled plasma - mass spectrometry, NMR = nuclear magnetic resonance spectroscopy, SERS = surface enhanced raman spectroscopy, Uv-vis = ultra violet – visible spectroscopy, EXAFS = extended X-ray absorption fine structure spectroscopy, TRLIF = time resolved laser induced fluorescence spectroscopy, ESI-MS = electrospray ionisation - mass spectroscopy

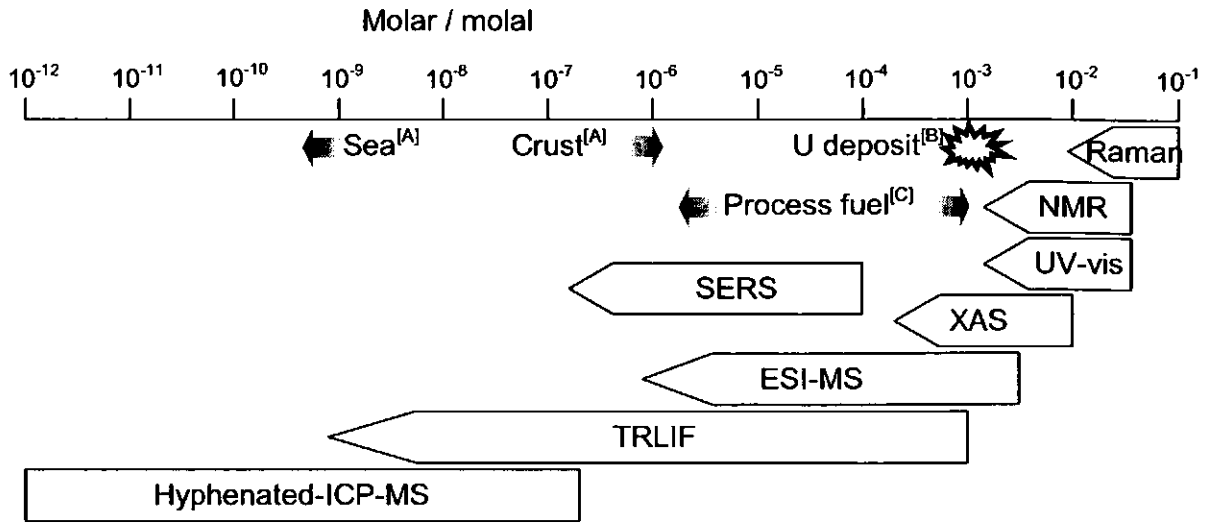

Figure 1.3 Working concentration ranges of analytical techniques used for the direct determination of radionuclide species. Concentrations of U typically found in various matrices are shown for comparison from; [A] Gruning *et al.*, 2004, [B] Payne and Airey 2006, [C] Moulin *et al.*, 1996)

1.8 Aqueous speciation analysis using electrospray ionisation-mass spectrometry

ESI-MS was chosen as a direct technique to determine radionuclide-ligand speciation in this project, as it has advantages over other techniques for this type of analysis. The major advantage of this technique over other mass spectrometric methods lies in its soft ionisation process, which enables the chemical structure of a solution phase molecule to be largely retained during ionisation to the gas phase affording detailed information on aqueous chemical complexation (Keith-Roach *et al.*, 2005). Many species can be detected simultaneously, which is advantageous in terms of speed and simplicity of analysis, and ESI-MS provides direct comparison of signal intensities from different species. This also allows speciation analysis without the need for prior separation of species, avoiding potential artefacts induced through interactions with the stationary phase, and the technique has nanomolar to micromolar detection limits.

The electrospray interface is illustrated in Figure 1.4. A full discussion of this analytical method is given in Cole (1997). In brief, the sample solution is carried in a mobile phase solvent or directly infused to the charged capillary where a cone shaped droplet forms, and solution ions of like charge to the polarity applied to the capillary tip accumulate at the droplet surface. When electrostatic repulsion becomes greater than the droplet surface tension, the droplet explodes and collision with the drying sheath gas (N_2) removes solvent molecules, and ionic solution species are drawn into the mass spectrometer for gas phase measurement. Altering the polarity of the capillary charge enables the identification of cationic species using the positive ion mode of analysis, or anionic species using the negative ion mode. The mass spectrum obtained using ESI-MS provides a signal of counts per second for a defined range of mass to charge ratios from which solution species can be deduced.

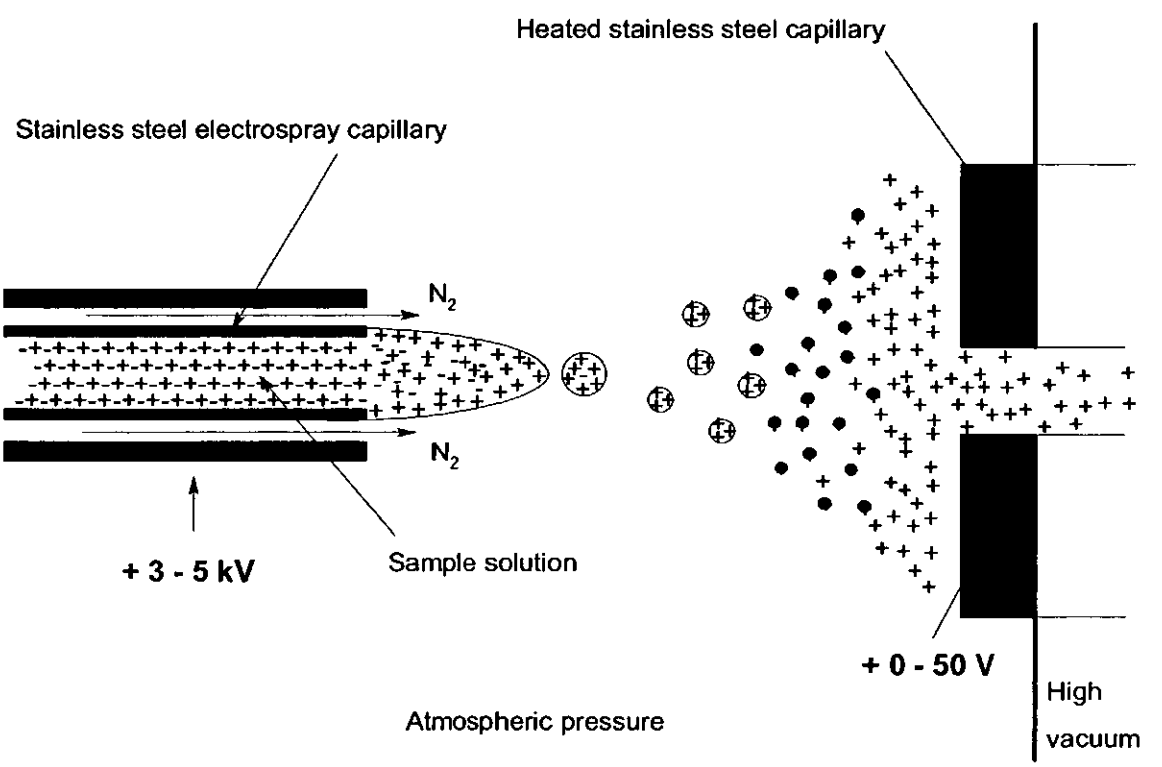

Figure 1.4 Schematic diagram of an ESI-MS capillary interface

The analytical response for a given analyte is sensitive to the instrument tuning parameters such as the voltage difference between the capillary emitter tip and capillary inlet (*e.g.* Agnes and Horlick, 1995) therefore the signal response should be optimised for an analyte prior to analysis of experimental solutions. Complications arising from the solution matrix have also been noted, matrix ions are able to adduct to analyte species of opposing charge (*e.g.* Pasilis *et al.*, 2006), and increased ionic strength can lead to suppression of the electrospray signal (Olesik *et al.*, 1997). However with judicious experimental design these effects can be addressed (Cartwright *et al.*, 2007).

DiMarco and Bombi (2006) have reviewed the application of ESI-MS to environmental analysis and highlighted the issues of polymerisation and electrochemical changes (*e.g.* pH and redox state; where oxidation of water can decrease pH in the positive ion mode, and reduction of ionic species can result in increased pH in the negative ion mode). Pasilis *et al.* (2006) also discussed artefacts in ESI-MS, including gas phase adduction in the positive ion mode, and charge reduction of the ligated metal centre in the negative ion mode of analysis suggesting the reduction of U(VI) to U(V) and U(IV) in the gas phase. Therefore care must be taken when interpreting ESI-MS data, such as using both positive and negative ion modes to reduce potential artefacts (Cartwright *et al.*, 2007).

ESI-MS has been applied to the determination of radionuclides, and actinide speciation results obtained have been confirmed by the use of complementary techniques such as TRLIF spectroscopy (*e.g.* Moulin *et al.*, 2000), or by comparison with previous experimental work or speciation modelling (*e.g.* Cartwright *et al.*, 2007), showing the suitability of the technique for determination of radionuclide speciation. Speciation studies of radionuclides using ESI-MS have largely focused on long-lived lanthanides (Stewart and Horlick, 1994), actinides (Keith-Roach *et al.*, 2005) or stable isotopes of

radioactive elements (*e.g.* Wang and Agnes, 1999); and have investigated hydrolysis reactions (Moulin *et al.*, 2001), complexation by inorganic ligands (Pasilis *et al.*, 2006), complexation by organic ligands in binary and ternary systems (Cartwright *et al.*, 2007), complex stoichiometry (Pasilis and Pemberton, 2003), speciation changes with increased pH (Cartwright *et al.*, 2007) and kinetics of complexation (Keith-Roach *et al.*, 2005).

Hydrolysis of thorium was observed using ESI-MS over a pH range of 0 to 3, (Moulin *et al.*, 2001). Mass spectra showed the Th^{4+} in solution at pH 0 as a perchlorate adducted thorium complex. With increasing pH from 1 to 3, the signal for this Th^{4+} adduct decreased, and hydrolysed Th species were observed, with increasing signals for $Th(OH)^{3+}$ and $Th(OH)_2^{2+}$. Complexation of UO_2^{2+} with 1-hydroxyethane-1,1-diphosphonic acid (HEDP) was investigated using ESI-MS, and a change in the dominant uranium complex could clearly be observed in the ESI-MS spectra from a UO_2^{2+}-adduct to a (UO_2)-HEDP species as the ligand concentration was increased (Jacopin *et al.*, 2003). Detailed equilibrium and kinetic information on the complexation of Th with two naturally produced iron-ligating siderophores was reported using ESI-MS (Keith-Roach *et al.*, 2005). Equilibrium speciation of Th-ligand species was observed over the pH range 5 and 9, and ESI-MS showed fast metal exchange when Fe^{3+} was added to solutions.

Novel complexes formed by Th with organic ligands (EDTA, NTA) have been observed in 0.05 M ammonium acetate at an environmentally relevant pH (Cartwright *et al.*, 2007, Chapter 2). ESI-MS spectra showed species not predicted by existing thermodynamic databases, including a mixed ligand species ($[ThNTAEDTA]^{3-}$ which had previously been predicted by potentiometry (Carey *et al.*, 1964). Figure 1.5

illustrates an ESI mass spectrum for one such species where [ThEDTAacetate]$^-$ is visible at a mass over charge of 579, with one possible ligand coordination to the metal centre suggested after (Grubisic *et al.*, 2006) inset. Changes in Th speciation as a function of pH over the range 2.5 - 11.0 were also observed, and the presence of aqueous Th species at high pH illustrates the need for better direct speciation methods to enable the effective management and environmental impact assessment of nuclear wastes.

The emerging use of nanoESI-MS for radionuclide analysis (*e.g.* Vercouter *et al.*, 2005), where an electric field is applied to a low volume (20 µL) nanoES emitter capillary to draw a low volume of sample (0.1 μL/min) to the mass spectrometer inlet capillary, has the advantages of reduced sample volume and increased sensitivity which are both important considerations in the analysis of radioactive samples.

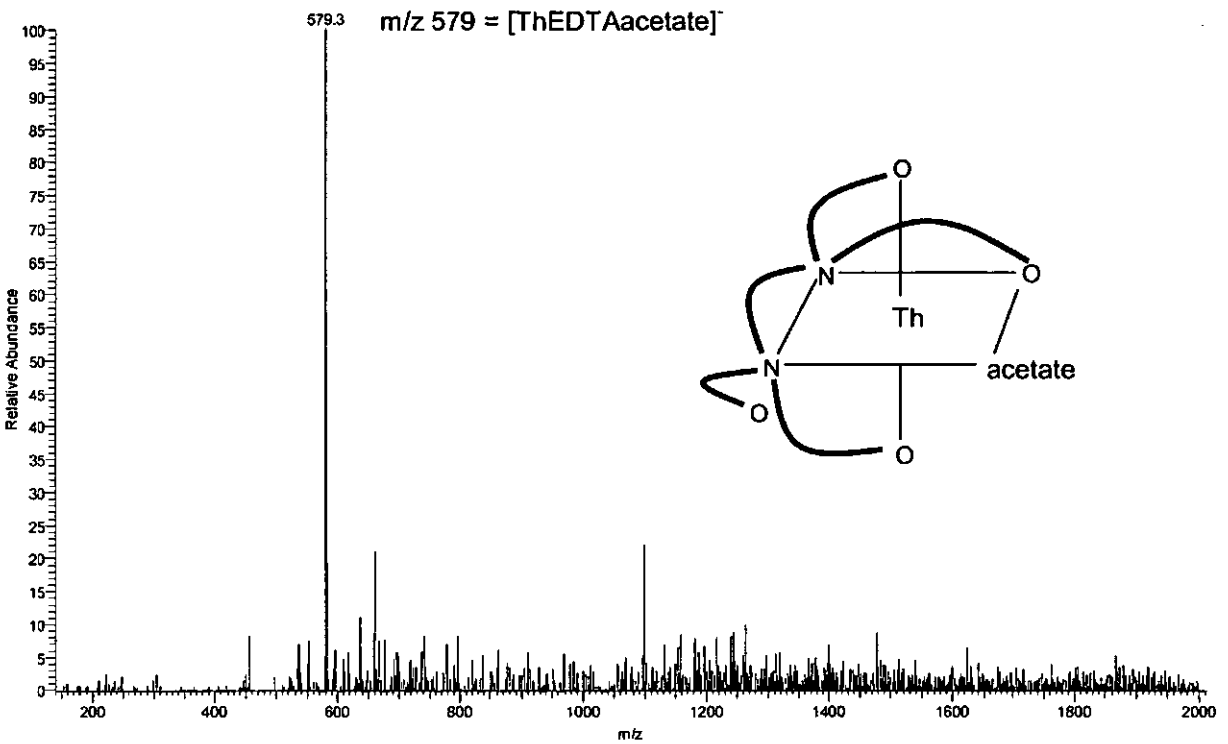

Figure 1.5 ESI mass spectrum showing Th-EDTA-acetate complex (inset shows a possible ligand coordination environment around the metal centre)

1.9 Project aims and objectives

Radionuclide solubility and mobility are ultimately controlled by aqueous radionuclide speciation, thus the aim of this thesis was to define Th and UO_2^{2+} speciation in the presence of co-contaminant chelating agents and to investigate the influence of speciation on processes controlling the mobility of Th and UO_2^{2+}. Three organic chelating agents that are present in waste streams were selected. Ethylenediaminetetraacetic acid (EDTA) and nitrilotriacetic (NTA), are strongly chelating anthropogenic organic ligands used in nuclear site decommissioning and iso-saccharinic acid (ISA) is a cellulose degradation product. Specific objectives were to:

- characterise the aqueous phase speciation of Th and UO_2^{2+} in the presence of EDTA and NTA using electrospray ionisation-mass spectrometry (ESI-MS).

- explore competitive interactions between ThEDTA and Fe using ESI-MS to define the species present, and inductively coupled plasma-mass spectrometry (ICP-MS) and flame atomic absorbance spectroscopy (FAAS) to determine total solution phase concentrations.

- define the processes by which EDTA, NTA and ISA impact on the sorption of Th and UO_2^{2+} to a natural dune sand matrix.

- investigate the effect of complexation by EDTA and NTA on the migration of Th through natural sand and fit the data using the k1-d reactive transport modelling code to elucidate geochemical interactions controlling Th migration.

- evaluate and discuss the experimental results in a wider environmental context relevant to nuclear waste contamination with suggestions for areas of pertinent future research.

1.10 Collaborator contributions

Part of the experimental work undertaken for Chapter 2 relating to optimisation of the ESI-MS instrument tuning for direct determination of actinide-ligand species, and the investigation of Th-EDTA and Th-NTA speciation as a function of pH was carried out in collaboration with Dr. Andy Cartwright during his related post-doctoral position within the BEACh group at the University of Plymouth. Results from these experiments were published (Cartwright *et al.*, 2007), and this author contributed to that publication with an extensive proportion of the original experimental work, chemical speciation modelling, and co-authorship of the paper.

Chapter 2

Speciation of Th and UO_2^{2+} co-contaminant complexes determined by electrospray ionisation-mass spectrometry

2.1 Introduction

The role of common organic compounds that have been co-disposed with radioactive wastes such as ethylenediaminetetraacetic acid (EDTA) and nitrilotriacetic acid (NTA) (Bolton *et al.*, 1996) is relatively poorly understood. Novel analytical techniques that provide direct information on speciation are therefore required to determine radionuclide complexes in challenging sample matrices containing a variety of metals, complexing agents and matrix ions.

Time-resolved laser-induced fluorescence (TRLIF) (Moulin *et al.*, 1996; Moulin *et al.*, 1998; Moulin *et al.*, 2000; Moulin, 2003) and extended X-ray absorption fine structure (EXAFS) (Sylwester *et al.*, 2001; Monsallier *et al.*, 2003) have been used to study solution phase speciation for nuclear fuel cycle and environmental purposes. However, these techniques have limitations, such as the range of elements that can be studied by TRLIF and the high detection limits of EXAFS (Moulin *et al.*, 2000). This has led to other analytical techniques being investigated, one of which is electrospray ionisation-mass spectrometry. This technique was initially applied to the determination of biomolecules, but its potential to be used for environmental process studies, including inorganic complex formation and mobility (Keith-Roach *et al.*, 2005) has been demonstrated.

The aims of this chapter are to demonstrate that ESI-MS is capable of sensitive radionuclide speciation analysis in the presence of EDTA and NTA, and that it can characterise changes in speciation resulting from changes in the chemical conditions, e.g. pH. Therefore, using Th(IV) and U(VI) as model actinides in key oxidation states, ESI-MS has been applied to (1) obtain optimum generic ESI-MS operating conditions for radionuclide-ligand speciation analysis using calcium-isosaccharinic acid to define

instrument tuning; (2) identify and characterise the Th and UO_2^{2+} species that form in the presence of EDTA and NTA over a pH range of 2–11; (3) identify and characterise Th and UO_2^{2+} speciation in the presence of increased ligand concentrations; (4) identify and characterise the species formed when Th or UO_2^{2+} is equilibrated with both ligands, to investigate competitive interactions; (5) compare the complexes found experimentally with published data derived from other speciation techniques and those predicted by existing speciation models.

2.2 Experimental

2.2.1. Chemicals and reagents

Methanol (Riedel-de-Haën, LC–MS grade), water (G-chromasolv grade), ammonium acetate (Sigma Ultra grade), NTA (trisodium salt) and Uranium (VI) were obtained from Sigma–Aldrich (Poole, Dorset, UK). EDTA (disodium salt) was obtained from Fisher Scientific UK Ltd. (Loughborough, Leicestershire, UK). Thorium (IV) nitrate was obtained from VWR International (Poole, Dorset, UK). The structures of EDTA and NTA are shown in Figure 2.1.

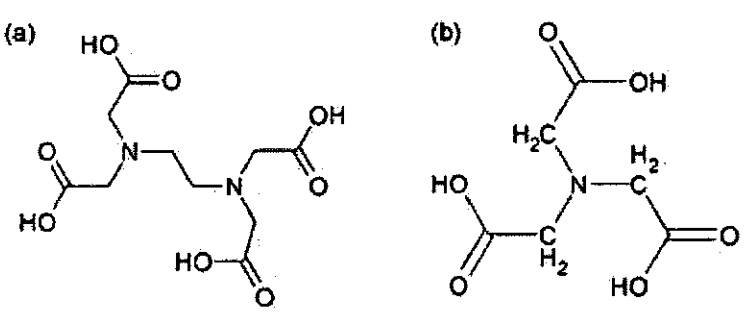

Figure 2.1 The structures of (a) EDTA and (b) NTA

2.2.2 Sample preparation

Fresh stock solutions of 4 mM Th, UO_2^{2+}, EDTA and NTA or 20 mM EDTA and NTA were prepared in LC–MS grade water (G-chromasolv) or 50 mM aqueous ammonium acetate, and then mixed in the relevant diluents and left overnight to equilibrate. Initially, the instrument was optimised for EDTA and NTA individually and also for mixtures of Th and EDTA, and Th and NTA; and of UO_2^{2+} and EDTA, and UO_2^{2+} and NTA; in order to establish the best operating conditions for the analyses. Calcium isosaccharinic acid ($CaISA_2$) was prepared (Whistler and BeMiller, 1963) and used to investigate the extent to which changing the operating conditions affected the peak distribution, because three large peaks were present in the mass spectrum. Optimisations were carried out using direct infusion as this provides a constant input of sample. A generic set of conditions based on a compromise between the optimisations was then adopted for all subsequent analyses (see Section 2.2.3).

Once the instrument had been optimised, analyses were carried out using flow injection of samples (5 μL) into a carrier stream of water (150 μL min^{-1}). Calibration graphs were constructed by summing the species formed between Th or UO_2^{2+} and EDTA or NTA in ammonium acetate buffer. Speciation experiments were then conducted to investigate speciation over a pH range of 2.5–10.8 (prepared in water) and speciation of Th or U in the presence of both EDTA and NTA at circumneutral pH. Acetic acid and ammonia were used to adjust the pH over the range investigated and the exact pH was measured using a freshly calibrated pH 213 microprocessor pH meter (Hanna Instruments, Leighton Buzzard, UK) equipped with a micro-combination pH electrode (MI-410P, Microelectrodes Inc., Bedford, NH, USA).

2.2.3 Electrospray ionisation-mass spectrometry

Water was delivered using a P580A binary pump (Dionex-Softron GmbH, Germering, Germany) at 150 μL min^{-1}. Sample injections (5 μL) were made manually with a metal-free Rheodyne injector (model number 9125, CA, USA). Mass spectrometric analysis was performed using an ion trap mass spectrometer fitted with an electrospray interface (ThermoQuest Finnigan Mat LCQ, San Jose, CA). Data were acquired and processed with Xcalibur 1.0 software. The following instrument parameters were used: source voltage, −4.50 kV; capillary voltage, −10 V; tube lens offset, −50 V; capillary temperature, 220 °C; nitrogen sheath gas flow rate, 60 (arbitrary units), and; nitrogen auxiliary gas flow rate, 20 (arbitrary units). Mass spectra were recorded in the negative ion mode within *m/z* 150–2000 with complementary analyses over the same *m/z* range in the positive ion mode. All analyses were performed in triplicate. Flow injection was used throughout as an effective, clean method of introducing the sample to the instrument, and the total ion count peaks were averaged over a standard time interval of 0.5 min.

2.2.4 Speciation modelling software

Geochemical modelling of aqueous complexation of Th and UO_2^{2+} with organic and inorganic ligands was carried out using three speciation models in the public domain. The diversity of data in the databases associated with the models meant that it was useful to compare all three with the experimental data. PHREEQcI v.2.12.5 (Parkurst and Appelo, 1999) is widely used by radiochemists, MEDUSA (Puigdomenech, 2006) has the most user-friendly interface and Visual MINTEQ v 2.4 (2006) has one of the most complete databases for organic ligand-radionuclide complexes (Serne *et al.*, 2002). Visual MINTEQ used the associated MINTEQ v4.0 database, which is derived from NIST databases (46.6 and 46.7). For PHREEQcI v.2.12.5, the MINTEQ v4.0 database

was selected as the default with thermodynamic data added for Th and EDTA and U(VI) and EDTA or NTA from the critical review by Smith and Martell (1989), and for $[ThNTA]^+$ from Anderegg (1977). MEDUSA was used with its counterpart database, HYDRA.

2.3 Results and discussion

2.3.1 Optimisation and effect of the operating parameters on the species distributions

Initially, all samples were analysed in both positive and negative ion modes to assess which mode of operation yielded the best signal-to-noise ratio. The positive ion mode generates positively-charged ions and vice versa, thus different species will electrospray more efficiently in either positive or negative mode. For the species analysed within this study, negative ionisation generally gave the most sensitive response and information-rich spectra. Some of the spectral peaks were due to adducts formed within the ionisation source as a result of the ionisation mode. The adducts originated from either the salt of the compound, for example nitrate from thorium nitrate, or from the sample matrix, for example acetate from ammonium acetate or protons from water. Therefore, the positive ion mode was used as a tool to verify whether the species associated with the Th^{4+} or UO_2^{2+} centre were ligated or adducted. An additional benefit of identifying a species in both modes is that potential artefact species that might be produced through reactions during the electrospray procedure are less likely to form under both electrospray conditions. Both negative ion mode (Dodi and Monnier, 2004; Moulin *et al.*, 2003) and positive ion mode (Baron and Hering, 1998; Moulin *et al.*, 2003) have previously been used for the analysis of metal EDTA complexes.

The electrospraying and subsequent detection of metal complexes is dependent on the electrospray ionisation operating parameters. If a metal and a complexing agent form a mixture of species, there is a possibility that the species distribution will also be sensitive to the operating parameters discussed (see section 2.3.3). This was investigated using direct infusion of $Ca(ISA)_2$ because three main species were observed in the negative ion mode (*m/z* 179 from $[ISA]^-$, *m/z* 577 from $[Ca(ISA)_3]^-$ and *m/z* 975 from $[Ca_2(ISA)_5]^-$). Each species was selected in turn to be the focus of the automatic instrument optimisation process and the observed species distribution was recorded (Table 2.1). Similar species distributions were obtained when the instrument was optimised on *m/z* 179 and 975; however optimisation on *m/z* 577 resulted in a significantly different distribution, most notably giving a lower relative abundance of the free ISA^- ion at *m/z* 179. This shows that instrument settings affect the species distribution as well as the total ion count, thus the technique does not give absolute ratios of species. However, the data provide an approximate species distribution with consistent identification of the two dominant species (*m/z* 577 and 975), regardless of the operating parameters used.

Table 2.1 The effect of mass tuning on the signal obtained for the three main masses for ISA observed in the negative ion mode

Mass tuned for	Normalised abundance			Max signal (cps)
	m/z 179	m/z 577	m/z 975	
179 m/z	77	92	100	11600
577 m/z	43	100	84	

2.3.2 Calibration and linearity of response for Th–EDTA, UO_2^{2+}-EDTA, Th–NTA and UO_2^{2+}-NTA complexes

A calibration series was prepared over the range 0.04 – 4 mM by equilibrating equi-molar concentrations of thorium or uranium and EDTA or NTA in 50 mM ammonium acetate. Ammonium acetate was required to buffer the pH and thus limit changes in speciation. In water, the pH varied between 5.7 and 2.2 over a Th–EDTA concentration range of 0.04 – 2 mM while in ammonium acetate it varied from pH 6.9 to 5.4. Calibration graphs were obtained for Th–EDTA, and Th–NTA species, assuming that Th was completely complexed which is reasonable within the experimental errors. Five point linear calibrations with R^2 values of 0.995 were obtained for both Th–EDTA and Th–NTA, using the sum of the counts corresponding to Th–EDTA or Th–NTA species against concentration. For UO_2^{2+}-EDTA and UO_2^{2+}-NTA four and five point linear calibrations over a concentration range of 0.04 – 0.8 mM were obtained with R^2 values of 0.979 and 0.998 respectively. Therefore, subsequent experiments were carried out within the relevant linear range.

2.3.3 Th speciation

Effect of pH on Th speciation with EDTA. The speciation of Th–EDTA complexes changed with pH, as shown in Figure 2.2 and Table 2.2. Under acidic conditions (Figure 2.2A), the mixed ligand species $[ThEDTAac]^-$ (*m/z* 579) dominated; the acetate was confirmed as a ligand, rather than an adducted ion, as the species was observed in the positive ion mode in the doubly protonated form (*m/z* 581). Acetate is present due to the pH adjustment with acetic acid. The second most abundant peak was that of the $[ThEDTANO_3]^-$ complex, detected at *m/z* 582. A nitrate-containing species was also observed in the positive ion mode. The co-ordination numbers exhibited here are consistent with Th chemistry (*e.g.* Cotton, 2006), although it has also been previously

noted that the electrospray process at this temperature may remove aqua ligands (Keith-Roach *et al.*, 2005), which were not observed in these spectra.

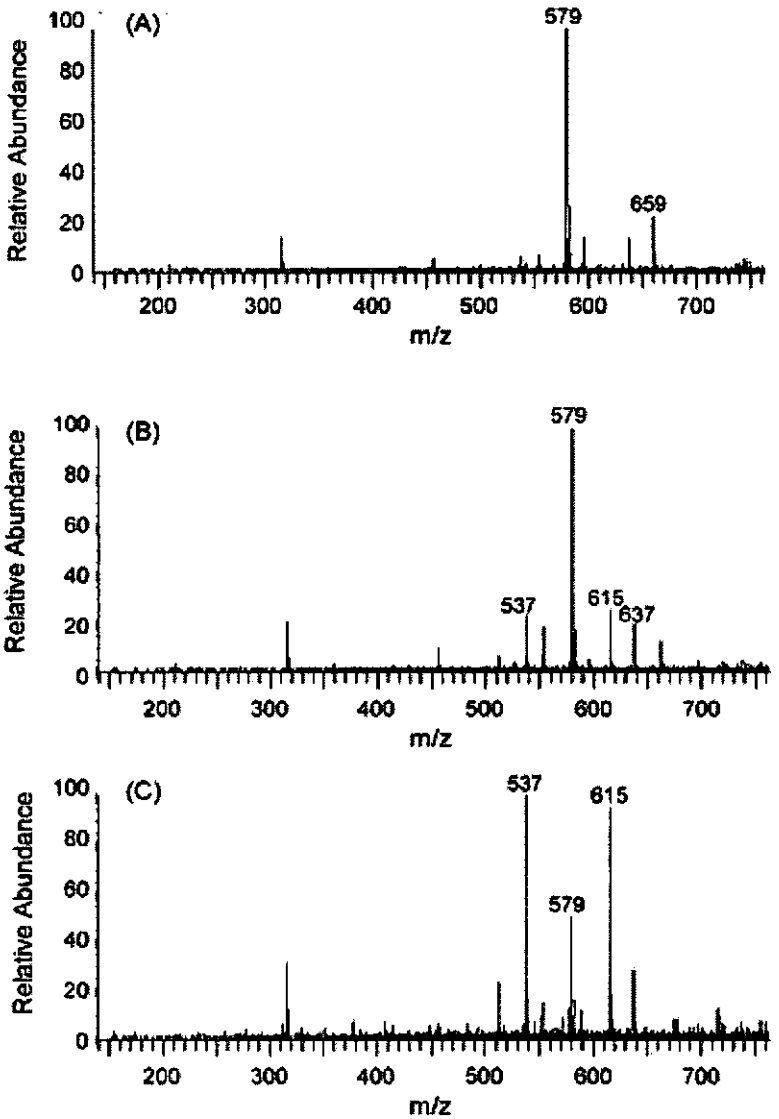

Figure 2.2 Negative ion mode ESI-mass spectra for 0.4 mM Th and 0.4 mM EDTA at: (A) pH 2.5; (B) pH 7.2; (C) pH 10.0

At circumneutral pH (Figure 2.2B), the mass spectrum was again dominated by the mixed ligand complex $[ThEDTAac]^-$ but $[ThEDTANO_3]^-$ was also observed. The nitrate-containing species (*m/z* 582) was the dominant form when the acetate concentration was low (e.g. at pH 6.0 and 8.3, Table 2.2). However, the hydroxy species

Table 2.2 The main species/adducts observed during negative ion mode ESI-MS of solutions containing Th(IV) with EDTA or NTA over the pH range 2.5–10.8 and the corresponding species

pH	Main species/adduct observed in EDTA experiments (observed *m/z*)	Corresponding species	Main species/adduct observed in NTA experiments (observed *m/z*)	Corresponding species
2.5	$[ThEDTAac]^-$ (579)	$[ThEDTAac]^-$	$[ThNTA(ac)_2]^-$ (538)	$[ThNTA]^+$
3.6	$[ThEDTAac]^-$ (579)	$[ThEDTAac]^-$	$[ThNTA(ac)_2]^-$ (538)	$[ThNTA]^+$
6.0	$[ThEDTANO_3]^-$ (582)	$[ThEDTANO_3]^-$	$[ThNTA_2Na]^-$ (631)	$[ThNTA_2]^{2-}$
7.2	$[ThEDTAac]^-$ (579)	$[ThEDTAac]^-$	$[ThNTA_2Na]^-$ (631)	$[ThNTA_2]^{2-}$
8.3	$[ThEDTANO_3]^-$ (582)	$[ThEDTANO_3]^-$	$[ThNTA_2Na]^-$ (631)	$[ThNTA_2]^{2-}$
10.0	$[ThEDTA(OH)_2acH_2]^-$ (615)	$[ThEDTA(OH)_2ac]^{3-}$	$[KHNTA]^-$ (228)	N/A
10.8	$[ThEDTA(OH)_2acH_2]^-$ (615)	$[ThEDTA(OH)_2ac]^{3-}$	$[KHNTA]^-$ (228)	N/A

$[ThEDTAOH]^-$ (*m/z* 537) and $[ThEDTA(OH)_2ac]^{3-}$, which was observed as $[ThEDTA(OH)_2acH_2]^-$ (*m/z* 615), also appeared in the spectrum. $[ThEDTAOH]^-$ was confirmed using positive ion ESI-MS but in the case of $[ThEDTA(OH)_2ac]^{3-}$, it was not clear from the positive ion spectra whether the species was $[ThEDTA(OH)_2ac]^{3-}$ or $[ThEDTA(OH)_2]^{2-}$. However, since other adducts of $[ThEDTA(OH)_2ac]^{3-}$, $[ThEDTA(OH)_2acHNa]^-$ and $[ThEDTA(OH)_2acNa_2]^-$ were also observed at *m/z* 637 and 659, respectively, acetate is likely to be a ligand. The absolute and relative importance of the two hydroxy species increased with increasing pH and dominated the spectra at pH 10.0 and pH 10.8 (Figure 2.2C; Table 2.2). A relatively small signal was also observed at *m/z* 315 throughout these experiments, corresponding to $[AlEDTA]^-$ from aluminium contamination. Free EDTA (H_3EDTA^-; *m/z* 291) was not observed.

The observation of mixed ligand species is important as the acetate and nitrate ligands, as well as the hydroxy and EDTA ligands, affect the charge of the species and thus potential interactions with solid binding phases in the environment. Although acetate and nitrate concentrations are low in most natural environments, they can be high, for example, in contaminated land and other ligands may also occupy this binding position. Mixed ligand actinide species have been previously identified for Th and EDTA and NTA (Carey *et al.*, 1964), Pu and EDTA (Boukhalfa *et al.*, 2004) and U(IV) and EDTA (Perfiliev *et al.*, 1986) and mixed ligand species may therefore be important in general for large actinide ions in contaminated environments.

Effect of pH on Th speciation with NTA. These experiments were carried out with 0.04 mM Th and NTA, as some precipitation was observed with 0.4 mM Th and NTA. The speciation again changed with pH, from a 1:1 cationic thorium-NTA complex at pH 2.5 (Figure 2.3A), observed as a diacetate adduct at *m/z* 538, to an anionic bis-NTA complex, $[ThNTA_2]^{2-}$, at pH 7.2, observed as a sodium adduct (*m/z* 631; Figure 2.3B).

NTA has a lower denticity than EDTA, allowing bis-NTA complexes to form. The data are in agreement with those of Carey *et al.* (1964) obtained from potentiometric titrations, who observed a shift from the 1:1 to the 1:2 complex as the pH increased. The bis-NTA complex is the key Th–NTA species in the most environmentally relevant pH range (pH 6.0–8.3). The hydroxy species $[ThNTA(OH)_2]^-$ (*m/z* 454) was observed, but only up to a maximum of 20% of the major peak intensity (at pH 8.3). No thorium species were observed at pH 10.0 or above (Figure 2.3C, Table 2.2), which may be due to precipitation of $Th(OH)_4$ or ThO_2; the main peak (*m/z* 228) corresponded to the potassium adduct of un-complexed NTA. This suggests that interactions between Th and NTA are weaker than between Th and EDTA.

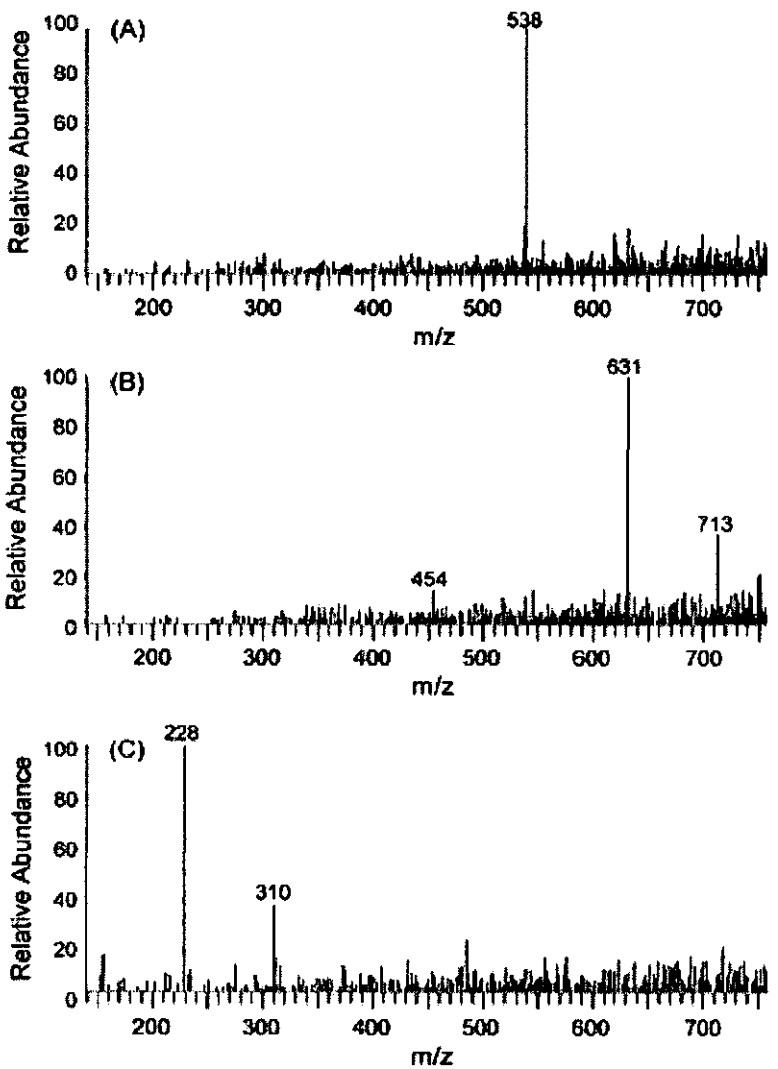

Figure 2.3 Negative ion mode ESI-mass spectra for 0.04 mM Th and 0.04 mM NTA at: (A) pH 2.5; (B) pH 7.2; (C) pH 10.0

The strong influence of the ligands on Th speciation can be seen by comparing the experimental data with Figure 4.2A, which shows the formation of thorium-hydroxy species with increasing pH.

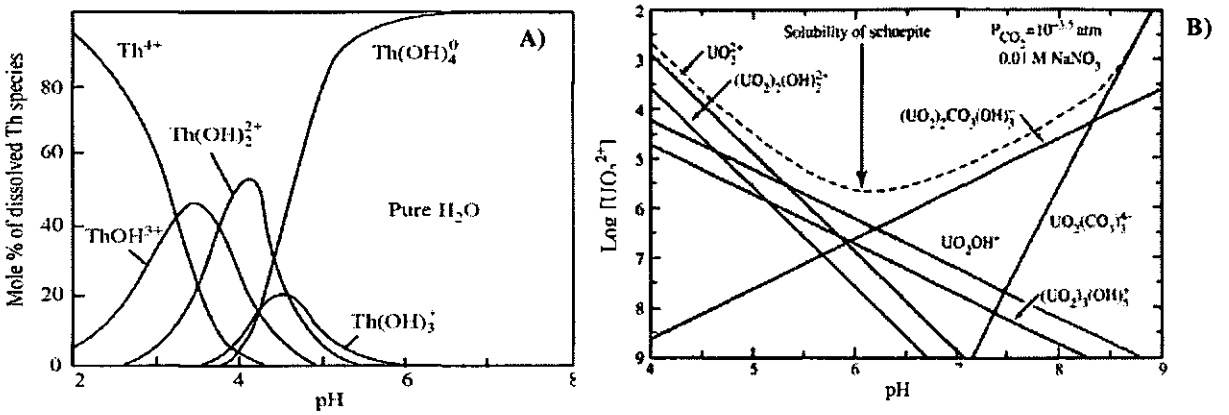

Figure 2.4 Example pH speciation diagrams for A) Th as a mole % (Guillardet et al., 2003); and B) UO_2^{2+} as log concentration (Siegel and Bryan, 2005)

Speciation of Th with increased ligand concentration .The effect of ligand concentration on the speciation of Th (0.4 mM) was investigated using mixtures of Th and EDTA or Th and NTA in the Th : L ratios listed in Table 2.3, in 0.05 M ammonium acetate. As the ratio of EDTA : Th increased, the spectral abundance of the $[ThEDTA_2]^{4-}$ species increased; which was observed as proton/Na adducts at *m/z* 811, 833, 855 and 877 ($[ThEDTA_2H_3]^-$, $[ThEDTA_2H_2Na]^-$, $[ThEDTA_2HNa_2]^-$ and $[ThEDTA_2Na_3]^-$ respectively).

In the case of NTA, $[ThNaNTA_2]^-$ remained the most abundant spectral peak as the NTA concentration increased. $[ThNTA_3]^{5-}$ was also observed at *m/z* 866 and 888 ($[ThNTA_3Na_3H]^-$ and $[ThNTA_3Na_4]^-$ respectively), however this complex was not confirmed in the positive ion mode and may therefore represent a Na_3NTA adduct of the Th-NTA_2 species.

Table 2.3 Speciation of Th (0.4 mM) with EDTA or NTA as a percentage of total ESI-MS counts for Th-ligand species (± % shows 1 σ of combined analytical uncertainty for triplicate analyses for all species)

Ratio	EDTA %			NTA %			
Th : L	ML	ML_2	± %	ML	ML_2	ML_3	± %
1 : 1	94	6	7	6	94	0	5
1 : 2	81	19	4	3	89	8	4
1 : 3	58	42	4	3	84	13	4
1 : 4	50	50	6	3	79	18	5
1 : 5	43	57	4	2	76	21	4

Speciation of Th in an EDTA and NTA mixed ligand system. Figure 2.5 shows that a mixture of products formed, including mixed ligand complexes, when 0.4 mM Th, EDTA and NTA (1:1:1) were mixed in 50 mM ammonium acetate. The sodium adduct of $[ThNTA_2]^{2-}$ produced the largest peak (*m/z* 631) and $[ThEDTAac]^-$ was also present (*m/z* 579). However, adducts of the mixed ligand species $[ThNTAEDTA]^{3-}$ produced signals at *m/z* of 710, 732 and 754, corresponding to $[ThEDTANTAH_2]^-$, $[ThEDTANTAHNa]^-$ and $[ThEDTANTANa_2]^-$ respectively. This Th-NTA-EDTA species was confirmed in the positive ion mode, and the counts for these adducts in the negative ion mode summed to make this species the most abundant spectral peak. The mixed ligand $[ThNTAEDTA]^{3-}$ species has been identified indirectly by potentiometric titration (Carey *et al.*, 1964) but this is the first direct confirmation of its existence. This result emphasises the importance of understanding mixed ligand complexation when investigating the behaviour of Th in co-contaminated environmental matrices.

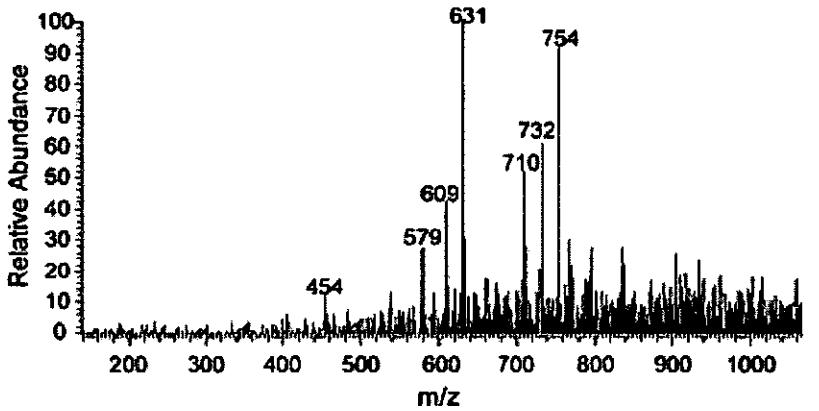

Figure 2.5 Negative ion mode ESI-mass spectrum of 0.4 mM Th, EDTA and NTA at circumneutral pH

2.3.4 UO_2^{2+} speciation

Effect of pH on UO_2^{2+} speciation with EDTA. There were significant peaks from Al-EDTA (*m/z* 315; [AlEDTA]$^-$) and inorganic UO_2^{2+} species in these spectra across the pH range (2.5 – 10.8), indicating incompleted complexation of UO_2^{2+} by EDTA. Structurally, the uranyl ion (O=U=O) prevents EDTA binding as a hexadentate ligand, which is consistent with the complex being less stable. Table 2.5 shows the most abundant spectral peak relating to UO_2^{2+} species; and the main UO_2^{2+}-EDTA complex observed at each pH investigated. Spectral peaks representing UO_2^{2+}-EDTA complexes were generally observed at 10 - 40 % of the most abundant inorganic UO_2^{2+} peak (*m/z* 456; $[UO_2(NO_3)_3]^-$. This peak was defined as a nitrate adduct of the uranyl ion, as no corresponding species was observed in the positive ion mode. A previous study has also suggested that such nitrate adduction to UO_2^{2+} occurred in the gas phase (Pasilis *et al.*, 2006).

Two types of UO_2^{2+}-EDTA species were observed in the negative ion spectra and confirmed in the positive ion mode: the 1:1 $[UO_2HEDTA]^-$species (*m/z* 559) and a 2:1 $(UO_2^{2+})_2$-EDTA species (*m/z* 969; $[(UO_2)_2NaEDTAacetate_2]^-$), where the EDTA is

Table 2.5 The main species/adducts observed during negative ion mode ESI-MS of solutions containing U(VI) with EDTA or NTA over the pH range 2.5-10.8 and the corresponding species

pH	Main UO_2 complex observed in EDTA experiments (observed *m/z*)	Corresponding species	Main UO_2EDTA species/ adduct observed (*m/z*)	Corresponding species
2.5	$[UO_2(NO_3)_3]^-$ (456)	UO_2^{2+}	$[UO_2HEDTA]^-$ (559)	$[UO_2HEDTA]^-$
3.6	$[UO_2(NO_3)_3]^-$ (456)	UO_2^{2+}	$[UO_2HEDTA]^-$ (559)	$[UO_2HEDTA]^-$
6.0	$UO_2HEDTA]^-$ (559)	$[UO_2HEDTA]^-$	$[UO_2HEDTA]^-$ (559)	$[UO_2HEDTA]^-$
7.2	$[UO_2(NO_3)_3]^-$ (456)	UO_2^{2+}	$[UO_2HEDTA]^-$ (559)	$[UO_2HEDTA]^-$
8.3	$[UO_2(NO_3)_3]^-$ (456)	UO_2^{2+}	$[UO_2HEDTA]^-$ (559)	$[UO_2HEDTA]^-$
10.0	$[UO_2HEDTA]^-$ (559)	$[UO_2HEDTA]^-$	$[UO_2HEDTA]^-$ (559)	$[UO_2HEDTA]^-$
10.8	N/A	N/A	N/A	N/A
pH	Main species/adduct observed in NTA experiments (observed *m/z*)	Corresponding species	Main UO_2NTA species observed (*m/z*)	Corresponding species
2.5	$[UO_2(NO_3)_3]^-$ (456)	$[UO_2]^{2+}$	$[UO_2NTA_2Na_3]^-$ (715)	$[UO_2NTA_2]^{4-}$
3.6	$[UO_2(NO_3)_3]^-$ (456)	$[UO_2]^{2+}$	$[UO_2NTA]^-$ (458)	$[UO_2NTA]^-$
6.0	$[UO_2NTA]^-$ (458)	$[UO_2NTA]^-$	$[UO_2NTA]^-$ (458)	$[UO_2NTA]^-$
7.2	$[UO_2NTA]^-$ (458)	$[UO_2NTA]^-$	$[UO_2NTA]^-$ (458)	$[UO_2NTA]^-$
8.3	$[UO_2NTA]^-$ (458)	$[UO_2NTA]^-$	$[UO_2NTA]^-$ (458)	$[UO_2NTA]^-$
10.0	$[KNTAacH_2]^-$ (310)	N/A	$[UO_2NTA_2Na_3]^-$ (715)	$[UO_2NTA_2]^{4-}$
10.8	$[KNTAacH_2]^-$ (310)	N/A	N/A	N/A

assumed to have a bridging position between the U centres. Additional peaks relating to the 2:1 complex were also observed at *m/z* 887 and 947 from $[(UO_2)_2EDTAacetate]^-$ and $[(UO_2)_2HEDTAacetate_2]^-$ respectively. The positive ion spectrum showed a peak from $[(UO_2)_2H_3EDTAacetate_2]^+$, suggesting that the acetate ions were present as ligands. A UO_2^{2+}-$EDTA_2$ complex was also observed (*m/z* 851; $[UO_2H_5EDTA_2]^-$), however this was not confirmed in the positive ion mode and may therefore result from gas phase adduction of the $[UO_2HEDTA]^-$ species by $[H_4EDTA]^0$.

$[UO_2HEDTA]^-$ was the dominant uranium peak at pH 6.0 and 10.0, and the primary UO_2^{2+}-EDTA species observed across the pH range relevant to natural waters (6.0 – 8.3). At pH 7.2 the $(UO_2^{2+})_2$-EDTA complex described above was also present in the mass spectra at 42 % relative abundance compared with the $[UO_2HEDTA]^-$ peak.

Effect of pH on UO_2^{2+} speciation with NTA. The speciation of UO_2^{2+} and NTA changed with pH as shown in Table 2.5, which lists the most abundant solution species and the main UO_2^{2+}-NTA species observed at each pH. There were significant spectral peaks from inorganic UO_2^{2+} species at low pH ($\leq$ 3.6), and from a K-NTA species (*m/z* 310; $[KH_2NTAacetate]^-$ at high pH ($\geq$ 10.0).

At acidic pH (2.5 and 3.6) a nitrate adduct of the uranyl ion was the dominant spectral peak (*m/z* 456, $[UO_2(NO_3)_3]^-$), with an uranyl-triacetate species also present (*m/z* 447, $[UO_2acetate_3]^-$). At pH 3.6, $[UO_2NTA]^-$ (*m/z* 458) was present at 60 % of the most abundant spectral peak, and a lesser signal was observed for a bis-NTA complex of UO_2^{2+} (*m/z* 715; $[UO_2Na_3NTA_2]^-$) at 10 % relative abundance. The importance of UO_2^{2+}-NTA species increased with pH and at circumneutral pH (6 - 8.3) the anionic $[UO_2NTA]^-$ complex was the most abundant peak in the mass spectrum. There were

also smaller signals for mixed ligand UO_2^{2+}-NTA-acetate complexes at *m/z* 540 $[UO_2NaNTAacetate]^-$, and *m/z* 622 $[UO_2Na_2NTAacetate_2]^-$. These species were confirmed in the positive ion mode (*m/z* 520; $[UO_2H_3NTAacetate]^+$, *m/z* 542; $[UO_2H_2NaNTAacetate]^+$, *m/z* 564; $[UO_2HNa_2NTAacetate]^+$ and *m/z* 624; $[UO_2H_2Na_2NTAacetate_2]^+$). A bis-NTA $[UO_2NTA_2]^{4-}$ complex was also evident as a Na^+ adduct at *m/z* 715 between pH 6.0 – 8.3 with additional signals for the complex from mixed H^+/Na^+ adducts. This complex was confirmed in the positive ion mode with a double proton adduct. The nitrate adducted uranyl ion (*m/z* 456) remained visible in these spectra at pH 6.0, 7.3 and 8.3 respectively, indicating that not all UO_2^{2+} was complexed by NTA.

At pH 10, $[UO_2NTA_2]^{4-}$ was the only UO_2^{2+} species visible in the mass spectrum, however the counts were an order of magnitude lower than observed for this species between pH 2.5 – 8.3, possibly due to the formation of UO_2-carbonate species (*e.g.* Figure 2.4B); no UO_2 species were observed in the spectrum at pH 11 suggesting precipitation of U at these higher pH values.

The strongest degree of complexation of UO_2^{2+} by NTA observed using ESI-MS was between pH 6 – 8.3, showing the importance of these species under conditions relevant to natural waters.

Speciation of UO_2^{2+} with increased ligand concentration. The effect of increased ligand concentrations on the speciation of UO_2^{2+} (0.4 mM) was investigated using mixtures of UO_2^{2+} and EDTA or UO_2^{2+} and NTA in the ratios of UO_2^{2+} : L listed in Table 2.6, all in 50 mM ammonium acetate. In 1 : 1 solutions of UO_2^{2+} with EDTA and UO_2^{2+} with NTA, 1 : 1 UO_2^{2+}-L complexes were the most abundant spectral peaks; however

significant peaks for $(UO_2^{2+})_2$-EDTA and UO_2^{2+}-NTA_2 species were also present in the mass spectra. Increased concentrations of EDTA showed limited effect on UO_2^{2+}-EDTA speciation; however with increasing concentrations of NTA, the $[UO_2NTA_2]^{4-}$ species described in Section 2.5.2 became more prominent in the mass spectra.

Table 2.6. Speciation of UO_2-ligand with EDTA or NTA as a percentage of total ESI-MS counts for UO_2-ligand species (± % shows 1 σ of combined analytical uncertainty for triplicate analyses for all species)

Ratio	EDTA %			NTA %		
UO_2 : L	ML	M_2L	± %	ML	ML_2	± %
1 : 1	64	36	10	72	28	6
1 : 2	75	25	9	72	28	3
1 : 3	43	57	9	70	30	6
1 : 4	55	45	7	64	36	2
1 : 5	58	42	6	57	43	3

Speciation of UO_2 in an EDTA and NTA mixed ligand system. In this study there was no evidence for mixed ligand species of UO_2^{2+}-EDTA-NTA from the ESI-MS mass spectra. In mixtures of 0.4 mM UO_2^{2+} with equi-molar EDTA and NTA, the $[(UO_2^{2+})_2NaEDTAacetate_2]^-$ complex (*m/z* 969) was the most abundant spectral peak. Lesser peaks representing $[UO_2NTA]^-$ and $[UO_2NTA_2]^{4-}$ species were observed at ~ 50 % of the major peak. Previous studies have reported mixed ligand species of U(IV) with EDTA (Carey and Martell, 1967; Perfil'ev *et al.*, 1986), and mixed ligand species of U(IV) with NTA (Carey and Martell, 1967); however to the author's knowledge there have been no reports of such mixed ligand complexes of UO_2^{2+} with EDTA or NTA.

2.3.5 Comparison of experimental data with speciation model outputs

The experimental data were compared with the outputs from the selected speciation models to assess how well the experimental data were predicted. All components were

included in the calculations (Th^{4+}, UO_2^{2+}, $EDTA^{4-}/NTA^{3-}$, ac^-, NO_3^-, NH_4^+, and CO_3^{2-} where appropriate), but mixed ligand or bis- species could not be predicted because the stability constants are not known (Table 2.7). Therefore, although acetate ligands were observed in $[ThEDTAac]^-$, for example, this species is considered to be [ThEDTA] for the purpose of this comparison.

Table 2.7 Stability constants given in various databases. The Smith and Martell (1989) data have been adjusted so that they are in the same format of data input as the constants in the HYDRA and MINTEQ databases. The original data show changes to a species, e.g. $ThEDTA + H_2O - H^+$, whereas the adjusted numbers show the data when all ligands are added to the metal ion, e.g. $Th + EDTA + H_2O - H^+$

Species	Stability constant (log k)			
	Hydra	MINTEQ v4.0	PHREEQcI data	Smith and Martell adjusted
ThEDTA	26.8	26.7	23.2[a]	23.2
$[ThEDTAH]^+$	28.8	28.6	1.98[a]	25.2
$[ThEDTAOH]^-$	19.5	-3.52	-7.04[a]	16.2
$Th_2EDTA_2(OH)_2]^{2-}$	62.7	-	-	
$[ThNTA]^+$	15.1	15.0	16.9[b]	
ThNTAOH	6.49	9.59	-	
ThO_2	-9.74	-2.7		
$Th(OH)_4$	-15.9	5.29		
UO_2HEDTA^-	19.7	19.63	7.32[a]	
$(UO_2)_2EDTA$	20.56	20.43	15.2[a]	
$(UO_2)_2EDTA_2^{4-}$	29.46	29.33	-	
$(UO_2)_2OHEDTA^-$	16.05	15.42	-	
UO_2NTA^-	10.85	10.78	9.56[a]	

[a]Smith and Martell (1989)
[b]Anderegg (1977)

Th–EDTA and Th–NTA solubility. Visual MINTEQ predicted that Th would precipitate in the systems studied when either ThO_2 or $Th(OH)_4$ was specified as the possible solid phase, particularly at circumneutral and alkaline pH. Precipitation was predicted to be complete at a more acidic pH when ThO_2 was used. HYDRA/MEDUSA also predicted

precipitation of $ThO_{2(am)}$ or $Th(OH)_4$ from circumneutral to alkaline pH in the presence of NTA, but with EDTA, the high stability of the $[Th_2EDTA_2(OH)_2]^{2-}$ dimeric species ($\log k = 62$), which was only included in this database, resulted in this soluble species dominating the predicted speciation throughout the pH range studied. ESI-MS analysis in the positive ion mode confirmed that the monomer, rather than this dimer, was present in the solutions analysed, and the dimer has also been discounted following solution phase EXAFS analysis of Th–EDTA species (Xia *et al.*, 2003). The dimer was therefore removed from the database and Th solubility was underestimated by the model at high pH. Therefore, the Th–EDTA and Th–NTA complexes present in solution are more stable than currently predicted by these speciation models, and for the solution phase speciation calculations below, it was necessary to exclude the formation of solid phases. Solid phases were not included in the database for PHREEQcI, as shown in Table 2.7.

Variations in Th–EDTA and Th–NTA speciation with pH. There are some significant discrepancies between the stability constants assigned to soluble Th–EDTA and Th–NTA species in the databases (Table 2.7) and, in some cases, different species are included in each one. However, it is important to note that data can be entered into the models in different ways and the absolute numbers given can reflect these differences. For example, the $[ThEDTAOH]^-$ constants are calculated from $Th^{4+} + H_2O + EDTA^{4-} - H^+$ in the HYDRA and MINTEQ databases, while for the Smith and Martell data used in PHREEQcI, it is calculated from $ThEDTA + H_2O - H^+$. Therefore, the data in Table 2.7 from Smith and Martell (1989) have been adjusted for direct comparison with the other two databases. Once the $[Th_2EDTA_2(OH)_2]^{2-}$ dimer and potential solid phases were removed from the HYDRA database, the predicted speciation outputs from PHREEQcI and HYDRA/MEDUSA were similar, with

[ThEDTA] dominating from pH 2 to 7 and $[ThEDTAOH]^-$ from pH 7.5 to 10.0. These results broadly agree with the experimental data, although the models do not include the dihydroxy species observed. The low stability constant for $[ThEDTAOH]^-$ in the MINTEQ database resulted in the apparent persistence of [ThEDTA] at highly alkaline pH, which suggests that these data are less appropriate.

The existing speciation and thermodynamic data for the Th–EDTA complexes have recently been challenged by Xia *et al.* (2003). Their experimental data suggested that either the stability constant for $[ThOHEDTA]^-$ ($\log k = 30.2$, (Martell and Smith, 1995) was underestimated by five orders of magnitude or that other Th–EDTA species were present. The authors felt that the discrepancy between model and experiment was most likely due to the presence of $[Th(OH)_2EDTA]^{2-}$, for which they calculated a stability constant ($\log k$) of 39.5. The ESI-MS data from this study show that $[Th(OH)_2EDTA]^{2-}$ (seen here with an additional acetate ligand) is important. However, since the species co-exists with $[ThOHEDTA]^-$, it is also likely that the two species have similar stability constants. The stability constant for $[ThOHEDTA]^-$ from Martell and Smith (1995) ($\log k = 30.2$) and that derived for $[Th(OH)_2EDTA]^{2-}$ are several orders of magnitude higher than those used in the programs here, explaining the vast underestimation of Th–EDTA solubility predicted in this study at alkaline pH. However, their use in conjunction with the associated $\log k$ of 23.2 (Martell and Smith, 1995) for [ThEDTA] results in misrepresentation of the speciation at lower pH. In general, the reported stability constants for $[ThOHEDTA]^-$, $[Th(OH)_2EDTA]^{2-}$ and [ThEDTA] need to be re-examined, taking into account their stability over Th precipitation and achieving the equilibrium species distribution with pH. The absence of data for the $[ThEDTA_2]^{4-}$ complex also needs to be addressed to improve model outputs.

In the case of Th and NTA, the dominant $[ThNTA_2]^{2-}$ species seen experimentally from pH 6.0 to 8.5 is not included in the stability constant databases, despite the characterisation of this species in 1964 (Carey *et al.*, 1964). Therefore, the predictions of the models did not agree with the experimental data, with an overemphasis on $[ThNTA]^{+}$ and, notably, [ThNTAOH], which was not significant experimentally. The stability of $[ThNTA_2]^{2-}$ needs to be further examined in relation to precipitated phases, to allow prediction of this solution species at pH 6.0–8.5 and Th precipitation at pH 10.0, as seen experimentally. Equally, elucidation of an anionic species, rather than a cationic or neutral species, should aid interpretation of the environmental behaviour of Th in the presence of NTA.

Variations in UO_2^{2+}–EDTA and UO_2^{2+}–NTA speciation with pH. PHREEQc and Visual MINTEQ predicted that UO_2^{2+} would remain soluble across the pH range studied; however, solid phases were not defined in Visual Minteq or in the PHREEQc input file, and when included in the Hydra-Medusa model, the formation of the crystalline $UO_2(OH)_2 \cdot H_2O$ species was predicted from pH 7.4 with EDTA, and pH 4.8 with NTA; however such phases would not form over the timescales of these experiments (48 – 60 h). There were similarities in the percent of UO_2^{2+} associated with EDTA predicted by each model. However, since different in the UO_2^{2+}-EDTA species were included in each database, and their stability constants varied, there were differences in the predictions of UO_2^{2+}-EDTA speciation with pH.

PHREEQc predicted that the UO_2^{2+} ion was the only UO_2^{2+} species at pH 2.5, while both Visual MINTEQ and Hydra-Medusa also predicted the $[UO_2HEDTA]^{-}$ species at this pH, at 48 % and 60 % respectively. As pH approached neutral values, UO_2^{2+}-EDTA species became increasingly important. Between pH 3.6 to 7.2, UO_2^{2+}-EDTA species

represented 96 to 100 % of the total UO_2^{2+} in the Visual Minteq and Hydra-Medusa models; and 21 to 88 % of total UO_2^{2+} in the PHREEQc model; in each case the highest degree of UO_2^{2+} complexation by EDTA was observed at pH 6.0. With PHREEQc UO_2^{2+}-EDTA was entirely present as $[UO_2HEDTA]^-$; whilst with Visual MINTEQ and Hydra-Medusa, a $(UO_2^{2+})_2$-EDTA-hydroxy species and a UO_2^{2+}-EDTA dimer which were not observed using ESI-MS, increased in importance with increasing pH (71 and 90 % respectively for the hydroxyl complex and ~ 10 % for the dimer, of the total UO_2^{2+}-EDTA species at pH 7.2). These species were not included in the PHREEQc model. At pH $\geq$ 8.3 uranyl-carbonates dominated UO_2^{2+} speciation, with no UO_2^{2+}-EDTA species were predicted. Although there were differences between species observed experimentally and those included in the models, there was general agreement between the trends in the experimental data and the speciation models for the formation of UO_2^{2+}-EDTA species.

With NTA, the $[UO_2NTA]^-$ complex was the only UO_2^{2+}-NTA species included in any of the three model databases. All three models predicted the maximum interaction between UO_2^{2+} and NTA at pH 6; however the percent UO_2^{2+} complexed by NTA varied between 25 % (PHREEQcI) and 95 % (Visual Minteq). Also the pH range where complexation by NTA was important varied between the models (pH 3.5 – 6.0 Hydra-Medusa; pH 6.0 – 8.3 PHREEQcI; pH 3.6 – 7.2 Visual Minteq). There was consistency between the theoretical and experimental data for the importance of UO_2^{2+}-NTA species at circumneutral pH. However, the $[UO_2NTA_2]^{4-}$ species identified in the experiments as an important species when NTA was in molar excess to UO_2^{2+} was not included in any databases and hence was not predicted. As with EDTA, uranyl-carbonates dominated UO_2^{2+} speciation at pH $\geq$ 8.3.

2.4 Conclusions

ESI-MS is a powerful analytical tool for studying Th and UO_2^{2+} speciation in the presence of EDTA and NTA over a wide pH range and in complex mixtures. Data generated in the negative ion mode showed the range and approximate abundance of species present and the exact species were then confirmed for most species in the positive ion mode. The use of both modes allows identification of adducts and minimises the potential for instrumental artefacts. The data obtained were supported by previous experimental work and highlight differences between experimental and modelled data for the Th species. There was reasonable agreement between experimental and theoretical modelled data for the UO_2^{2+} species, although not all species observed were included in the databases, and some species that were included were not observed experimentally. The detection limit of 0.04 mM for these Th and UO_2^{2+} complexes is suitable for applying the technique to contaminated land scenarios and this allows a wide and informative *m/z* range (150–2000) to be used. The specific conclusions of the study are that (1) ESI-MS is well suited to these analyses and provides clear spectra that can be related directly to Th and UO_2^{2+} speciation, even when several species co-exist; (2) the bis-NTA species of Th and UO_2^{2+}, which are excluded from speciation databases, are important within an environmentally relevant pH range of 6.0–8.3; (3) mixed ligand species of Th have been confirmed, and; (4) experimentally observed Th–EDTA and Th–NTA speciation and UO_2^{2+}-EDTA and UO_2^{2+}-NTA was not predicted well by the three modelling programs. These data represent an important step forward in understanding actinide speciation in the presence of EDTA and NTA, and in identifying current limitations in speciation models. ESI-MS therefore offers opportunities to define solution-phase speciation in more detail than was previously possible, and increasingly complex samples can be studied, working towards examination of real environmental matrices.

Chapter 3

Competitive interactions in the ternary Th-Fe-EDTA system

3.1 Introduction

Geochemical models of aqueous speciation often assume chemical equilibrium is reached, which may not always be true in the heterogeneous natural environment where competitive processes may affect speciation. The kinetics of complexation reactions are important for elucidating environmental processes. The complexation kinetics of EDTA with transition metals has been reviewed by Ogino and Shimura (1986). Exchange kinetics in the Zn-EDTA-Fe system in natural waters have shown slow exchange between EDTA complexed Fe(III) and divalent cations, with the concentration of the incoming metal an important factor in the rate of metal exchange (Xue *et al.*, 1995). Nowack and Sigg (1997) found the dissolution of Fe minerals by metal-EDTA complexes to be dependent on the complexed metal, with dissociation of the complex the rate limiting step in the case of Fe dissolution from hydrous ferric oxide. To the author's knowledge however, there have been no direct speciation studies of the kinetics of exchange between EDTA- complexed radionuclides and trace metals such as Fe that have a strong affinity for the ligand.

Fe is abundant in environmental mineral phases and may also be present in canisters used to store nuclear wastes, and hence in contact with wastes as corrosion products when repository barrier systems are breached by natural waters. According to thermodynamic databases available in the literature, both iron and thorium form stable complexes with EDTA (e.g. Log k of 26 and 23 respectively (Smith and Martell, 1989)). However, there is some variability in literature constants, particularly for radionuclides. For example, for the ThEDTA complex, Anderegg (1977) reported log k values from different studies of 23.2 ± 0.1, 23.29 ± 0.04, 21.3, and 21.84 ± 0.04 and suggested a tentative value of 23.25 ± 0.11 at an ionic strength of 0.1 and a temperature of 20°C. Furthermore, reported equilibrium constants do not allow for reaction kinetics

to be considered, which are important in dynamic heterogeneous environmental systems, where kinetically limiting reaction pathways may prevent speciation equilibrium from being reached over the timescales of groundwater transport.

The aim of this study was therefore to investigate the competition between thorium and iron for EDTA, when Th had been pre-equilibrated with the ligand in order to determine the competitive processes occurring in the ternary Th-Fe-EDTA system within a kinetic framework. Specific objectives were to:

1) Quantify solution phase Th and Fe concentrations in the aqueous Th-Fe-EDTA system over time using inductively coupled plasma mass spectrometry (ICP-MS) for Th determination, and flame atomic absorption spectrometry (FAAS) for Fe determination.

2) Directly monitor changes in solution speciation over time using electrospray ionisation mass spectrometry (ESI-MS).

3) Determine the processes controlling kinetic interactions.

4) Discuss the results in the wider context of potential nuclear waste contamination of the terrestrial environment.

3.2 Experimental

3.2.1 Chemicals & reagents

Methanol (Riedel-de-Haen, LC-MS grade), water (G-chromasolv grade), ammonium acetate (ultra grade), nitric acid and iron(III) chloride were obtained from Sigma-Aldrich, (Poole, U.K.). EDTA disodium salt and ^{232}Th, ^{238}U and ^{56}Fe atomic spectroscopy standards were obtained from Fisher Scientific (U.K.) Ltd. (Loughborough, U.K.), and thorium nitrate salt from VWR International, (Poole, U.K.).

Ultra pure water was obtained from a Milli-Q purification system (Millipore ≥ 18.2 MΩ cm^{-1})

3.2.2 Sample preparation

Sample preparation was carried out in an ISO 9001:2000 accredited laboratory, and solutions were prepared under a laminar flow hood to minimise contamination. Working stock solutions of Th, Fe and EDTA were prepared by weighing the required mass of the relevant salt into a volumetric flask and making up to 50 mL with aqueous 0.05 M ammonium acetate. These were mixed vigorously by hand for a few minutes and it was necessary to place the EDTA stock solution in a sonic bath for 1 h to dissolve completely as some solid was visible after shaking by hand. Working stock solutions of Th or EDTA were prepared at a concentration of ~ 4.3 (± 0.3) mM, and Fe was prepared fresh prior to use at ~ 10 mM. Metals and ligands were then diluted and mixed as necessary to prepare control and experimental solutions. All glass- and plastic-ware was cleaned for > 12 h in 2 % Decon solution, thoroughly rinsed with reverse osmosis (RO) water, cleaned for > 12 h in a 10 % v/v HCl acid bath, rinsed thoroughly with ultra-pure water (Milli-Q ≥ 18.2 MΩ) and dried in a laminar flow hood.

3.2.3 Experimental design

An experimental strategy was designed to investigate the interactions of Fe(III) with Th-EDTA complexes. Figure 3.1 shows a flow diagram of the experimental design. Solutions were prepared from the working stock solutions at concentrations detailed in Figure 3.1, with molar ratios of Fe : Th of 1 : 1, 2 : 1, 3 : 1, 4 : 1 and 5 : 1. All solutions were prepared in aqueous 0.05 M ammonium acetate in order to buffer pH. 48 h after mixing the first two analytes to ensure equilibrium speciation (Cartwright *et al.*, 2007), Fe was added to solutions of Th and EDTA in the ratios given in Figure 3.1, and the

1 : 1 : 1 solutions were prepared in triplicate. Sub-samples from 1 : 1 : 1 solutions of Th : Fe : EDTA were taken at a high frequency over the first 48 h after addition of the second analyte and again after 1 week. Thereafter samples were taken on the same schedule as solutions where Fe was in molar excess over Th, *i.e.* every 10 days – 2 weeks for two months subject to instrument availability. Sub-samples of these solutions were filtered using Milli-pore syringe filters (0.45 μm; cellulose nitrate) and used undiluted for speciation analysis by ESI-MS, and diluted two-fold to 2 % HNO_3 for the determination of soluble Fe using FAAS, and a further 1000-fold dilution with 2 % HNO_3 for the determination of soluble Th using ICP-MS. Soluble Fe and Th fractions were therefore defined operationally as passing through a 0.45 μm filter membrane. Solutions of Th, Fe, equi-molar Th and EDTA, and equi-molar Fe and EDTA were prepared for use as experimental controls and were processed in the same manner. The pH of each solution was measured using a Mettler Delta 340 pH meter (Mettler-Toledo, Leicester, U.K.).

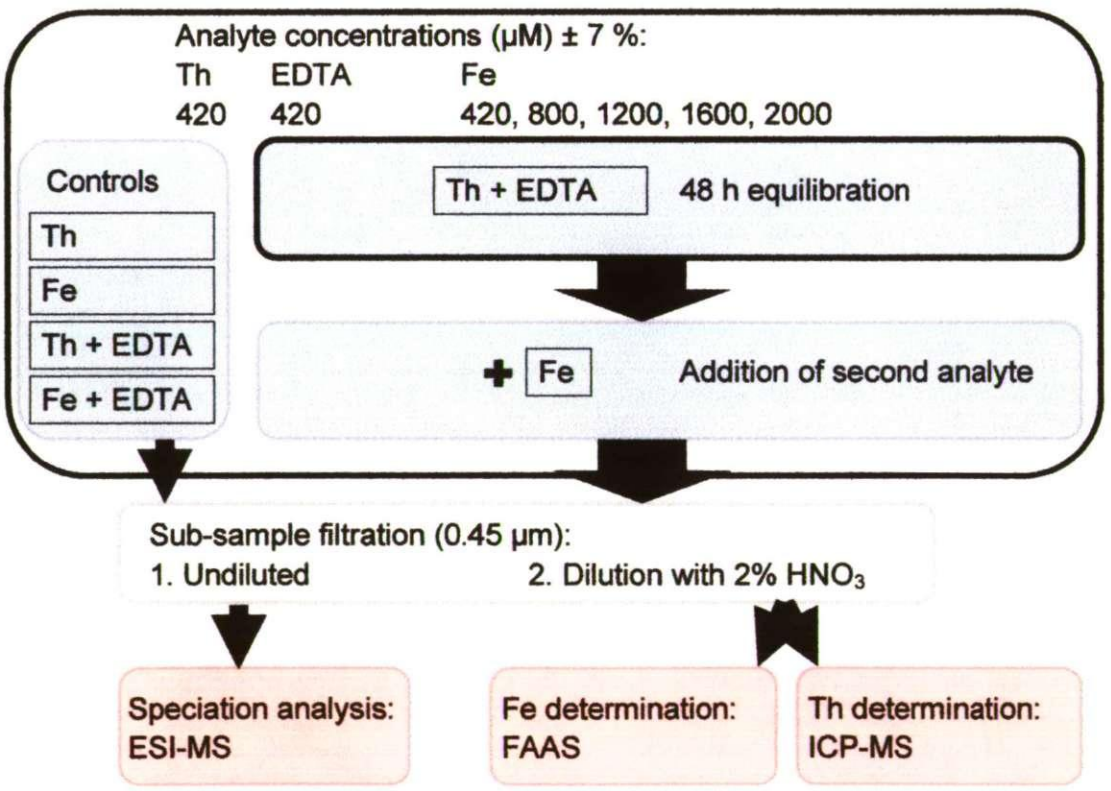

Figure 3.1 Flow diagram of experimental design

3.2.4 Analytical methods

An ion trap mass spectrometer fitted with an electrospray interface (ThermoQuest Finnigan Mat LCQ, San Jose, Ca, U.S.A.) was used to perform electrospray ionisation mass spectrometry (ESI-MS). Water was delivered by a P580A binary pump (Dionex-Softron GmbH, Germering, Germany) at a flow rate of 150 μL min^{-1}. Flow injections were made manually using a Rheodyne injector (model number 9125, CA, U.S.A.) as a clean, efficient method of sample introduction, with a 5 μL sample loop. Instrument tuning parameters are detailed in Table 3.1 for negative ion mode of analysis. Xcalibur 1.0 software was used to acquire and store data. ESI-MS counts were averaged over a 30 s time period around the spectral peak following each injection to provide consistent and comparable data using QualBrowser software. Data were then processed using Excel to obtain counts for relevant mass to charge ratios for the complexes of interest.

Table 3.1 ESI-MS tuning parameters

Tuning parameter	Negative ion mode
Capillary voltage	-45 V
Source voltage	-4.5 kV
Tube lens offset	+5 V
Capillary temperature	220 °C
N_2 sheath gas flow rate	60 (arbitrary units)
Auxiliary gas flow rate	20 (arbitrary units)

Determination of aqueous phase Th was carried out using inductively coupled plasma mass spectrometry (ICP-MS) (VG Plasmaquad PQ2+ Turbo, Winsford, Cheshire) using ^{238}U as an internal standard. The instrument was tuned prior to each analytical run using a calibration standard to obtain the optimum signal. Soluble Fe was determined using FAAS (Varian, Palo Alto, U.S.A.).

3.3 Results and discussion

3.3.1 Precipitation of Th and Fe in control solutions

Solutions of Th, Fe, and pre-equilibrated Th with EDTA and Fe with EDTA were sampled over time acting as experiment controls to quantify loss of soluble metal in the absence of competitive processes. Figure 3.2 shows the percentage of the metal remaining in solution over time for A) Fe and B) Th in the control solutions. Iron was rapidly lost from solution in the absence of EDTA (non-detectable after 7 min; LOD = 1.0 μM, defined as: mean of the blank plus 3σ over the gradient of the calibration line, probably due to the formation of solid phase Fe-hydroxides, as the concentration of iron that was used in these experiments was greater than the solubility of Fe(III) at the experimental pH (6.1 ± 0.2) (10^{-9} M, Stumm and Morgan, 1996). However, in solutions where EDTA was present, 99.5 ± 0.7 % of the Fe remained stable as aqueous phase Fe over the time period investigated (Figure 3.2A), suggesting that Fe was complexed by the ligand.

Th control solutions decreased within 1 h to 90.0 ± 2.6 % of the initial Th concentration, and remained stable in solution at this concentration over the time period. Th in the Th and EDTA solutions decreased to 90.7 ± 3.2 % of the initial concentration within 12 h, and then remained stable (Figure 3.2B). The similarity of the results, including the 10 % loss from solution, indicated that not all Th was complexed by the EDTA.

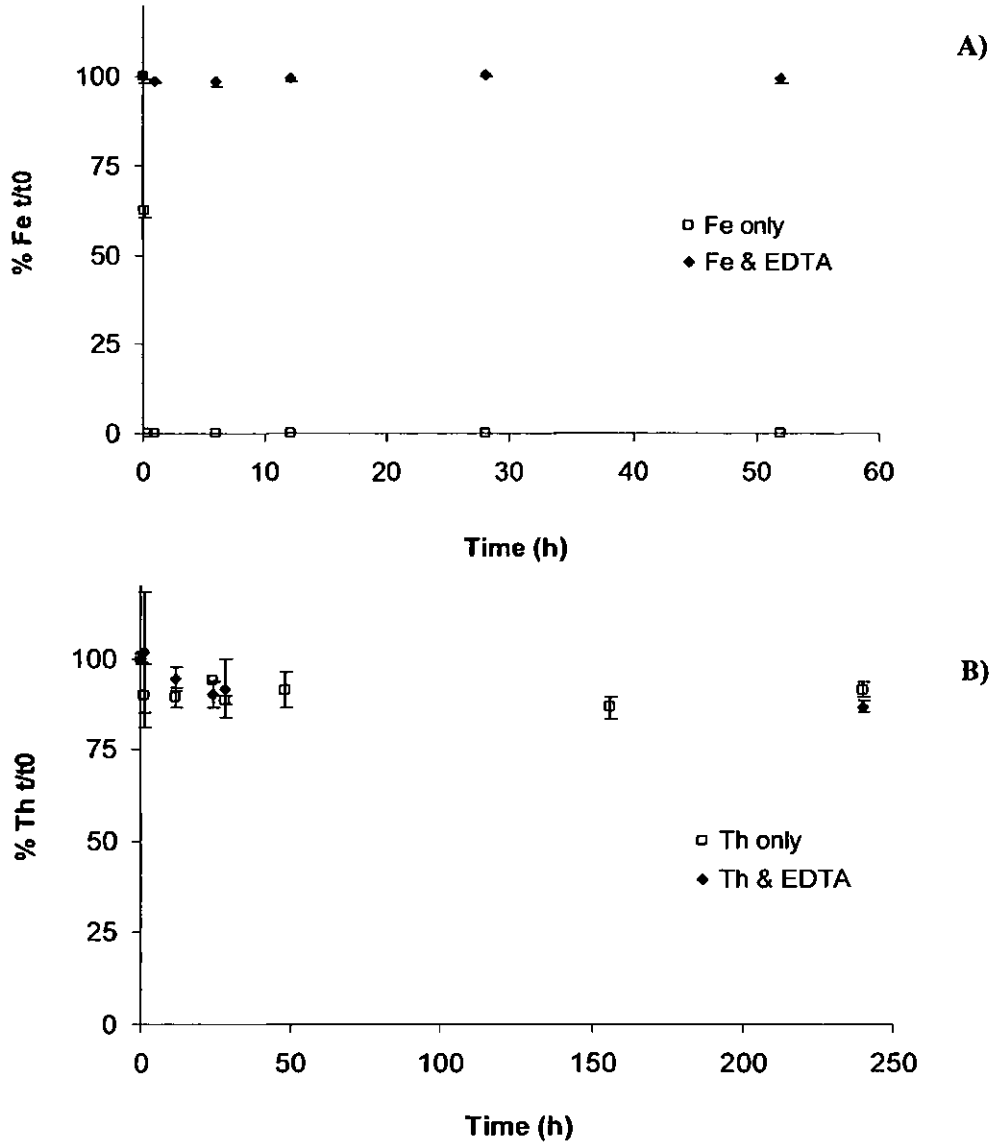

Figure 3.2 A) Fe and B) Th concentrations over time (as % of [t = 0]) for solutions containing each metal only and each metal with an equi-molar concentration of EDTA. Error bars show 1 standard deviation around the mean of triplicate sample concentrations

3.3.2 Competition in a system of pre-equilibrated ThEDTA with added Fe

The effect of Fe on ThEDTA complexation in the equi-molar Th : Fe : EDTA solution in 0.05 M ammonium acetate was quantified by determination of soluble Th and Fe over time using ICP-MS and FAAS respectively.

Th and EDTA were mixed and equilibrated for 48 h prior to the addition of Fe. On addition of Fe, there was a rapid of loss of Fe from solution within the first 48 h, with the minimum Fe concentration (4 % of the t = 0 concentration) reached by 160 h (7 d) (Figure 3.3A). The rate of loss in the first 48 h was significantly slower than the precipitation observed in the Fe control solutions, where Fe concentrations were below instrumental detection limits after 7 min. Interaction with the ThEDTA complex therefore appeared to limit the kinetics of Fe precipitation in these systems. Th was also removed from solution during this period at a greater rate than was observed in the control solution, and decreased to 74 ± 2 % of the initial concentration after 48 h (Figure 3.3B).

The rate of change in the concentration of each metal during the first 48 h was obtained from the gradient of the log of concentration over time, assuming a concentration dependent first order reaction as the simplest case; uncertainties represent error of the slope (S_b). The rate of loss of Fe ($-4 \times 10^{-6} \pm -9 \times 10^{-7}$ s^{-1}) was greater than the loss of Th ($-8 \times 10^{-7} \pm -5 \times 10^{-8}$ s^{-1}) from solution, which suggests that Th was removed from solution via sorption to the Fe precipitate rather than via co-precipitation. The negative charge imparted by acetate binding to Th as a second ligand (Chapter 2), facilitated sorption of the ThEDTA complex to solid phase Fe. The correlation coefficient (R^2) for the concentration of soluble Th versus the assumed Fe precipitate ($[Fe]_{t0} - [Fe]_{ti}$) was 0.93, with a slope of -0.34 ± 0.03, showing a loss of 34 μM Th per 100 μM Fe precipitated. From 160 to 1400 h (58 days), solution phase Fe concentrations increased from 4 ± 1 % to 26 ± 1 % of the initial Fe concentration, whilst the solution phase Th concentration continued to decrease slowly from 74 ± 2 % to 56 ± 1 % by 1400 h (58 days). The total percent changes in the metal concentrations of 22 ± 2 % and 18 ± 3 % were within analytical uncertainty of each other. Therefore, following the initial

precipitation of Fe, there was a slow process of Fe resolubilisation with a concomitant decrease in solution phase Th, suggesting exchange at the solid surface of the Fe precipitate. This is in accordance with literature studies, which have shown the displacement of aqueous phase EDTA complexed cations by solid phase Fe, resulting in increased solution phase Fe as the Fe-EDTA complex (*e.g.* Friedly *et al.*, 2002; Nowack and Sigg, 1996).

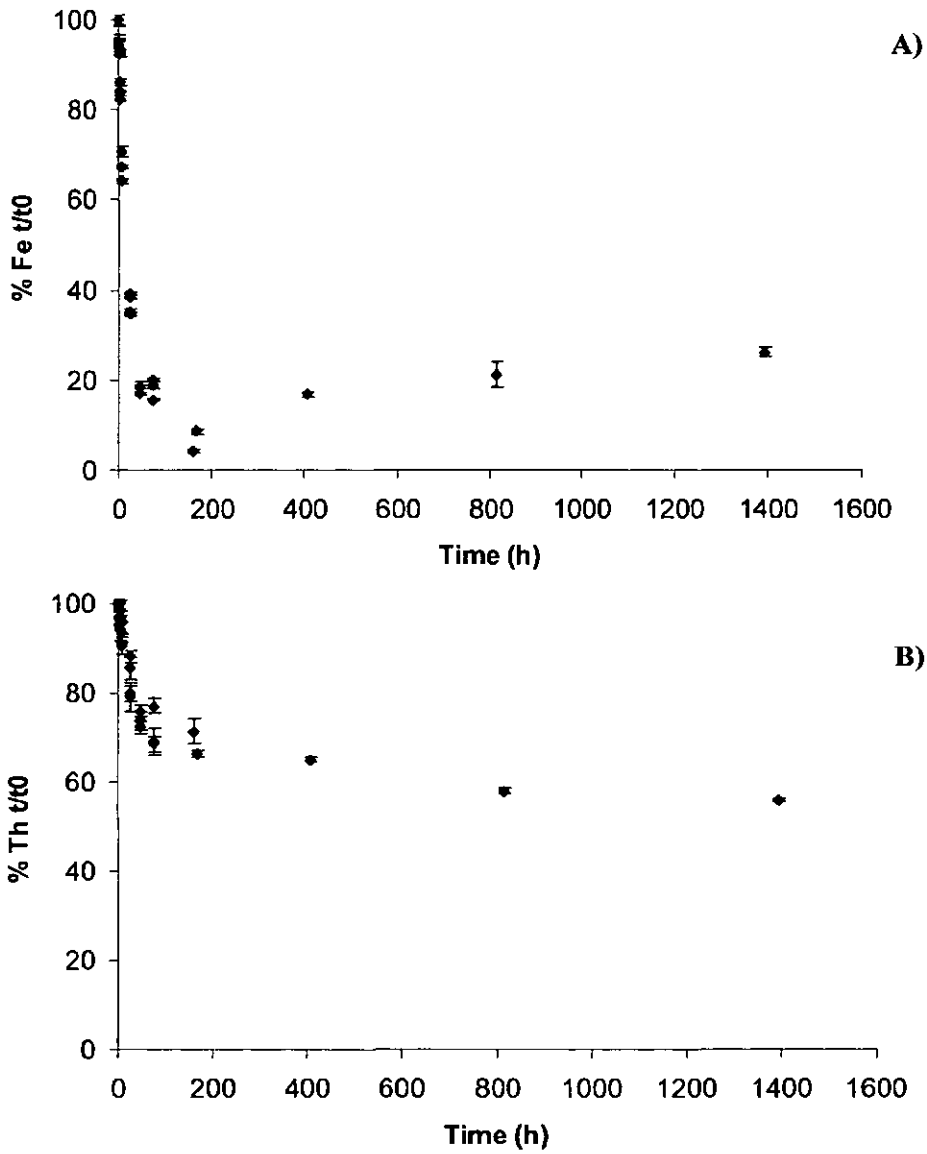

Figure 3.3 A) Measured solution [Fe]; and B) [Th] over time for 1:1:1 Th:Fe:EDTA (420 ± 30 µM), where Fe was added to a solution of ThEDTA that had been mixed 48 h before. Error bars represent analytical uncertainty (1 σ, n = 3) (< 5 %)

Characterisation of changes in solution speciation within the Th-EDTA-Fe system discussed above was provided using ESI-MS. Electrospray ionisation-mass spectrometry allows the direct observation of both Th and Fe EDTA solution phase complexes, as shown in Figure 3.4. ESI-MS analysis of the control solutions showed that no signal for Fe was observed in the mass spectra of solutions containing only Fe, probably due to its rapid removal from solution by precipitation. Thorium was observed with adducted nitrate and/or hydroxyl matrix ions and coordinated acetate anions.

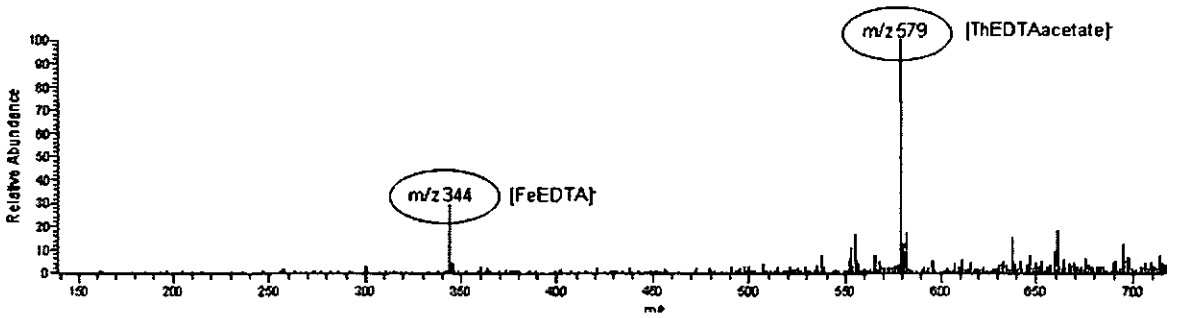

Figure 3.4 Example electrospray ionisation mass spectrum showing aqueous complexes of [ThEDTAacetate]$^-$ (m/z 579) and [FeEDTA]$^-$ (m/z 344) from a sample of 420 ± 30 μM Th pre-equilibrated for 48 h with 420 μM EDTA before the addition of 800 μM Fe, in 0.05 M ammonium acetate after 49 days

The change in solution speciation over the first 48 h in the 1 : 1 : 1 Th : Fe : EDTA system is shown in Figure 3.5. Results are presented as percent ThEDTA or FeEDTA species based on the ESI-MS signal for all metal-ligand species. Whilst this does not provide a quantitative measure of the change in solution speciation over time, it does provide semi-quantitative, direct observation of the exchange reactions. It was assumed that inter-day variability in the electrospray signal affected the response of both metal-EDTA complexes in the same manner and hence observed changes were due to changes in solution speciation and not analytical artefacts.

During the first 2 h, the ESI-MS data showed that only Th was bound to EDTA, explaining the observed precipitation of Fe. The formation of the FeEDTA complex was seen within 8 h, at 5 ± 5 % of the total metal-EDTA species distribution. By 48 h this species accounted for 11 ± 6 % of the observed metal-EDTA species. The complementary analytical techniques therefore showed that during the first 48 h, while Fe precipitation was the dominant process there was some formation of FeEDTA.This agrees with the quantitative data which showed a minimum Fe concentration of 4% of the initial value.

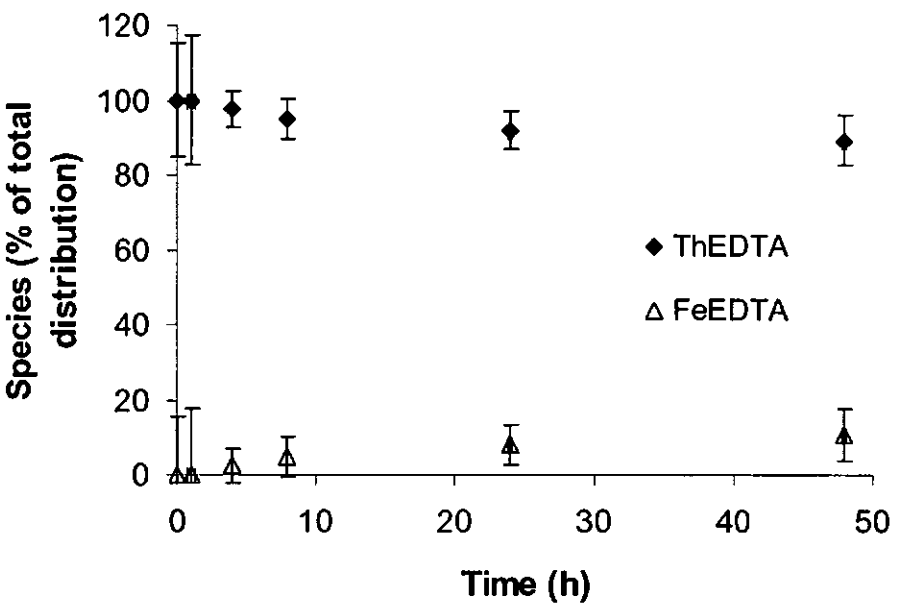

Figure 3.5 Speciation change over time as a percentage of total metal-ligand species ESI-MS counts for solutions of 420 ± 30 μM Th pre-equilibrated for 48 h with 420 μM EDTA before the addition of 420 ± 30 μM Fe

3.3.3 Competition in systems with excess Fe

The effect of higher concentrations of Fe on the stability of the ThEDTA complex was investigated by adding different concentrations of Fe to solutions of pre-equilibrated equi-molar Th and EDTA. Solutions were again sub-sampled over time to provide

quantitative determination of solution phase Th and Fe. Figures 3.6 A) and B) show the concentrations of solution phase Th and Fe respectively over time for different ratios of Fe : Th (1 : 1, 2 : 1, 3 : 1, 4 : 1 and 5 : 1), with 420 ± 30 μM of Th and EDTA in each system. The greatest removal of both Th and Fe from solution was over the first seven days (160 h) and there was a strong correlation between the loss of Th from solution and the amount of Fe precipitate formed during this time (slope of -0.23 ± 0.08 μM Th/μM Fe; R^2 = 0.98). This was within the experimental uncertainty of the relationship seen for Th removal from solution as a function of Fe precipitation in the 0 – 48 h period for the equimolar system (-0.34 ± 0.03 μM Th/μM Fe; R^2 = 0.93). The concentration of Fe remaining in solution after 7 days was higher in solutions of higher initial Fe concentration. With 5-fold excess of Fe to Th, the total soluble metal concentration in solution after 7 days was greater than the concentration of EDTA in solution (410 μM Fe and 110 μM Th). Since the earlier experiments indicated that Fe precipitation should be complete by this time, the extent to which Fe replaced Th in the EDTA complex is not clear.

After this period, Th concentrations continued to decrease in the solution phase while Fe concentrations increased in the 1 : 1, 2 : 1 and 3 : 1 Fe : Th systems. Using all the data from these three systems, the concentration of soluble Fe formed is directly dependent on the amount of Th removed from solution, (gradient of 1.02 ± 0.09; R^2 0.94); thus metal exchange was the predominant process taking place. However with higher Fe concentrations (4 : 1 and 5 : 1 Fe : Th systems), ongoing precipitation masked any exchange which may have been taking place.

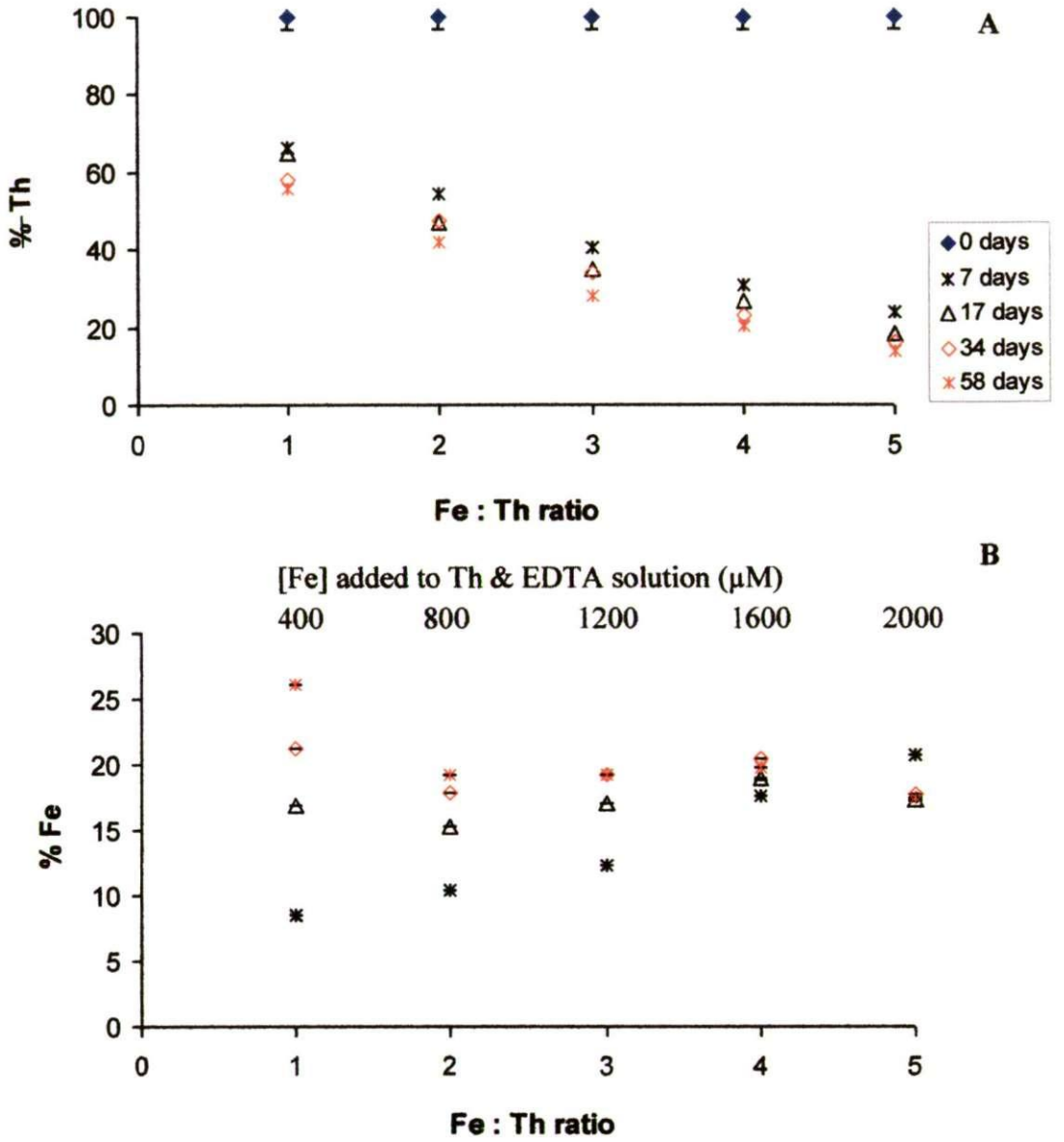

Figure 3.6 Determination of Th (A) and Fe (B) measured over time as a function of initial Fe : Th ratio in solutions where Th and EDTA were pre-equilibrated for 48 h prior to the addition of Fe. (Note different initial concentrations of Th and Fe). Error bars represent analytical uncertainty (1 σ, n = 3) (< 5 %)

Figure 3.7 shows the dynamic species distribution of ThEDTA and FeEDTA, using ESI-MS, in solutions with varied Fe concentrations as discussed above. Results are presented as a percentage of ThEDTA or FeEDTA species based on the ESI-MS signal for all metal-ligand species. The 16 - 49 day data points show the mean of three time points (16, 29 and 49 days), as analyses of variance showed there to be no significant difference in this data at a 95 % confidence interval ($p = 0.9671$). As observed for the 1 : 1 : 1 solutions, the mass spectra from the first analyses (< 2 h) were as would be expected from a solution containing only Th and EDTA (*e.g.* Chapter 2), with no evidence of FeEDTA species in solution. By day 16, the $[FeEDTA]^-$ complex had formed in solution, thus explaining the observed quantitative increase over time in solution phase Fe. The percent distribution of FeEDTA relative to ThEDTA species was greater in solutions with higher Fe concentrations and was greater than the signal for ThEDTA when Fe was in 5-fold molar excess over Th.

With respect to the quantitative data, the speciation analysis demonstrated that ThEDTA persists to a significant extent in the 5-fold excess Fe system. Therefore, some of the Fe in solution was not complexed by EDTA, which helps to explain the on-going precipitation of Fe in this system over longer time periods. There was good linearity in the percent species distribution with increasing Fe concentrations, and the trend agreed well with the equivalent quantitative decrease in Th concentration (Fig. 3.6 A). However, the species distribution for Th was higher than the quantitative data indicated, thus the Th complex appeared to electrospray 3 times more efficiently than the Fe complex.

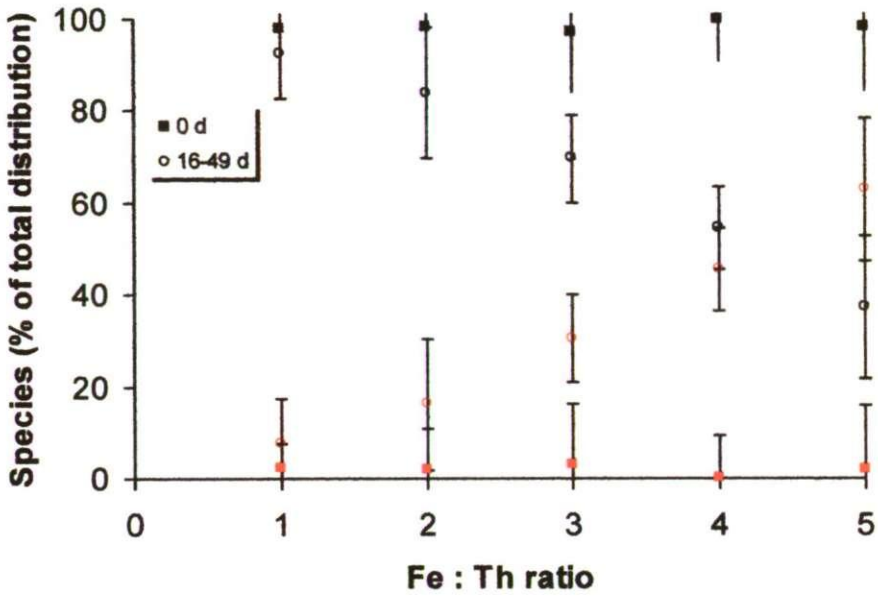

Figure 3.7 Speciation change over time as a percentage of total metal-ligand species ESI-MS counts for solutions of 420 ± 30 μM Th pre-equilibrated for 48 h with 420 μM EDTA before the addition of 420, 800, 1200, 1600 or 2000 μM ± 7% Fe. Solid squares are species counts % at t = 0 days (~ 0 – 2 h), open circles the mean count % of t = 16, 29 and 49 days, showing the formation of FeEDTA (grey) and loss of ThEDTA (black) species over time. Error bars represent one standard deviation around the mean of triplicate analyses at t = 0 d, and one standard deviation around the mean % species counts of three time points for 16-49 days.

3.4 Conclusions

The ability of co-contaminant organic complexes to enhance radionuclide solubility, and hence mobility, and the challenges of accurately modelling radionuclide-ligand speciation in simple aqueous systems was discussed in chapter 2. Speciation models assume that systems are in chemical equilibrium, and the resulting equilibrium speciation distributions underpin the reactive transport models used to predict contaminant radionuclide migration through the sub-surface environment. However, the

results discussed in this chapter show that the addition of one metal to a simple chemical system greatly increases the complexity of the observed chemical behaviour over time, with relatively slow kinetic processes precluding equilibrium speciation in the short term.

The environmental implications arising from the data suggest that in the presence of Fe corrosion products from steel waste canisters at repository sites, and mineral phase Fe in the far field, the persistence of EDTA-complexed tetravalent actinides will be dependent on the concentration of solid phase Fe species. The presence of amorphous Fe in the local environment will lead to exchange with complexed radionuclides, and subsequent immobilisation at the solid surface, as discussed above. However, the relatively slow kinetics of this exchange process also means that radionuclide migration will be dependent on the residence time of the contaminant plume through the host medium. At sites with fast groundwater flow rates through saturated formations (approaching 100 m y^{-1} (Mackay *et al.*, 1985)), groundwater residence times are a few days. Therefore transport will be greater than observed in less dynamic hydrogeological systems, where contaminant plume residence times are sufficient to allow equilibrium to be reached over the timescales of these experiments. It is clear from the data that in order to accurately model radionuclide transport, solution equilibrium assumptions cannot be relied upon and knowledge of kinetic reaction rates are required to define basic solution speciation before applying such theoretical data to predictive transport models.

Chapter 4

The impact of the organic co-contaminants EDTA, NTA and ISA on the sorption of Th(IV) and U(VI) to a natural sand matrix

4.1 Introduction

Understanding the behaviour of potential radioactive contamination in the environment is a pre-requisite for the safe management and disposal of nuclear wastes. Sorption processes are a fundamental factor determining the mobility of nuclear contaminants in the environment, where complex interactions between solid and solution phase radionuclides (see Figure 4.1) can be governed by local environmental chemical parameters such as ligand availability.

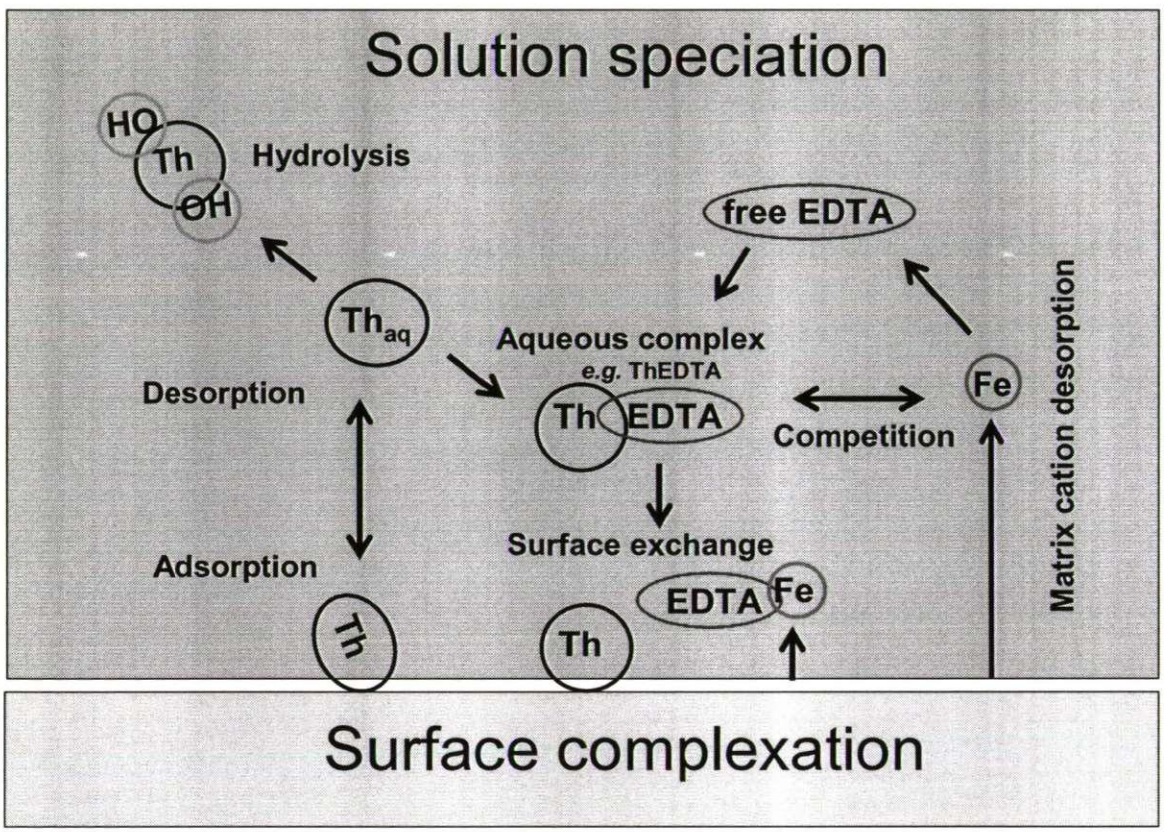

Figure 4.1 Potential solid-solution interactions affecting radionuclide sorption using thorium as an example

Contaminant sorption is commonly studied through the use of the sorption Kd, the coefficient that describes the equilibrium distribution of a contaminant between the solid and solution phases (equation 1).

$$Kd\ (L\ kg^{-1}) = \frac{[C]_s\ (moles\ kg^{-1})}{[C]_{aq}\ (moles\ L^{-1})} \quad \text{eq. 1}$$

Where $[C]_s$ is the concentration of the contaminant sorbed to the solid, and $[C]_{aq}$ is the concentration of the contaminant in solution (*e.g.* Fetter, 1999).

The Kd of a radionuclide in a given oxidation state is dependent on the binding capacity of the solid phase, which is determined by surface reactive functional groups. Sand assemblages have a lower sorption capacity than other permeable geological strata such as clays. Therefore a sand matrix allows examination of the impact of co-contaminant organics on radionuclide sorption (and hence transport) in a worst case scenario of contaminant release. This is significant with respect to nuclear waste repositories, for example a proposed repository at Sellafield lies on a Sherwood Sandstone aquifer (Bath *et al.*, 2003). Important binding phases for actinides on heterogeneous natural sand matrices include silanol groups, associated Fe-hydroxides and natural organic material.

The influence of EDTA and NTA on sorption of Th to an environmental solid phase has not previously been reported, while the influence of EDTA on uranyl sorption was investigated by Pathak and Choppin (2007b). When considering radionuclide mobility, competition from surface binding sites and inorganic ligands for radionuclides, and competition from matrix metals for ligands may limit the solubilising impact of the ligands investigated.

The aim of this study was to use batch sorption experiments to investigate the effect of the key organic co-contaminants EDTA, NTA and ISA on the sorption of Th(IV) and U(VI) to a natural dune sand, as a relatively simple, environmentally relevant solid matrix, with the following objectives: quantify the net effect of the co-contaminants on the sorption of Th(IV) over a concentration range from 5 to 500 μM (representing

varied contaminant scenarios), elucidate the nature of the solid/solution Th interactions from quantified changes in the solution phase trace cations and organic carbon concentrations, and compare the results with the sorption of 500 μM U(VI).

4.2 Experimental

4.2.1 Chemicals and reagents

Ultra pure water was obtained from a Milli-Q purification system (Millipore ≥ 18.2 MΩ cm^{-1}), U(VI) nitrate was obtained from Riedel-de-Haen (Hanover, Germany), Th(IV) nitrate from VWR International (Poole, U.K.). EDTA (disodium salt) was obtained from Fisher Scientific U.K. Ltd (Loughborough, U.K.), NTA (trisodium salt) and nitric acid (trace select, 69%) from Sigma Aldrich (Dorset, U.K.). $CaISA_2$ was prepared after the method of Whistler and BeMiller (1963). Dune sand was collected from a location close to the site of the U.K.'s low level nuclear waste storage facility near the village of Drigg (Cumbria).

4.2.2 Sand characterisation

Drigg dune sand was prepared by sieving to < 2 mm and dried overnight at ~ 110 °C. The sand was analysed to determine surface area using the standard BET method of nitrogen adsorption to surface area (Gemini 2375 V4.01 Instrument, Micromeritics (Norcross, U.S.A.). Particle size distribution (PSD) was obtained using low angle laser diffraction, (Mastersizer Long-bed X, Malvern Instruments Ltd, Malvern, U.K.). Total trace cations were determined in a HNO_3 digest using 1.5 g sand and 20 mL of concentrated acid (69 % v/v). Sand was weighed in pre-weighed perfluoroalkoxy vessels (Savillex, Minnetonka, USA), then freeze dried, re-weighed and refluxed in concentrated HNO_3 at a temperature of ≥ 140 °C for > 8 h. The supernatant was then

diluted to 2 % HNO_3 for cation determination by ICP-OES (Varian, Palo Alto, U.S.A.). EDTA extractable cations were determined by 0.16 M EDTA extraction (5 g sand : 10 mL solution shaken for 24 h). Samples were centrifuged (< 0.45 μm) (Sorvall Legend RT centrifuge, Thermo Scientific, Basingstoke, U.K.), and supernatent waters diluted in 2% HNO_3 for cation determination by ICP-OES (Al, Ca, Fe, K, Mg, Na, Ti and Zn). Total organic carbon associated with the sand matrix was determined by mixing 5 g sand : 10 mL ultra-pure water (Milli-Q) for 7 d on an orbital shaking table, with the supernatant waters acidified with 25 % v/v HCl and analysed to determine total organic carbon using a Shimadzu TOC analyser (Shimadzu, Milton Keynes, U.K.). The pH of sand-solution (ultra-pure water) mixtures were measured using a pH meter (Mettler-Delta 340, Mettler-Toledo, Leicester, U.K).

4.2.3 Sample preparation

Initial studies showed decreased aqueous radionuclide concentrations in the sand-water mixtures from 0 to 7 days. There was no significant difference in concentration from 7 to 10 days within a 95 % confidence level, indicating that 7 days was a suitable mixing period to reach an equilibrium solid-solution phase distribution. Solid : solution ratios from 1 to 20 g : 10 mL showed that 5 g : 10 mL was the optimum experimental set up to provide a measurable change in aqueous radionuclide concentrations and hence sorption. Sample preparation was carried out in an ISO 9001:2000 accredited laboratory. Working stock solutions of radionuclides and ligands were prepared by weighing the required mass of the relevant salt into a volumetric flask and making up to 50 mL with pure water. Working stock solutions of Th or UO_2^{2+} were prepared at a concentration of 4.3 (± 0.3) mM, and the ligands at 4.3 or 40 mM. Solutions of relevant mixtures of radionuclides and ligands were pre-mixed from these working stocks 24 h prior to addition to the solid phase at a solid : solution ratio of 5 g : 10 mL

in 50 mL centrifuge tubes, to ensure the formation of stable aqueous radionuclide-ligand complexes. Figure 4.2 shows a flow diagram of the experimental design. Sample tubes were wrapped in aluminium foil to prevent photo-catalytic reactions and shaken on an orbital shaking table (KS125 basic, JK IKA Labortechnik Staufen, Germany) for a 7 d mixing period at 200 rpm, sufficient to suspend solid material and ensure a well mixed system. After 7 days, samples were separated (< 0.45 μm) by centrifugation, and the supernatant was sub-sampled for elemental determination. Samples were acidified in 2 % HNO_3 for the determination of Th(IV) or U(VI) by ICP-MS (VG Plasmaquad PQ2+ Turbo, Winsford, Cheshire).

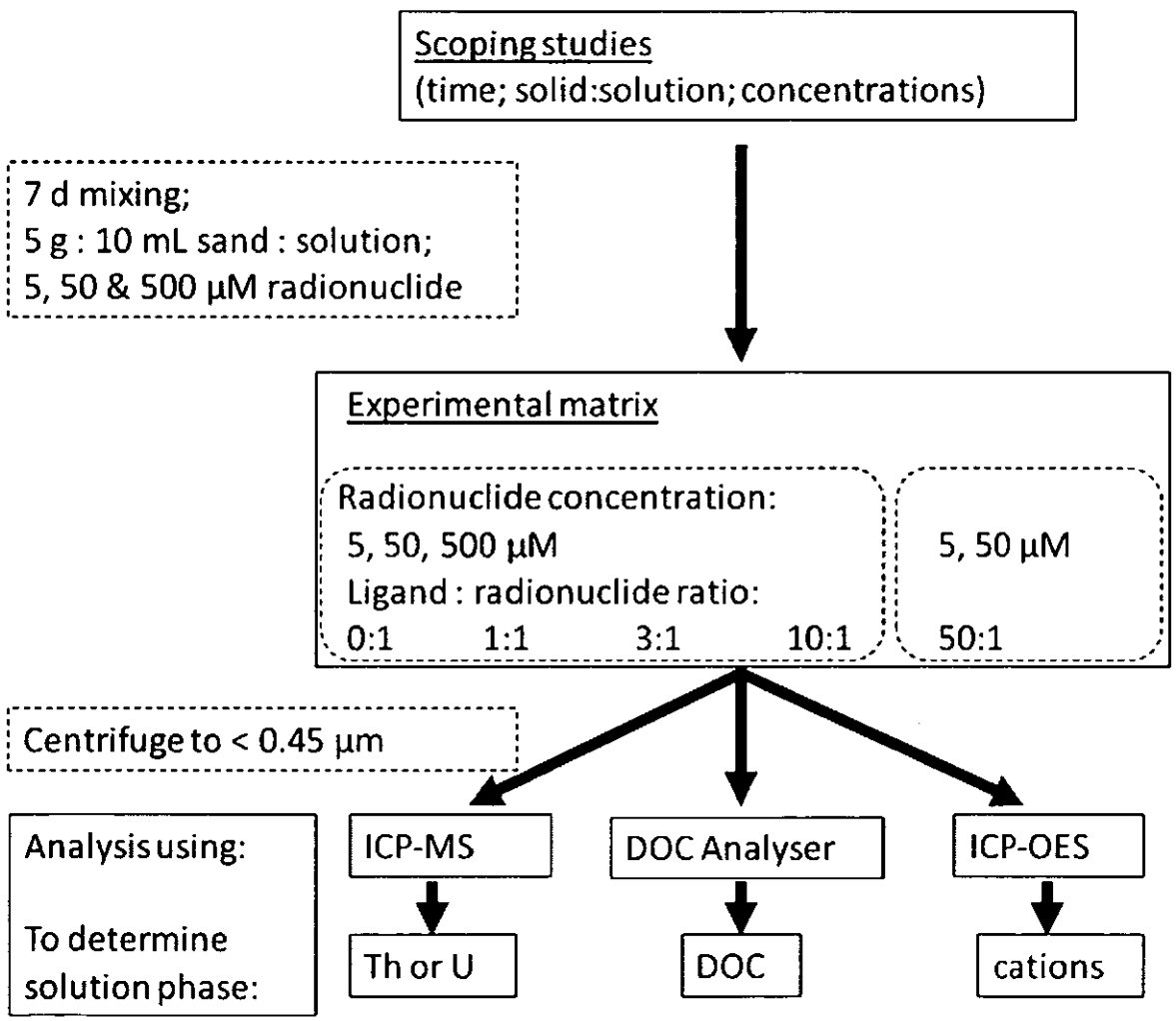

Figure 4.2 Flow diagram showing experimental design for batch sorption study

4.3 Results and discussion

4.3.1 Characterisation of Drigg dune sand

Particle size distribution analysis showed > 98 % of the sand particles were within the 63 – 2000 μm size fraction, corresponding to very fine to very coarse sand grain size, with 67% within the fine to medium sand grade (125 – 500 μm). The specific surface area of the sand, as determined by the N_2-BET method, was 0.1193 $m^2\ g^{-1}$ (E. Reinoso Maset, pers comm.). Selected cation concentrations liberated during HNO_3 digestion and EDTA extraction are shown in Table 4.1, data is only presented for cations significantly affected by EDTA or NTA in the experimental systems. 1800 ± 80 μM organic carbon desorbed from the sand into MQ water. In all systems studied, the solid phase buffered system pH to 7.2 ± 0.2 within 8 h.

Table 4.1 Cation concentrations liberated by digestion of 5 g of Drigg dune sand in concentrated HNO_3 and extraction by 0.16 M EDTA

		Concentration (μM)			
		Ca	Fe	Mn	Zn
HNO_3	mean	345000	253000	600	630
	% RSD (n = 3)	16	10	12	7
EDTA	mean	53000	840	350	20.0
	% RSD (n= 3)	8	2	2	10

4.3.2 The effect of organic co-contaminants on the sorption of 500 μM thorium to Drigg dune sand

The aqueous concentrations of Th, matrix cations and DOC were determined in systems containing different ratios of each ligand : Th, to identify processes controlling ligand solubilisation of Th. In the absence of complexing agent, the Kd of Th was 55.4 ± 8.2 (all confidence intervals are ± 1 s.d. for n = 3). Sorption of Th occurred at the expense of Ca, since an additional 981 ± 15 μM of Ca, and negligible concentrations of other cations, desorbed as 485 ± 73 μM of Th was removed from solution. Cation exchange

of Ca with Th has previously been reported with high Ca concentrations (Xu *et al.*, 2007), and assuming Th binds as Th^{4+}, this indicates direct, charge balanced exchange at the sand surface.

EDTA. The addition of EDTA lowered the Th Kd to 3.5 ± 0.8 in the 10 : 1 EDTA : Th system and there was a non-linear change in Kd with increasing EDTA (Figure 4.3 A). Therefore, although EDTA increased Th solubility, it did not solubilise Th completely even in 10-fold excess in a system with a relatively low Th Kd. Increased concentrations of EDTA also increased the solubility of matrix metals (Figure 4.3 B), indicating an element of competition in the system for the ligand. The dissolved organic carbon concentrations (a surrogate measurement for EDTA) determined in the supernatant waters at the end of the mixing period showed some interaction between EDTA and the solid phase, which decreased as a percentage of EDTA added, to 9 ± 1 % in the 10:1 system (Figure 4.3C).

The concentration ratios of Th, the sum of Fe, Mn and Zn, and Ca to EDTA determined in solution are shown in Table 4.2. The Ca data have been adjusted for the ion exchange process with Th reported above; the high Ca:EDTA ratios suggest that the Ca in solution was not all bound to EDTA. Overall, the ratios of metal solubilised to EDTA added decreased as the EDTA concentration increased and this was most marked for Th, which decreased to < 20 % of the 1 : 1 ratio in the 10 : 1 system. Typical surface complexation models consider two types of surface binding sites: weakly binding yet numerous sites, and stronger binding but less numerous sites (*e.g* Dzombak and Morel 1990). In this context, the trends suggest that EDTA was competing for metals, especially Th, from increasingly strong binding sites as the EDTA concentrations increased. However, given that increased EDTA also increased the number of binding

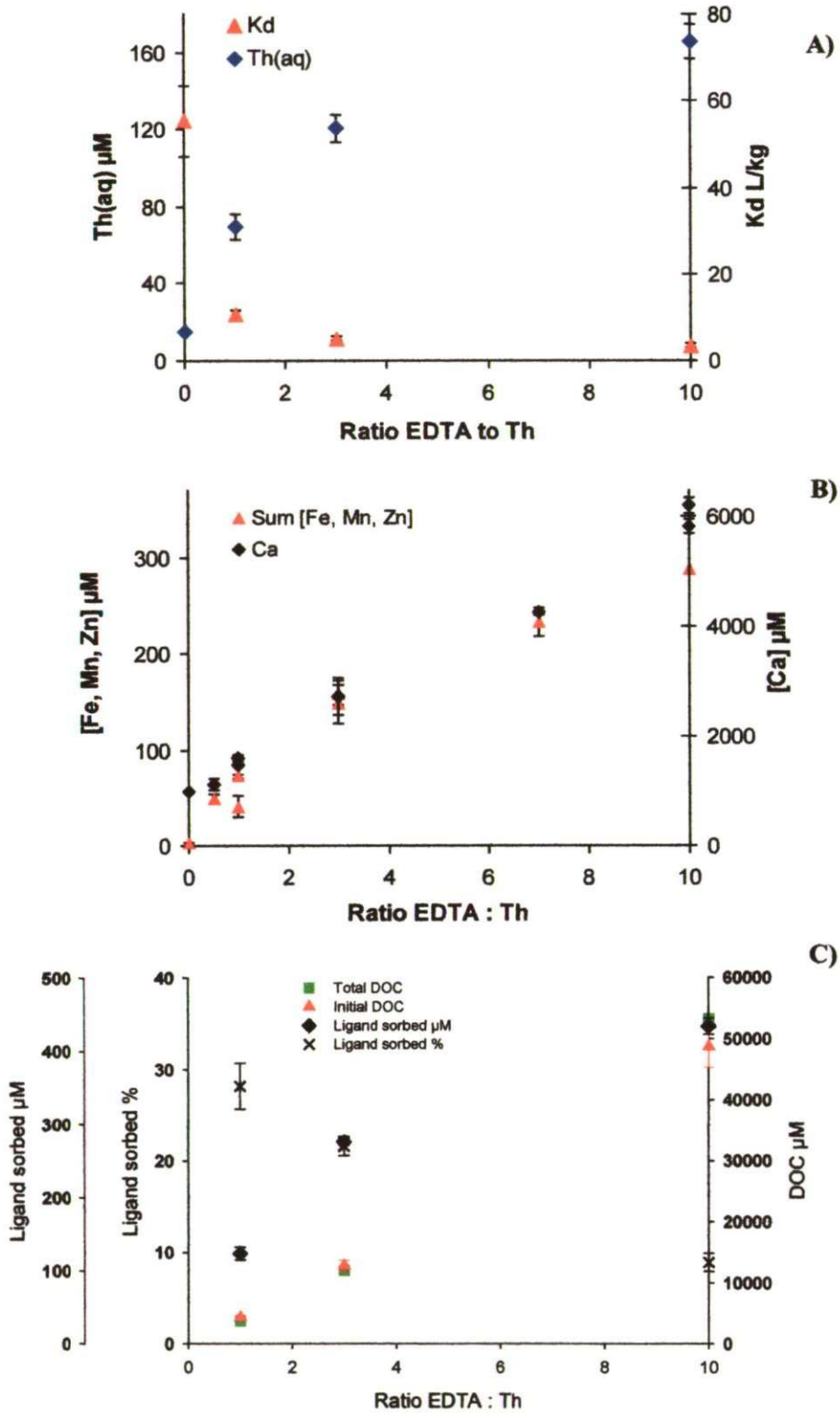

Figure 4.3 Influence of EDTA on Th sorption: A) Th sorption Kd and aqueous [Th], B) matrix cations desorbed (following blank subtraction), C) initial and total dissolved organic carbon, and [EDTA]sorbed

sites for Th sorption through the solubilisation of matrix metals, this effect could also be due to the number of sites available. EDTA complexes of Ca have the lowest stability constant of the metals investigated (Table 4.3). Therefore the high association of Ca with EDTA was due to an abundant supply of Ca (see table 4.1) and its weak association with surface binding sites. This was also shown in the solid phase digestions (Table 4.1), where despite little difference in solid phase Ca and Fe concentrations, 15.4 % of the total Ca was extractable by 0.16 M EDTA compared with 0.3 % of the total Fe.

Table 4.2 Solution phase metal : ligand ratios, using the metal and EDTA or NTA concentrations determined in solution. Ion exchange between Ca and Th was corrected for by subtracting twice the concentration of sorbed Th from the solution Ca concentration.

	Ratio of solution metals to ligand (μM/μM)		
EDTA (μM)	Th	∑Fe, Mn, Zn	Ca_{Tot}-Ca_{exch}
315	0.22	0.13	2.39
1003	0.12	0.15	1.96
4436	0.04	0.09	1.25
NTA (μM)			
300	0.08	0.03	0.73
1180	0.04	0.02	0.44
5210	0.04	0.02	0.55

NTA. In the presence of NTA (Figure 4.4 A) there was again a clear trend of decreased Th sorption with increased ligand concentration. The Kd of 2.1 ± 0.3 in the 10 : 1 NTA : Th system was significantly lower than the Th Kd in the equivalent EDTA system ($p = 0.017$). However the aqueous Th concentrations followed a linear trend with increased NTA concentration compared with the non-linear response with increased EDTA concentration. Therefore EDTA was more effective at solubilising Th at lower ligand concentrations and NTA was more effective at higher concentrations.

Table 4.3 Log K for metal-ligand complexes (EDTA and NTA from [25], 1996; ISA constants from [26]) and radionuclide-ligand complexes (EDTA from [27], NTA from [29])

Metal	EDTA	Log K	NTA	Log K	ISA	Log K
Ca^{2+}	CaL	12.4	CaL	7.6	CaL	4.3
	CaHL	16.0				
Fe^{3+}	FeL	27.7	FeL	17.9	n/a	
	FeHL	29.2	FeL_2	26.3		
	FeOHL	33.8				
	$Fe(OH)_2L$	37.7				
Mn^{2+}	MnL	15.6	MnL	8.7	MnL	7.3
	MnHL	19.1	MnL_2	11.6		
Zn^{2+}	ZnL	18.3	ZnL	12.0	ZnL	10.2
	ZnHL	21.7	ZnL_2	14.9		
	ZnOHL	19.9	ZnOHL	15.5		
Th^{4+}	ThL	26.2	ThL	16.6	n/a	
UO_2^{2+}	UO_2L	7.36	UO_2L	9.56	n/a	

NTA solubilised cations to a lesser extent than EDTA at all concentrations examined. Desorption of Ca was not significant until 5 mM NTA was present (10 : 1 system), whilst a linear relationship between the sum of Fe, Mn and Zn concentrations and NTA was observed (Figure 4.4 B). Since NTA was less effective than EDTA at competing with surface sites for matrix metals, fewer binding sites were created as the metals were taken into solution. The linear relationship between Th concentration and NTA added may therefore reflect this more limited competition from binding sites for Th. These data, together with those from the EDTA systems, suggest that it is the number, rather the type, of binding site that is important here, as NTA ultimately solubilised more Th than EDTA. The total concentration of metals (including Th) in solution was less than the NTA concentration in each system (Table 4.2). Table 4.3 shows that $FeNTA_2$, $MnNTA_2$ and $ZnNTA_2$ species formed, and solution speciation studies have shown that $[ThNTA_2]^{2-}$ forms at the pH (7.2) of these experiments (Cartwright *et al.*, 2007, Chapter 2 section 2.3.3); this is broadly consistent with the relatively low metal solubilisation.

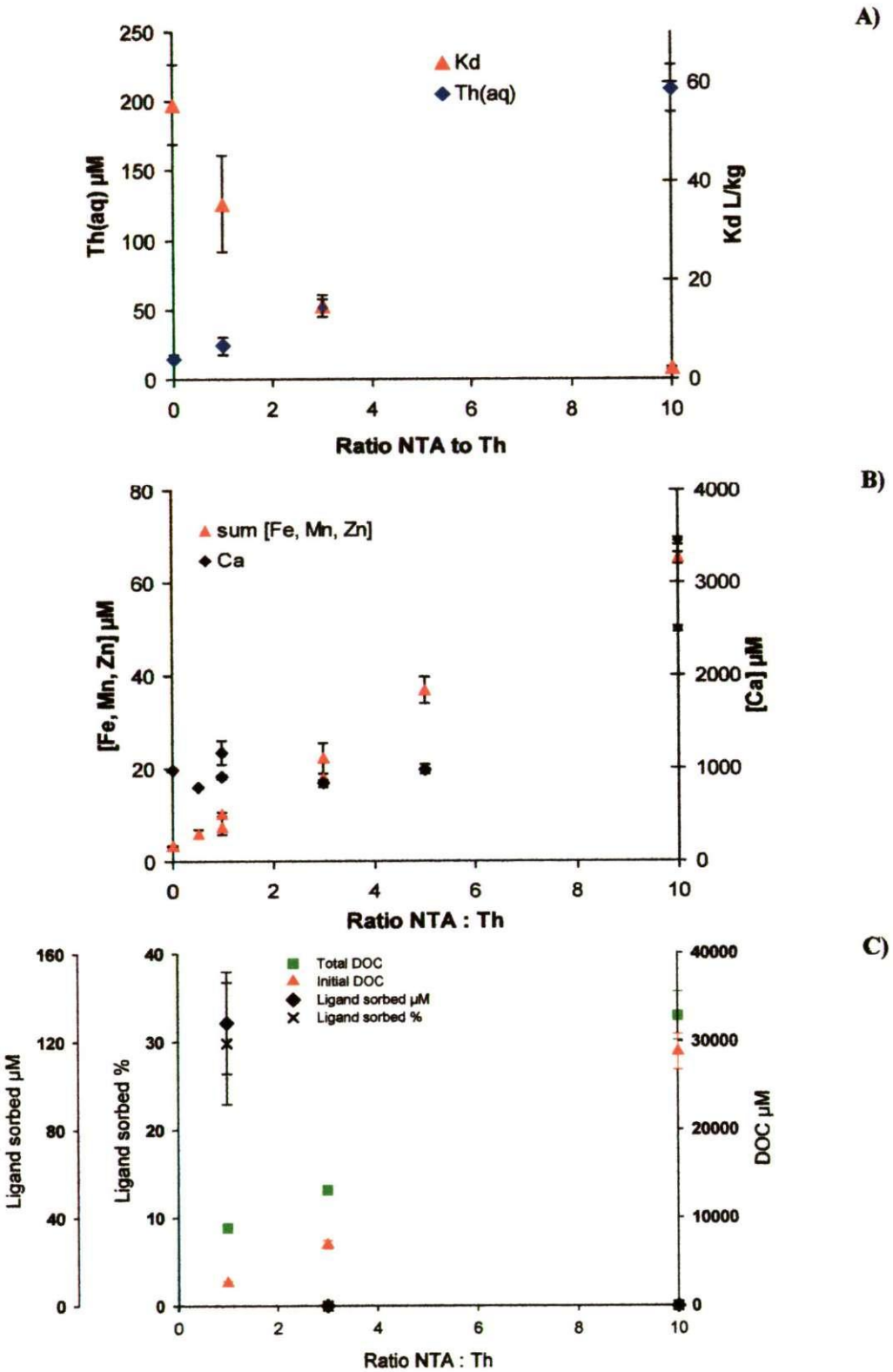

Figure 4.4 Influence of NTA on Th sorption: A) Th sorption Kd and aqueous [Th], B) matrix cations desorbed (following blank subtraction) and C) initial and total dissolved organic carbon, and [NTA]sorbed

ISA. ISA had no influence on the sorption of Th to the solid phase (Figure 4.5 A). The DOC data for these systems (Figure 4.5 B) suggest that there was a strong interaction between ISA and the solid surface when compared with EDTA and NTA. No desorption of Fe, Mn or Zn was observed with ISA, and the increase in aqueous Ca concentrations observed arose from the use of the $CaISA_2$ salt. Therefore these data are not presented.

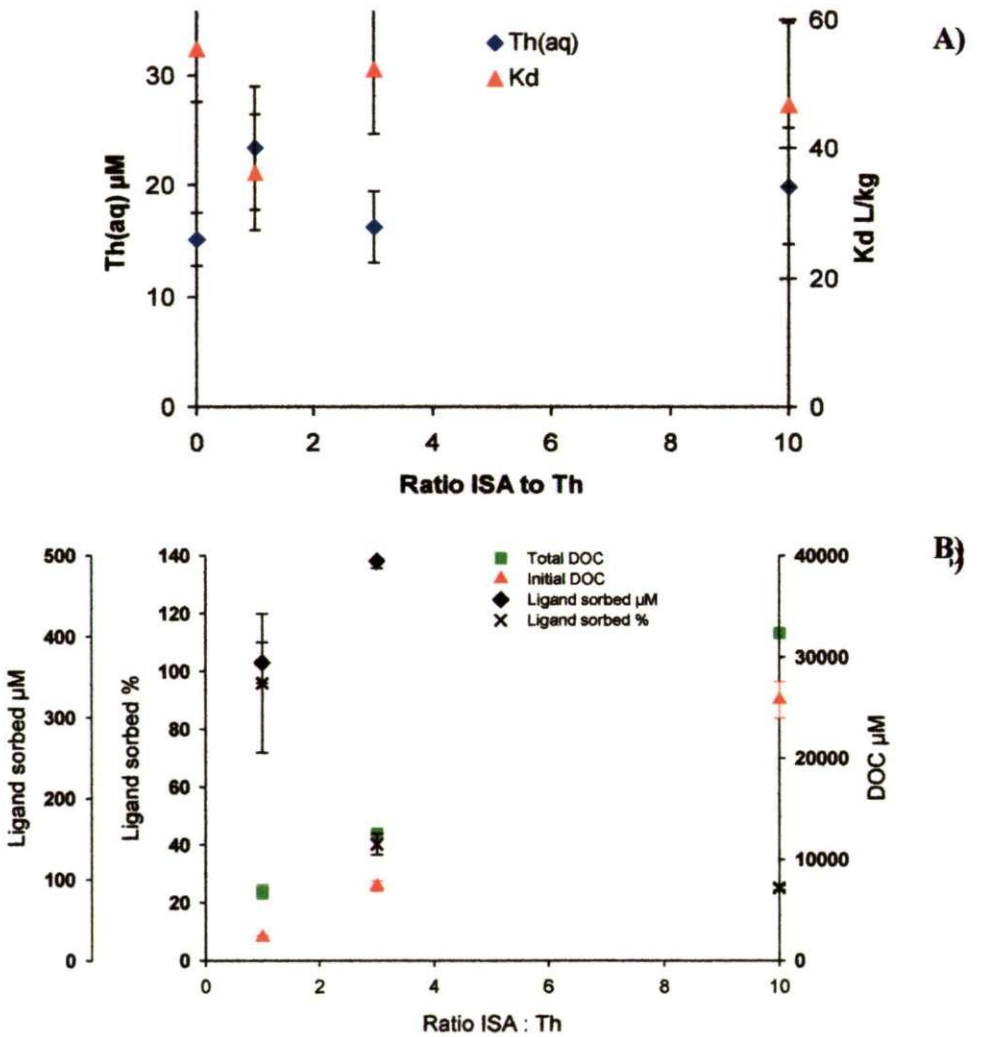

Figure 4.5 Influence of ISA on Th sorption: A) Th sorption Kd and aqueous [Th] and B) initial and total dissolved organic carbon, and [ISA] sorbed

4.3.3 The effect of organic co-contaminants on the sorption of 5 μM and 50 μM thorium to Drigg dune sand

The effect of EDTA and NTA was investigated at lower Th concentrations (5 and 50 μM) to assess the impact of the ligands on Th sorption relevant to a less contaminated site. ISA was not investigated, as the ligand showed no influence on Th sorption at the higher Th concentration.

5 μM Th. With 5 μM Th, the sorption Kd in the Th only system was 5.1 ± 1.4, an order of magnitude lower than observed in the 500 μM system. The relative binding site availability is higher with a lower Th concentration, which suggests that precipitation contributes to the solid phase association with 500 μM Th. Each ligand investigated increased the sorption of Th (Figure 4.6 A) relative to that observed in the Th only control system. However, other investigators in the author's laboratory (Reinoso Maset *et al.*, 2008) have shown that the difference observed at this Th concentration (5 μM) was a kinetic effect, driven by the relatively slow sorption kinetics of Th alone compared with Th in the presence of complexing agents. In the absence of complexing agents, 5 μM Th alone reached its equilibrium solid-solution distribution at some time between 7 and 23 d. This observation is consistent with the results from the EDTA systems reported here (Figure 4.6 A), in which the increasing concentrations of EDTA did not change the Th Kds outside of experimental uncertainty ($p = 0.084$) until EDTA was present in a 50-fold excess. NTA increased apparent Th sorption to a lesser extent than EDTA, which is consistent with the lower efficacy of NTA for extracting cations from the sand surface.

50 μM Th. With 50 μM Th, in the absence of either ligand, the sorption Kd of 50 μM Th was 5.0 ± 1.9, the same as the Kd in the 5 μM Th system. With EDTA and NTA

(Figure 4.6 B), the Kds were also comparable with the 5 μM Th systems. These data suggest that at low Th concentrations relative to the matrix metal concentrations and available binding sites in this system, the equilibrium Kd of Th is largely independent of the type or concentration of the complexing agent present. However, in a dynamic environmental system with groundwater flow, the differential kinetics displayed in the presence/absence of the complexing agents could impact on Th binding, with greater retention of Th in a system co-contaminated with complexing agents.

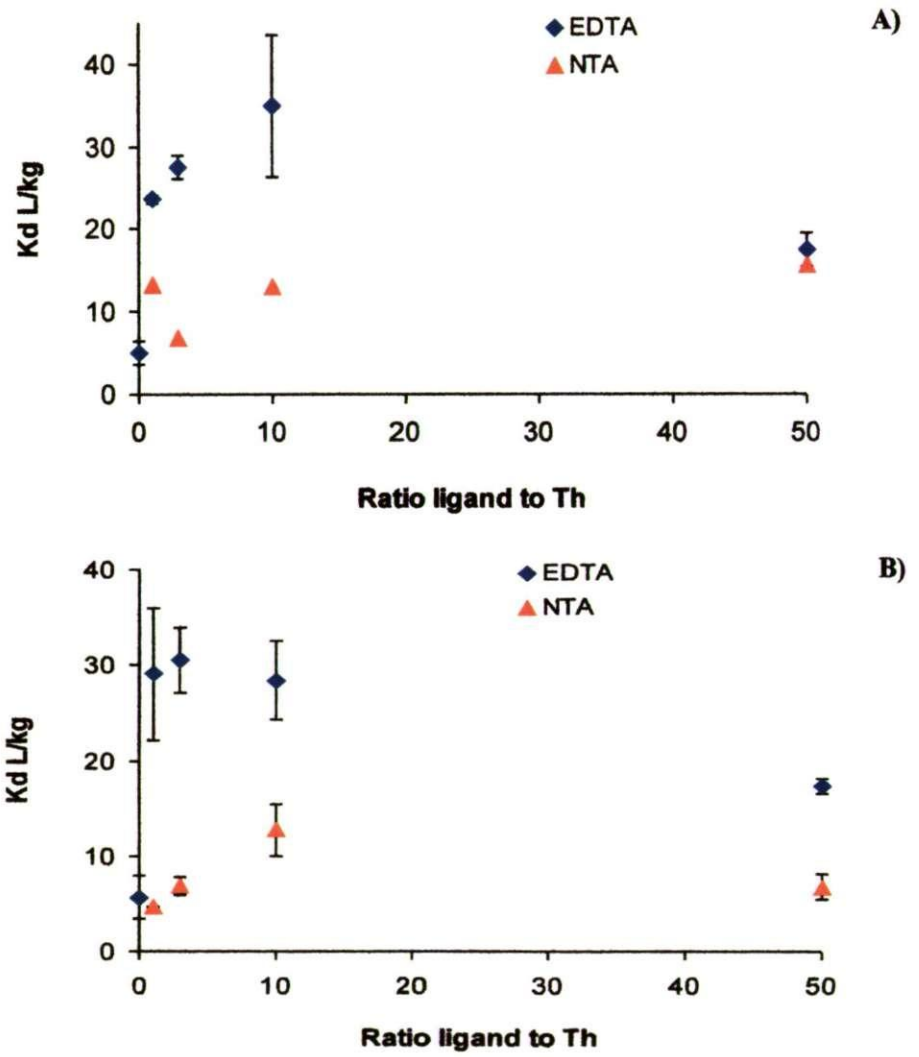

Figure 4.6 Influence of ligand availability on sorption of: A) 5 μM Th and B) 50 μM Th to Drigg dune sand

4.3.4 The effect of organic co-contaminants on the sorption of 500 μM UO_2^{2+} to Drigg dune sand

The difference in the effect of the EDTA and NTA on sorption of tetravalent and hexavalent actinides can be seen by comparing 500 μM Th with EDTA (Figure 4.3 A) and with NTA (Figure 4.4 A) with 500 μM UO_2^{2+} (Figure 4.7) For UO_2^{2+} sorption in the absence of the ligands, the Kd was lower than observed for Th (8.4 ± 0.8 compared with 55.4 ± 8.2 L kg^{-1}), consistent with the formation of stable solution phase uranyl carbonate species at pH 7.2 (*e.g.* Zhou and Gu, 2005; Prikryl *et al.*, 2001).

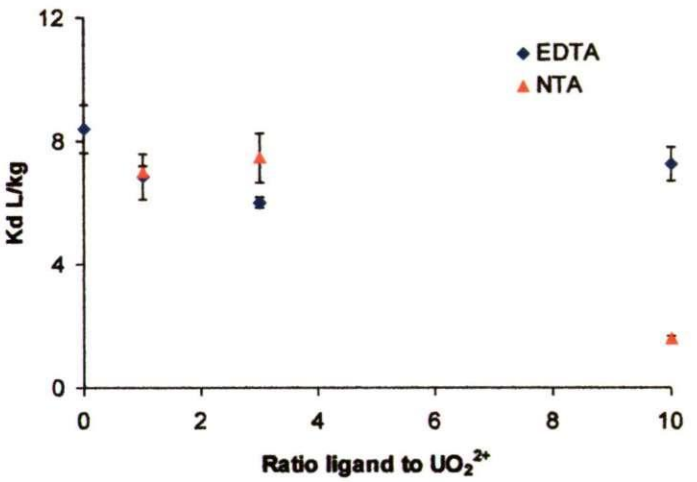

Figure 4.7 Influence of ligand availability on sorption of 500 μM UO_2^{2+} to Drigg dune sand

Desorbed Ca may also have played a role in stabilising aqueous UO_2^{2+}, as observed by Fox *et al.* (2006), who found that in systems of constant CO_2, increased Ca concentrations decreased sorption of UO_2^{2+} to quartz due to the formation of mixed aqueous uranyl-calcium-carbonate species. EDTA and NTA did not significantly affect sorption of UO_2^{2+}, except at high concentrations of NTA (5 mM) which enhanced UO_2^{2+} solubility (Kd of 1.6 ± 0.1 in the 10 : 1 NTA : Th system). Serne *et al.* (2002)

reported UO_2^{2+} sorption to natural solid phases to be independent of EDTA, whilst Pathak and Choppin (2007b) have shown that EDTA decreased UO_2^{2+} sorption to hydrous silica at low pH (2.9 – 3.9), but had no effect on UO_2^{2+} sorption at pH 4.7. This pH dependent behaviour is consistent with the results presented here at pH 7.2, where carbonate species dominate UO_2^{2+} speciation and effectively compete with the ligands for UO_2^{2+}.

4.4 Conclusions

The novel data presented in this study have highlighted the role played by EDTA and NTA in controlling sorption of Th to a natural solid phase, with implications for the mobility of tetravalent actinides in the terrestrial environment. Two contrasting effects of the ligands were observed depending on the radionuclide concentration.

At low thorium concentrations (5 and 50 μM) EDTA significantly enhanced Th sorption relative to the Th only control system over the timescales of the experiments (7 days). However, this appears to be due to the slow kinetics of Th sorption in the absence of complexing agents and, accordingly, the concentration of complexing agents did not affect the solution phase concentration of Th from a ratio of 1:1 to 1:10. NTA showed a similar influence, enhancing short term Th sorption, but to a lesser degree than EDTA. This effect appears to be driven by the relative concentrations of Th to matrix metals, with the matrix metals dominating association with the complexing agents.

With the highest thorium concentration (500 μM), the Kd for Th in the absence of complexing agents was higher than in the other systems, suggesting some degree of precipitation. Increased concentrations of EDTA or NTA significantly decreased sorption of Th to the solid phase. Thorium concentrations increased linearly with

increasing NTA concentration. EDTA had a greater effect than NTA at low ligand concentrations (500 to 2500 μM), but NTA was the more effective complexing agent for Th when at the highest ligand concentration (5 mM). These trends relate to the higher efficiency of EDTA for solubilising surface bound cations, thus, as the EDTA concentration increased; there was increased competition from exposed surface binding sites for Th. This shows that it is important to consider how matrix cations affect radionuclide-complexing agent interactions, both in terms of competition for the complexing agent and through the creation of surface binding sites.

At the pH of the experiments, ISA did not influence Th sorption, suggesting its presence in mixed wastes will not affect actinide mobility in the far field. The ligands showed no impact on UO_2^{2+} sorption to the sand at the experimental pH (7.2), and hence carbonate complexation dominated UO_2^{2+} speciation.

Extrapolating these results to the environmental migration of radionuclide contaminants, it can be seen that the co-contaminants EDTA and NTA will significantly influence the mobility of tetravalent actinides. At low radionuclide concentrations, their presence will result in lower radionuclide mobility in dynamic groundwater regimes by increasing the rate of radionuclide sorption. With high radionuclide contaminant loading, increased concentrations of these ligands will very significantly enhance radionuclide mobility. For hexavalent species such as UO_2^{2+}, inorganic ligands present in groundwaters may exert a greater influence on radionuclide mobility than co-contaminant organic species.

Chapter 5

Effect of complexation by EDTA and NTA on Th migration through a natural sand matrix

5.1 Introduction

Understanding migration pathways of potential contaminant radionuclides through terrestrial matrices is vital for the effective management of nuclear wastes, in planning potential disposal sites and remediation of accidental contamination (*e.g.* Dozol *et al.*, 1993).

The role of organic chelates in enhancing radionuclide transport has therefore been the focus of studies using laboratory based column experiments to simulate groundwater flow through terrestrial matrices. Complexation by EDTA has been shown to enhance mobility of ^{60}Co (Mayes *et al.*, 2000; Brooks *et al.*, 1996) and uranium (Read *et al.*, 1998), whilst the complexation of ^{90}Sr by EDTA resulted in enhanced retention of the radionuclide (Pace *et al.*, 2007). Experimental and field data can be modelled using reactive transport computer codes such as CRAFLUSH (Jardine *et* al., 2002), CHEMTARD (Sims *et al.*, 1996) and k1D (Schüßler *et al.*, 2001) to determine hydrogeochemical factors such as sorption kinetics that influence radionuclide transport, in order to extrapolate behaviour from controlled laboratory studies to predict migration at specific contaminant sites. The k1D reactive transport code used in this study has been successfully applied to model the humic acid borne transport of Am(III) (Schüßler *et al.*, 2001) and the migration of UO_2^{2+} released from depleted uranium corrosion products (Handley-Sidhu *et al.*, 2009).

The aim of this study was to determine the effect of Th complexation by EDTA and NTA on the migration of Th through a natural sand matrix. This is a solid phase relevant to the site of a U.K. low level waste repository near Drigg, Cumbria. Specific objectives to achieve this aim were to: 1) determine the effect of Th complexation by EDTA and NTA on the migration of Th in a simulated groundwater through a natural

sand matrix using laboratory column experiments; 2) simulate the experimental data using the k1D reactive transport computer code; and 3) discuss the applicability of the findings to the wider issues of environmental nuclear waste contamination.

5.2 Experimental

5.2.1 Chemicals and reagents

Ultra pure water was obtained from a Milli-Q purification system (Millipore $\geq$ 18.2 MΩ cm^{-1}). Th(IV) nitrate from VWR International (Poole, U.K.). EDTA (disodium salt) and salts of Ca, Mg, Na, K, Cl, SO_4^{2-}, NO_3^-, HCO_3^- and KBr were obtained from Fisher Scientific U.K. Ltd (Loughborough, U.K.), NTA (trisodium salt) and nitric acid (trace select, 69%) from Sigma Aldrich (Dorset, U.K.). Dune sand was collected from a location close to the site of the U.K.'s low level nuclear waste repository near the village of Drigg (Cumbria).

5.2.2 Column experiments

A synthetic groundwater was prepared (Table 5.1). The ionic concentrations were within the range of literature values reported for shallow groundwater at Sellafield (Bath *et al.*, 2003). A conservative bromide tracer solution (250 mM) was prepared from the potassium salt. Solutions of Th, EDTA and NTA were prepared from relevant salts in the simulated groundwater matrix and diluents were mixed to the required concentrations (4 $\pm$ 0.3 mM Th, EDTA and NTA; and 40 $\pm$ 3 mM EDTA and NTA). Th was pre-equilibrated alone, or with EDTA and NTA in 1 : 1 and 1 : 10 molar ratios in the simulated groundwater for 24 h prior to sample injection. In order to be able to determine Th in the column eluent, the Th concentration (~ 4 mM) was an order of magnitude greater than used in previous chapters. Batch sorption experiments were

carried out as described in section 4.3 using the simulated groundwater in place of the pure water system, with 0.4 and 4 mM Th and the ratios of ligand : Th used in the column experiments, to investigate the influence of the higher concentration of Th, and pre-equilibration in the synthetic groundwater, on Th sorption.

Table 5.1 Ionic concentrations for simulated groundwater preparation. Ground water (GW) components Dr. J. Small, Nexia Solutions, pers. comm., July 2008

Ion	Prepared (M)	GW components (M)
Ca^{2+}	0.0007	0.0009
Mg^{2+}	0.0002	0.0002
Na^{+}	0.0007	0.0007
K^{+}	0.0001	0.0001
Cl^{-}	0.0008	0.0008
SO_4^{2-}	0.0002	0.0002
NO_3^{-}	0.0006	0.0005
HCO_3^{-}	0.0008	0.0011

Drigg dune sand was sieved mechanically to obtain the 63 μm – 2 mm sand fraction, which was then equilibrated with the simulated groundwater for 48 h before use. Figure 5.1 illustrates the experimental set-up used in the column transport experiments. The polyetheretherketone (PEEK) self pack column (50 mm × 10 mm; Applied Biosciences, Foster City, USA) with 0.2 μm in-line filter frit, was packed by adding a small amount of sand and tapping gently to allow it to settle, and the process was repeated until the column was full (6.2 ± 0.2 g). This eliminated air pockets and removed excess water. The column was then attached to the peristaltic pumping system (Multiflow Lambda,

Zurich, Switzerland) with 2 mm PVC tubing (Nalgene, Hereford, UK); with flow upwards through the column to ensure column saturation.

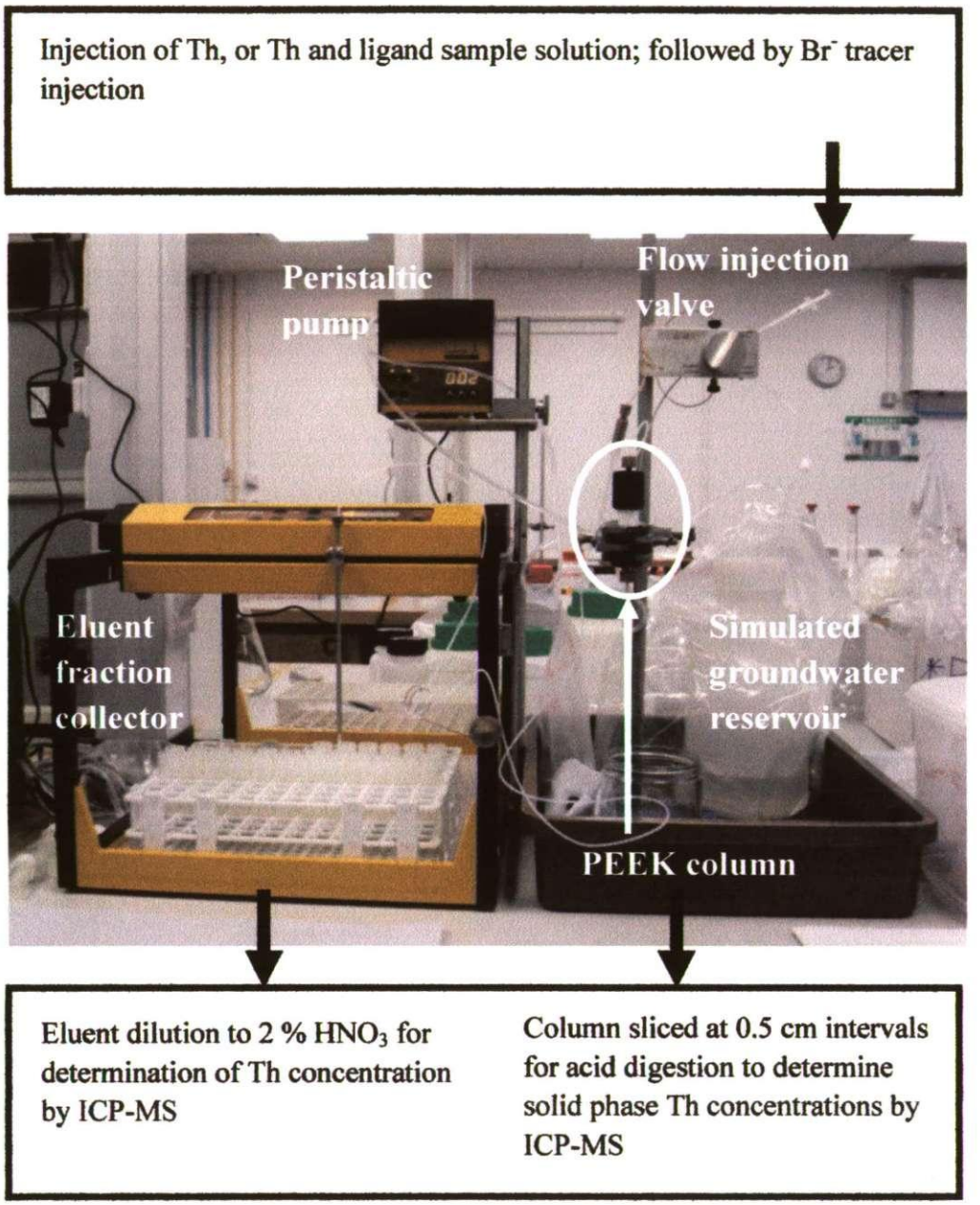

Figure 5.1 Column transport experimental set-up

Two experimental flow rates were used, 0.29 mL h^{-1} and 0.97 mL h^{-1}, corresponding to flow velocities of 32.4 and 108 m y^{-1} through the sand. The higher flow rate was used for all samples, and the lower flow rate was also used for the 1 : 1 Th : EDTA solution.

These velocities are consistent with the lower and higher end groundwater velocities reported under natural hydrogeological conditions for sand aquifers (Mackay *et al.*, 1985). Th or Th-ligand sample solutions were introduced by manual injection using a Rheodyne injection valve (Bergstrasse, Germany) with a 50 μL sample loop. Fifty μL of the Br solution was injected at the conclusion of each sample run in order to define the physical parameters of the column. The column, tubing and injection syringe were acid washed (10 % HCl vol/vol), thoroughly rinsed with ultra-pure H_2O, and conditioned with simulated groundwater solution between each column run. Three aliquots of each sample were taken for total Th and Br analysis immediately after injection.

Column outflow was collected at regular intervals using the automated sample fraction collector, with collection timings determined by the relevant sorption Kd values obtained for each analyte mixture from previous batch sorption experiments (Chapter 4) and column hydrological properties. Pre-weighed vessels were placed at regular intervals on the collection grid and were re-weighed after sample collection to monitor flow rates. Uncertainty associated with the flow rate in each experiment was < 5 %. Outflow sub-samples were diluted to 2% HNO_3 for later determination of Th; or frozen and later diluted to 2 % HNO_3 for determination of Br^-; using ICP-MS. The measured pH of the synthetic groundwater solution was 7.2 ± 0.2, and in each case the column outflow pH was 7.3 ± 0.2 (Mettler-Delta 340, Mettler-Toledo, Leicester, U.K).

After each sample run, the column was opened and the packed sand pushed out using a polypropylene rod. The sand was sliced at approximately 0.5 ± 0.1 cm intervals and collected in pre-weighed perfluoroalkoxy vessels (Savillex, Minnetonka, USA). Samples were then freeze dried, re-weighed and refluxed in concentrated HNO_3 at a

temperature of ≥ 140 °C for > 8 h. The supernatant was then diluted to 2 % HNO_3 for Th determination using ICP-MS.

5.2.3. Modelling

Model simulations were performed using the k1D reactive-transport code at the Centre for Radiochemistry Research at the University of Manchester School of Chemistry under the supervision of Dr. Nick Bryan. Input parameters required by the model are given in Table 5.2. A value of zero for diffusion was defined, as diffusive processes were assumed to be negligible relative to advective/dispersive transport.

Table 5.2 Model input parameters of the k1D transport code

Parameter	Value (unit)	Derivation of parameter
Length	0.05 (m)	Known
Cross sectional area	7.85×10^{-5} (m^2)	Known
Sub-divisions	30	Chosen such that the result of the calculation is insensitive to its value
Porosity	varied, Table 5.4 (void vol/vol)	Defined by breakthrough time of Br peak
Injection rate	varied ($m\ s^{-1}$)	Calculated from flow rate, column dimensions and porosity
Diffusion	n/a	Assumed insignificant compared to effects of advection and dispersion.
Dispersivity	varied, Table 5.4 (m)	Defined by width of Br peak
Simulation end time	varied (s)	Known
Species concentration	varied (M)	Experimentally defined
Chemical reaction, see text		
Th + EDTA ↔ ThEDTA	1.382×10^{7} ($L\ mol^{-1}$)	Smith and Martell (1989)*

In this study, the aqueous stability constant reported by Smith and Martell (1989) for the ThEDTA complex (Table 2.7) was used in all model simulations. Speciation modelling using PHREEQcI pH showed that Th and EDTA would be present as a range of species at the experimental rather than simply Th^{4+} or $EDTA^{4-}$. Therefore the stability constant was adjusted to take account of the background speciation, and gave a conditional constant for the species (log K = 7.14).

The K1D code allows chemical reactions to be defined, and the values for these reactions were obtainted through an iterative process which identified the best fit to the elution profiles. A dimensionless sorption Kd that defined the strength of Th binding to surface sites was used in all simulations. An additional stronger Th binding site was included to achieve a dual binding site model, and rate constants were added in the kinetic model. Model output data were exported to Microsoft Excel and compared with the experimental results.

5.3 Results and discussion

5.3.1 Batch sorption experiments for thorium in synthetic groundwater

The Kd values in systems of comparable Th concentrations (0.4 mM; Table 5.3) were approximately one order of magnitude greater in synthetic groundwater than in the pure water systems, although the same overall trend of increased ligand concentrations enhancing Th solubility was observed. With the higher concentration of thorium that was also used in the column experiments (4 mM), the Th sorption Kd was a factor of two greater again when no ligand was present, however pre-equilibration with the ligands enhanced Th solubility to a greater extent than at the lower Th concentration.

Table 5.3 Batch sorption studies of Th with EDTA or NTA in simulated groundwater (10 mL/5 g)

Analytes	Ratio	0.4 mM Th Kd (L kg^{-1})	RSD % (n = 3)	4 mM Th Kd (L kg^{-1})	RSD % (n = 3)
Th		670	16	1400	11
Th & EDTA	1 : 1	200	19	67	4
	1 : 10	91	3	35	6
Th & NTA	1 : 10	65	5	42	10

5.3.2 Column characterisation

The physical and hydrodynamic properties of the column are given in Tables 5.2 and 5.4. The porosity and dispersion associated with each column were determined by fitting the conservative Br^- tracer model profile to that of the experimental Br^- data, with the Br^- elution peak breakthrough volume and peak width (Figure 5.2) giving the porosity and dispersion, respectively. It should be noted that in the case of the higher flow rate 1 : 1 Th : EDTA and 1 : 10 Th : NTA columns the data collection frequency resulted in poor peak resolution which increased the uncertainty of the modelled dispersivity. There was also some variation in the peak elution volumes, and hence column porosity, indicating either heterogeneity of the sand or minor inconsistencies in packing the columns.

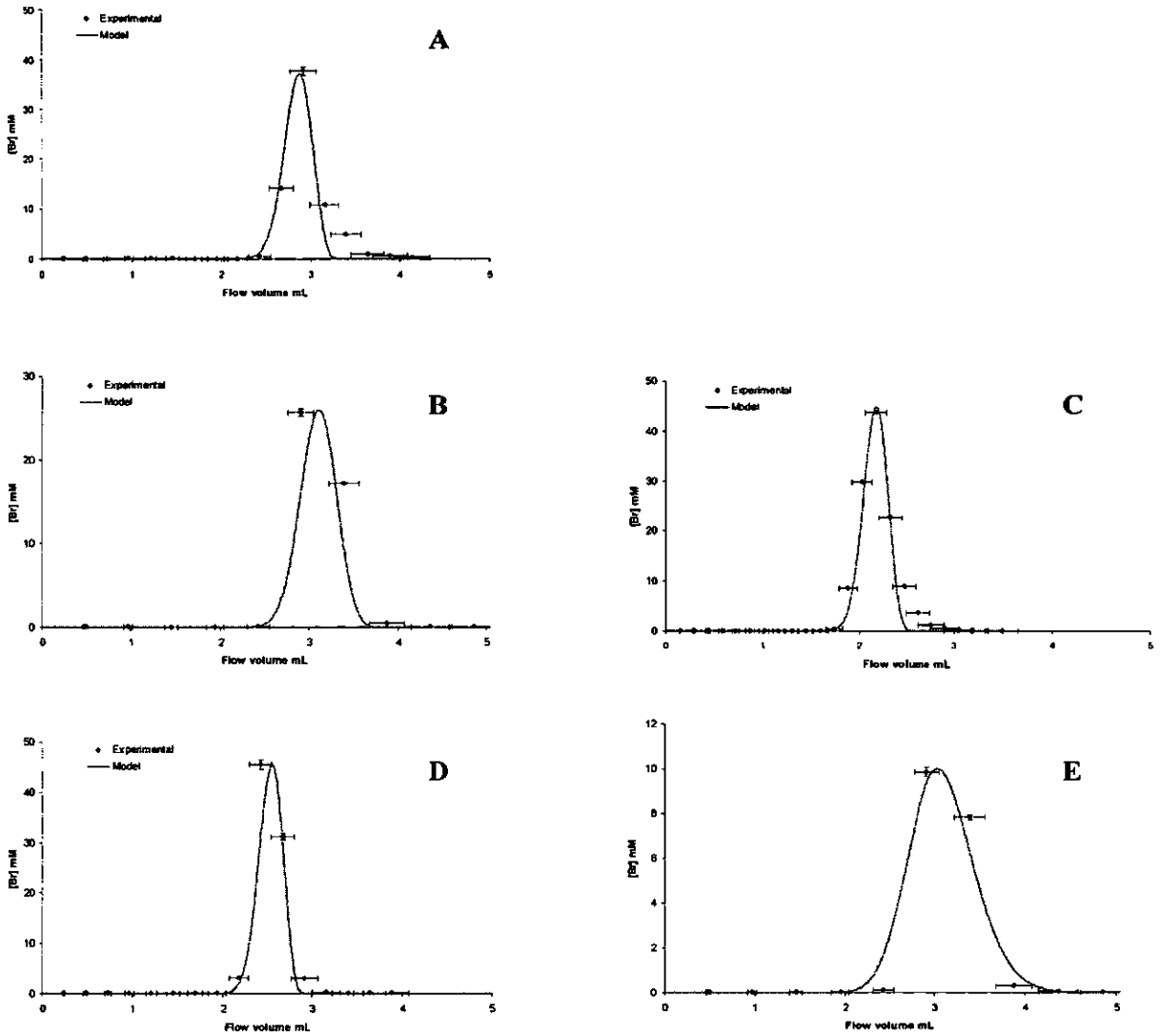

Figure 5.2 Experimental and modelled Br^- tracer elution data for columns of: A) Th; B) 1 : 1 Th : EDTA; C) 1 : 1 Th : EDTA (low flow rate); D) 1 :10 Th :EDTA and E) 1 : 10 Th : NTA

Table 5.4 Th transport experimental parameters

Experimental System	Pump flow[+] rate mL h^{-1}	Br^- peak[+] mL	Dispersivity m	Porosity[+]	Th breakthrough[+] mL	maximum [Th] M
Th only	0.97	2.91	0.00060	0.70	n/a	n/a
Th & EDTA $1:1_a$	0.97	2.91	0.00010	0.78	4.24	8.28×10^{-6} ($\pm 1 \times 10^{-7}$)
Th & EDTA $1:1_b$	0.29	2.18	0.00007	0.54	4.35	9.44×10^{-6} ($\pm 9 \times 10^{-8}$)
Th & EDTA 1:10	0.97	2.43	0.00005	0.63	3.15	3.87×10^{-5} ($\pm 4 \times 10^{-7}$)
Th & NTA 1:10	0.97	2.91	0.00035	0.78	2.85	4.86×10^{-5} ($\pm 2 \times 10^{-6}$)

	Th injected M ($\pm 3 \times 10^{-4}$)	Th injected moles ($\pm 2 \times 10^{-8}$)	Th eluted moles ($\pm 4 \times 10^{-9}$)	Th eluted %	Solid phase Th moles ($\pm 2 \times 10^{-8}$)	Th recovery %
Th only	3.85×10^{-3}	1.93×10^{-7}	4.35×10^{-10}	0	1.97×10^{-7}	102
Th & EDTA $1:1_a$	4.98×10^{-3}	2.49×10^{-7}	4.62×10^{-8}	19	2.03×10^{-7}	100
Th & EDTA $1:1_b$	3.75×10^{-3}	1.88×10^{-7}	3.75×10^{-8}	20	2.32×10^{-7}	144
Th & EDTA 1:10	4.98×10^{-3}	2.49×10^{-7}	8.66×10^{-8}	35	1.61×10^{-7}	99
Th & NTA 1:10	4.23×10^{-3}	1.88×10^{-7}	2.33×10^{-8}	11	n/a	n/a

[+] Error associated with flow rates ≤ 5 %

5.3.3 The effect of EDTA and NTA on Th migration through sand packed columns

This section describes the experimental results of the column migration experiments. Th elution data from these experiments are presented in Figure 5.3, and determination of Th associated with the solid phase by acid digestion after completion of each column run in Figure 5.3.

Elution profiles In the 4 mM Th only column, very low concentrations of Th were detected in the eluent throughout the 4 day experiment and there was no clear Th elution peak (Figure 5.3A). This is consistent with the batch sorption Kds for Th systems (Table 5.3) which showed a high degree of sorption to the solid phase.

Pre-equilibration with equi-molar EDTA had a significant effect on Th migration, as expected from the batch Kd values, and enhanced Th transport. Two flow rates (0.97 and 0.29 mL h^{-1}) were used for this ratio and similar Th elution profiles were seen at both flow rates, with breakthrough flow volumes of 4.4 ± 0.2 mL and 4.2 ± 0.2 mL, respectively (Figures 5.3 B and 5.3 C). Both peaks were retarded relative to the Br^- tracer, by 146 ± 10 and 200 ± 14 % respectively for the high and low flow rates. The maximum Th concentrations in the eluent were 8.3 μM and 9.5 μM, respectively. Overall 19 and 20 % of the total Th injected was eluted from these columns over the experimental period (Table 5.3). The elution profiles were characterised by a high peak concentration and an extended tail of lower concentrations. Such tailing is normally indicative of a kinetic process slowly releasing the sorbed species (*e.g.* Handley-Sidhu *et al.*, 2009). However, contrary to this, the similarity of the two profiles suggests that desorption kinetics were rapid with respect to the two flow rates, i.e. desorption was at equilibrium in the fast flow system.

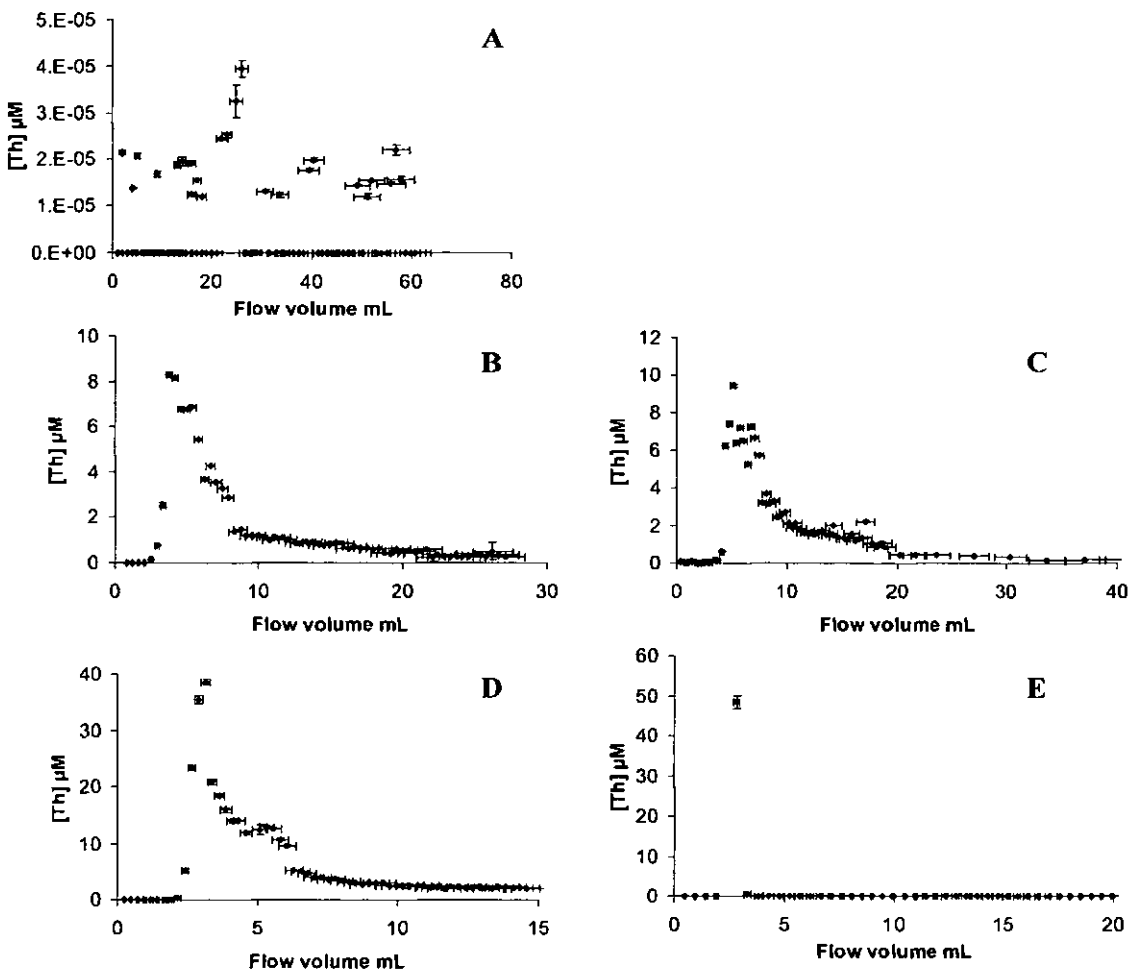

Figure 5.3 Experimental Th elution data for columns of: A) Th; B) 1 : 1 Th : EDTA; C) 1 : 1 Th : EDTA (low flow rate); D) 1 : 10 Th : EDTA and E) 1 : 10 Th : NTA

Pre-equilibration with a 10-fold excess of EDTA resulted in a similar Th elution profile (Figure 5.3D) to those observed in the equimolar Th : EDTA columns, with a high Th concentration peak followed by a tail. The peak exhibited a similar retardation to that observed in the 1 : 1 column at the same flow rate, breaking through at 130 ± 9 % of the tracer breakthrough flow volume. The maximum Th concentration in the eluent was an order of magnitude greater (39 µM) than in the equimolar Th - EDTA columns. Additionally, a shoulder was evident on the peak at 5.34 mL, corresponding to the main peak breakthrough volume in the 1 : 1 systems. In total, 35 % of the Th injected into the

column was eluted, compared with 19 % in the comparable equimolar Th - EDTA column. From the speciation data presented in chapter 2, adducts or mixed ligand complexes of the ThEDTA and $ThEDTA_2^{4-}$ complexes would be expected to dominate the speciation in the equimolar and 1 : 10 systems, respectively, with the negative charge on the $ThEDTA_2^{4-}$ complex consistent with it being more mobile.

The elution profile for 1: 10 Th : NTA (Figure 5.3 E) contrasted with the Th - EDTA profiles, with only one fraction of high Th concentration eluted (4.9×10^{-5} M) at a flow volume of 2.4 – 2.9 mL, *i.e.* unretarded relative to the Br^- tracer. The peak was not well resolved because of the collection frequency, but it was clearly narrow compared with the EDTA data, with no significant tailing. This suggests that a simple mechanism governed the migration of Th-NTA, which was likely to be present as the $ThNTA_2^{2-}$ species (see Chapter 2). However, as only 10 % of the Th eluted from the column, 90 % of the Th associated strongly with the sand and was retained on the column, as seen when Th was added on its own. Therefore, solid phase binding sites compete quite effectively with NTA for Th, and cause dissociation of the complex, as was observed for the migration of the SrEDTA complex by Pace *et al.* (2007).

Solid Phase Digestion: Acid digestion of the sand following the column experiments confirmed that Th had a strong interaction with the sand, with total retention of the Th on the column in the Th only system (100 ± 10 % recovery (Table 5.4)). However, 42 % migrated beyond the first section of the column (0 - 0.5 cm; Figure 5.4), showing some mobility. Consistent with the elution data, pre-equilibration with EDTA resulted in significantly lower Th concentrations remaining on the column. However, it is interesting to note that the solid phase concentration gradient was also reduced, and this was particularly marked for the excess EDTA column. This, along with the on-going

elution of Th, suggests that the Th - EDTA species were largely stable in this system. Unfortunately solid phase data were not available for the Th - NTA column.

The column data provide an insight into the effect of EDTA and NTA on the migration of Th and underline the importance of EDTA as a ligand. The data for NTA were far more limited, but indicated a mobile complex that dissociates as it is transported through the column, due to competition from solid phase binding sites.

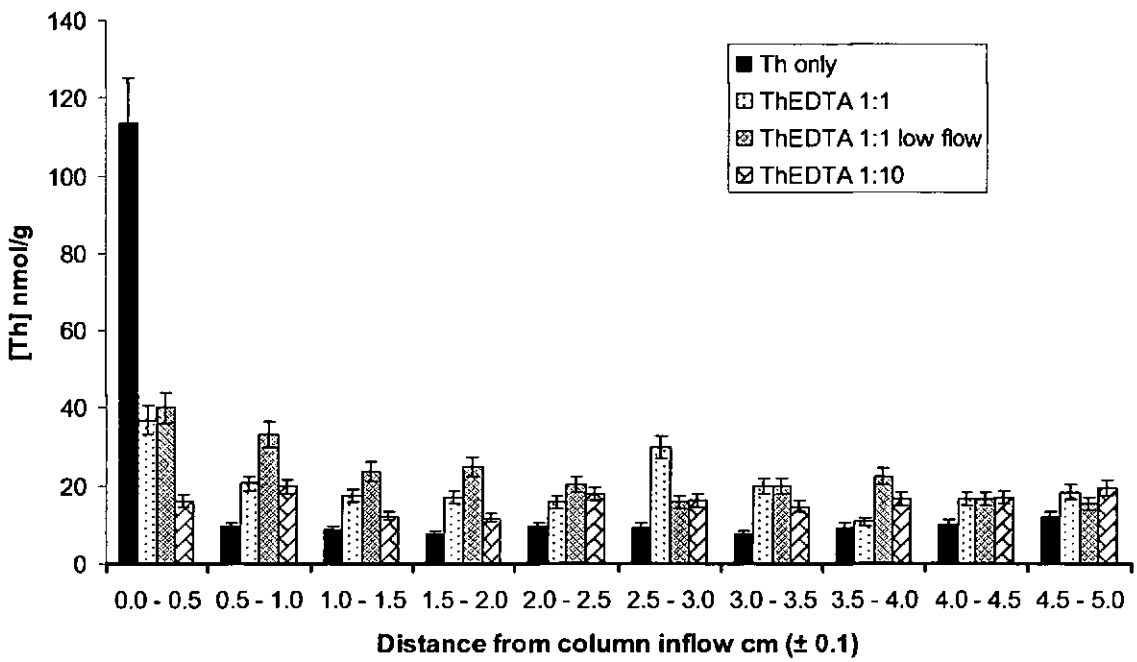

Figure 5.4 Column digestion results showing distribution of Th along the column, sand blank Th concentrations of 6.7 ± 1.4 nmol g^{-1} have been subtracted from the data (error bars show 10 % RSD resulting from combined analytical and experimental uncertainty)

5.3.4 Th-EDTA transport modelling

Modelling of the experimental data can provide information on the type of mechanism responsible for retarding contaminant transport, such as equilibrium or kinetic sorption

processes. Different approaches were used to model Th transport in the presence of EDTA, to identify possible chemical controls. Thorium was not eluted from the Th only column, and the data from the Th-NTA column were too limited to be modelled meaningfully.

Equilibrium speciation model. A simple equilibrium speciation model was used to simulate the 1 : 10 Th : EDTA column. A single aqueous [ThEDTA] complex was entered into the model using the adjusted constant (log K = 7.14). A surface binding site was defined with a Kd, which was adjusted until the simulated peak breakthrough concentration matched the experimental data. The best fit value of the Kd was 18000, an order of magnitude greater than the Kd observed in the equivalent static batch experiment (Table 5.3). However, these are not directly comparable as the transport Kd is dimensionless, and the difference in Kd values is consistent with those reported between batch sorption and column values in a previous study for the migration of neptunium (Kumata and Vandergraaf, 1998).

In the model, the equilibrium Th speciation was calculated for each transport step using the stability constant for aqueous Th-EDTA species and the strength of surface binding sites for Th. This means that migration of Th-EDTA species was implicit, and Th breakthrough was sensitive to the transport of EDTA. It was therefore necessary to include sorption of EDTA to the surface with a Kd of 0.15 in order to model the Th peak breakthrough volume accurately. However, the symmetrical equilibrium model curve obtained using these two equilibrium reactions only did not reproduce the tail observed in the experimental data (Figure 5.5 A). When this model was applied to the 1 : 1 column of the same flow rate essentially no Th eluted in the model data; peak

concentrations were in the order of 10^{-17} M. This model therefore demonstrated that a simple instantaneously reversible chemical interaction does not explain the experimental results obtained.

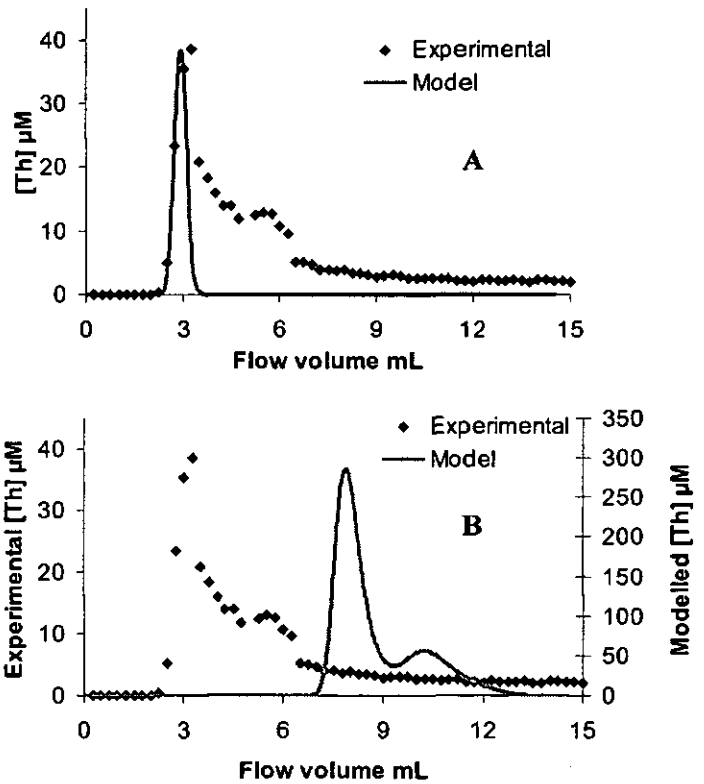

Figure 5.5 Modelled transport of Th in the 1 : 10 Th : EDTA column using: A) equilibrium speciation; and B) dual binding site model

A second surface binding site was added to the model matrix with a lower site density but a stronger Th sorption Kd, following the surface complexation model of Dzombak and Morel (1990). The 1 : 10 Th:EDTA data were used to fit a Kd of 2.6×10^8 for this site. This resulted in a reasonable peak shape, although it was narrower and retarded relative to the experimental data (Figure 5.5 B). The maximum modelled elution Th concentration was one order of magnitude greater than the experimental data and only 5.6 % of the Th injected was predicted to elute. Adjusting the model to improve the amount of Th eluted and peak width served only to further retard the peak. Moreover,

adding a second Th-EDTA complex ($ThEDTA_2^{4-}$), as observed in chapter 2, to the equations did not improve the peak shape. Clearly, a simple approach using simple instantaneously reversible chemical reactions was fundamentally unable to reproduce the observed behaviour.

Kinetic model. A kinetic model can be used to define elution peaks characterised by tailing concentrations as demonstrated by UO_2^{2+} migration through a sand column based on kinetically slow desorption processes (Handley-Sidhu *et al.*, 2009). Therefore two kinetic reactions were entered into the model in addition to the constants used in the equilibrium model, with a single sorption site defined. The interactions defined by these parameters and the related equations are shown in Figure 5.6.

As the modelled Th elution data followed the modelled EDTA elution data, these reactions described kinetic sorption of EDTA to the solid surface using forward (adsorption) and backward (desorption) rate constants. The best fit values were:

Reaction 1: $k_{f1} = 5 \times 10^{-4}\ s^{-1}$ $k_{b1} = 1 \times 10^{-4}\ s^{-1}$

Reaction 2: $k_{f2} = 5 \times 10^{-4}\ s^{-1}$ $k_{b2} = 1 \times 10^{-3}\ s^{-1}$

where k_{f1} and k_{f2} are the adsorption rate constants for reactions 1 and 2, respectively, and k_{b1} and k_{b2} are the corresponding desorption rate constants.

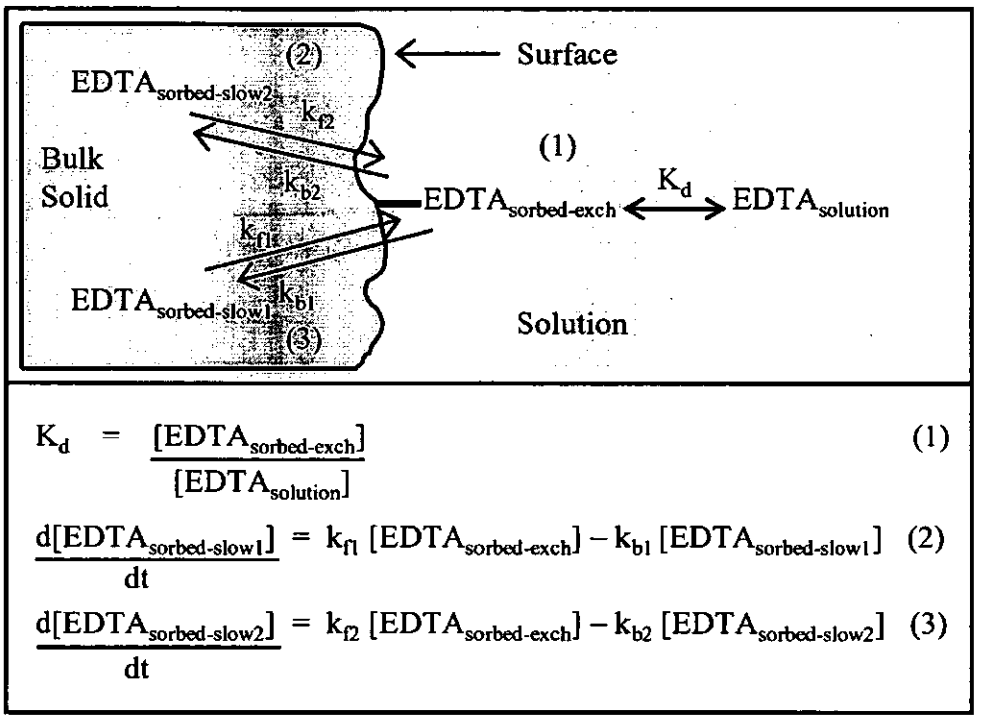

$$K_d = \frac{[EDTA_{sorbed\text{-}exch}]}{[EDTA_{solution}]} \quad (1)$$

$$\frac{d[EDTA_{sorbed\text{-}slow1}]}{dt} = k_{f1}[EDTA_{sorbed\text{-}exch}] - k_{b1}[EDTA_{sorbed\text{-}slow1}] \quad (2)$$

$$\frac{d[EDTA_{sorbed\text{-}slow2}]}{dt} = k_{f2}[EDTA_{sorbed\text{-}exch}] - k_{b2}[EDTA_{sorbed\text{-}slow2}] \quad (3)$$

Figure 5.6 Chemical processes included in the kinetic transport model; ↔ represents equilibrium (instantaneous), and ⇆ kinetic (slow) reactions

The model provided a good fit to the experimental data for the 1 : 10 Th : EDTA column (Figure 5.8 A). The equations and constants that gave the fit in Figure 5.8 A were then applied to model the 1 : 1 Th : EDTA column at the same flow rate (0.97 mL h^{-1}), and lower flow rate (0.29 mL h^{-1}). Although the peak shape generated by this model (Figure 5.7 B and C) was a better fit to the experimental data than provided by the equilibrium model, the eluent Th concentrations were underestimated by 15 orders of magnitude for the higher flow rate column and 12 orders of magnitude for the lower flow rate column. If migration of Th was governed by kinetic sorption of chemical species, the model should be able to match the experimental data for different flow rates and concentrations. Therefore these simulations confirmed that kinetic sorption of simple chemical species was not controlling Th transport in these systems.

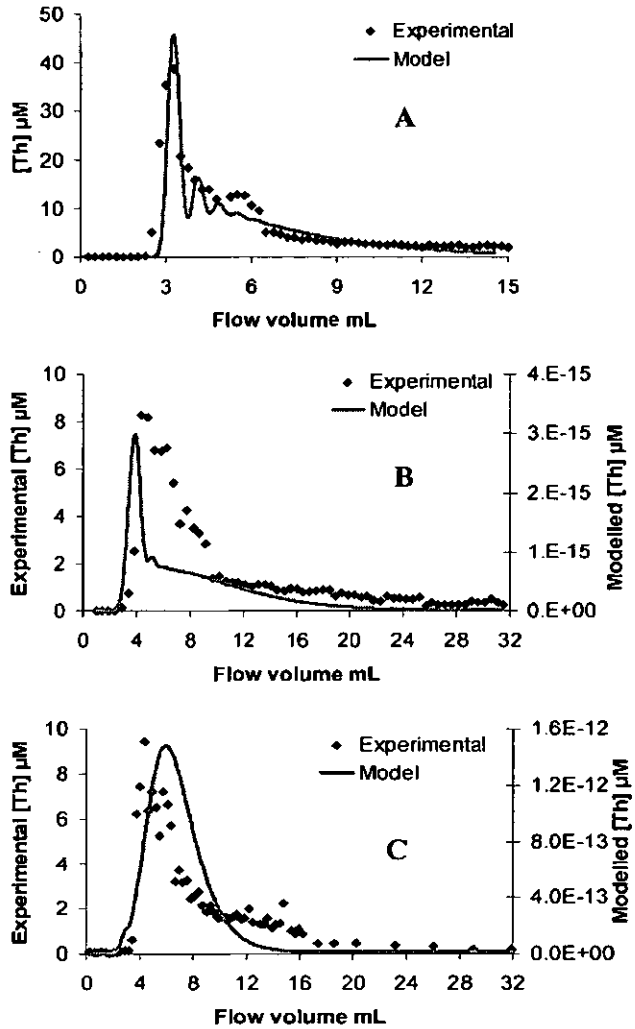

Figure 5.7 Modelled transport of Th using two kinetic interactions between solution and surface phase Th for columns: A) 1 :10 Th : EDTA; B) 1 : 1 Th : EDTA; and C) 1 : 1 Th : EDTA (low flow rate)

Colloidal Th species. The modelling confirmed that the observed elution behaviour of Th-EDTA in the columns was not consistent with the transport of simple chemical species. The breakthrough peaks in the Th-EDTA systems showed quite low retardation but were disperse, which is indicative of a transport mechanism based on a physical retardation process (N Bryan [Manchester University] 2009, pers comm., 19 September).

Formation of colloids could result in this type of profile, since different size colloids can follow different flow paths. It is known that at higher pH, tetravalent actinides such as Th will readily polymerise and form colloids (*e.g.* Yun *et al.*, 2006). Given that the Th concentration used was greater than its solubility, and speciation modelling of Th using PHREEQcl at the pH of the experiments (7.2) predicted Th to be present predominantly as $Th(OH)_4$, Th colloids would be predicted in the stock solution. Colloidal species tend to be strongly sorbing when they possess a net positive charge (McCarthy and Zachara, 1989) and very mobile in natural systems with a net negative charge where they may act as ligands (*e.g.* Champ *et al.*, 1984). Humic substances have been shown to adsorb to positively charged colloidal species, with the organic coating imparting an overall negative charge, resulting in mobility through the environment typical of anionic species (McCarthy and Zachara, 1989). Increased humic concentrations also enhanced the transport of Am through sand columns by the formation of colloidal humic-Am species which reduced Am sorption to the solid phase (Artinger *et al.*, 1998). Tetravalent Pu and Th have been shown to strongly associate with low molecular weight organic colloids in surface soil waters (Santschi *et al.*, 2002). To the author's knowledge there have been no investigations into the migration of Th-EDTA colloidal species. However, EDTA has been shown to adsorb to Th precipitate (Xia *et al.*, 2003), which is consistent with the concept of colloidal Th-EDTA transport.

The batch sorption data support the concept of colloidal Th formation. The Kd observed in the Th system in synthetic groundwater was an order of magnitude greater than the equivalent pure water system, and this suggests that the solution matrix ions played a role in enhancing precipitation of Th. Therefore, although distinct chemical species were seen in pure water systems using ESI-MS, it is reasonable to conclude that colloids

formed in the synthetic groundwater systems, and interactions with EDTA increased their mobility.

Overall it appears that the observed profiles are the result of EDTA mediated transport of polydisperse Th colloids. The absence of Th elution in the Th only column and the broadened peak in the Th-NTA column, indicate that the presence of EDTA was fundamental to any colloidal Th transport.

5.4 Environmental implications

The experimental data showed that both EDTA and NTA enhanced the mobility of Th through the sand matrix, and that the ligand concentration was an important factor in the amount of Th eluted. In the absence of any organic complexant, the radionuclide was readily immobilised through sorption to the sand matrix, whereas 19 % and 35 % of the total Th injected were eluted with 4 and 40 mM EDTA respectively. The ligands enhanced migration either through the formation of stable aqueous species as suggested by the Th-NTA data or, in the case of EDTA, by stabilising colloidal species. This has implications for the mobility of analogous tetravalent actinides such as Pu(IV) through the terrestrial environment, which pose a very significant risk to environmental health.

For ligand-mediated transport of radionuclide colloids, the groundwater flow rate will have little impact on the magnitude of contaminant transport, rather, this will be dependent on the relative and absolute concentrations of actinide and organic co-contaminants present in mixed wastes. The data reinforce the conclusions of contaminant site field studies (*e.g.* Means *et al.*, 1978) that organic co-contaminant chelating agents such as EDTA enhance the environmental mobility of tetravalent actinides.

Chapter 6

Conclusions and future work

6.1 Conclusions

The overall aim of this project was to define Th and UO_2^{2+} speciation in the presence of co-contaminant chelating agents and to investigate the influence of speciation on the mobility of UO_2^{2+} and Th in the terrestrial environment. The work highlighted a number of issues that are of importance in understanding and predicting actinide migration: the need to re-examine the chemical speciation and associated stability constants of actinide-EDTA and -NTA complexes; the relatively slow kinetics of sorption and metal-radionuclide exchange in the complexes, and co-contaminant chelating agents interactions with actinides in both ionic and colloidal forms.

The power of ESI-MS for direct speciation analysis of complexes was demonstrated through the identification of speciation change with pH and relative ligand concentration, and highlighted shortcomings in the species currently included in stability constant databases. Mixed ligand species were important at neutral pH, and Th-NTA_2 and Th-$EDTA_2$ complexes were increasingly important as the ligand concentration increased relative to Th. Such species are likely to be important when considering the environmental mobility of actinide contaminants. Equally, the technique provided crucial information for the experimental work in Chapter 3, which elucidated the process of slow metal exchange kinetics in the Th-EDTA-Fe system at the Fe precipitate surface. This process is important with respect to Th-EDTA movement through a wide range of environments due to the ubiquitous nature of Fe oxyhydroxides, and will be most important in slow moving groundwater, due to the slow exchange kinetics involved.

A limitation of flow-injection ESI-MS is that high background signals limit direct analysis of species in "real" water samples, as found for the waters from the sand experiments. However, these batch experiments identified several processes affecting the net solubility of Th in the presence of the complexing agents. The relative concentration of Th to matrix ions is critical, both from the perspective of competition for the complexing agents and, where matrix metals are solubilised, the creation of additional binding sites for Th. With increased concentrations of EDTA, the chelating agent was more effective in competing with binding sites for Th. Thus, EDTA and NTA raised the solubility of high concentrations of Th (500 μM), and lowered the short-term solubility of lower concentrations of Th (5 and 50 μM), by increasing the rate of Th sorption through the creation of surface binding sites.

Despite the distinct chemical species observed with 0.4 mM Th using ESI-MS (Chapter 2), the column studies for Th-EDTA (4 mM) in synthetic groundwater suggested that EDTA-mediated colloidal transport occurred. The higher concentration of Th and the synthetic groundwater matrix used in the column experiments enhanced the formation of Th colloids. EDTA-mediated transport of actinide colloids in groundwater therefore poses a significant threat to environmental health, as chemical retardation processes will not immobilise such species, or reduce radionuclide concentrations. The amount of radionuclide transported by this mechanism will be dependent on the relative concentrations of ligand and radionuclide present, but independent of groundwater flow rates.

Overall, these investigations of radionuclide-ligand species in relatively simple chemical systems under laboratory conditions have shown the complexity of the chemical interactions that influence actinide migration through the environment. The

processes identified and speciation information generated are important contributions to the current understanding of the role of chelating agents at contaminated sites, and for the assessment of new legacy wastes which will not undergo reprocessing and hence pose a greater radiotoxic risk to the environment.

6.2 Future work

Speciation.

The importance of EDTA-mediated Th colloid transport, identified in Chapter 5, should be examined further. Simple solution studies to investigate the formation of colloidal Th should be carried out over a similar concentration range to that used in chapters 2 and 4 in pure aqueous and synthetic groundwater solutions, and sampled over time. Addition of EDTA to solutions before and after Th colloids have formed, and subsequent analyses over time, would show the influence of EDTA on Th colloid stability. Flow Field-Flow Fractionation (FlFFF) has been recommended as a separation technology suited to the characterisation of colloids over the size range 0.001 to 50 μm (Gimbert *et al.*, 2003), and could be coupled with ICP-MS (*e.g.* Siripintanond *et al.*, 2002) for Th determination to provide Th colloid size distributions and Th concentrations. With knowledge of solution behaviour established, a Th-EDTA colloid system with sand should be investigated to understand the interactions of Th-EDTA colloids with sand.

Sorption.

Sorption was shown to be dependent on complexation by the ligands, and chapter 2 showed the pH dependence of radionuclide-ligand speciation over a broad pH range. Therefore the role of the ligands on sorption of UO_2^{2+} and Th should be investigated over a wider pH range relevant to contaminant migration from a nuclear waste

repository (*e.g.* 7 – 13). Having defined the underlying radionuclide-ligand speciation using ESI-MS such analyses would improve the understanding of sorption mechanisms.

Migration.

Th-EDTA migration was of colloidal nature at the experimental concentrations used. To evaluate the influence of the Th-EDTA solution species observed in chapter 2, column experiments using lower concentrations of Th (*e.g.* 500 μM) should be performed under similar experimental conditions with Th determination using high resolution ICP-MS to enable low eluent concentrations to be measured (*e.g.* Roth *et al.* (2005) reported an LOD for Th of 20 pg L^{-1} using high resolution-sector field-ICP-MS).

References

Agnes, G. R. and Horlick, G., 1995. Effect of operating parameters on analyte signals in elemental electrospray mass-spectrometry. *Applied Spectroscopy* **49**, 324-334.

Altmaier, M., Neck, V., Muller, R., and Fanghanel, T., 2005. Solubility of $ThO_2 \cdot H_2O_{(am)}$ in carbonate solution and the formation of ternary Th(IV) hydroxide-carbonate complexes. *Radiochimica Acta* **93**, 83-92.

Ambard, C., Delorme, A., Baglan, N., Aupiais, J., Pointurier, F., and Madic, C., 2005. Interfacing capillary electrophoresis with inductively coupled plasma mass spectrometry for redox speciation of plutonium. *Radiochimica Acta* **93**, 665-673.

Anderegg, G., 1977. *Critical Survey of Stability Constants of EDTA Complexes.* Pergamon Press, Oxford.

Arai, Y., McBeath, M., Bargar, J. R., Joye, J., and Davis, J. A., 2006. Uranyl adsorption and surface speciation at the imogolite-water interface: Self-consistent spectroscopic and surface complexation models. *Geochimica et Cosmochimica Acta* **70**, 2492-2509.

Artinger, R., Kienzler, B., Schussler, W., and Kim, J. I., 1998. Effects of humic substances on the Am-241 migration in a sandy aquifer: column experiments with Gorleben groundwater/sediment systems. *Journal of Contaminant Hydrology* **35**, 261-275.

Askarieh, M. M., Chambers, A. V., Daniel, F. B. D., FitzGerald, P. L., Holtom, G. J., Pilkington, N. J., and Rees, J. H., 2000. The chemical and microbial degradation of cellulose in the near field of a repository for radioactive wastes. *Waste Manage. (Oxford)* **20**, 93-106.

Baldwin, T., Chapman, N., Neall, F., 2008. Geological disposal options for high-level waste and spent fuel. *Report for the U.K. Nuclear Decommissioning Authority.*

Baron, D. and Hering, J. G., 1998. Analysis of metal-EDTA complexes by electrospray mass spectrometry. *Journal of Environmental Quality* **27**, 844-850.

Bath, A., Richards, H., Metcalfe, R., McCartney, R., Degnan, P., and Littleboy, A., 2003. Geochemical indicators of deep groundwater movements at Sellafield, UK *Joint Meeting of the European-Geophysical-Society/American-Geophysical-Union and European-Union-of-Geoscience*, Nice, FRANCE.

Bitea, C., Muller, R., Neck, V., Walther, C., and Kim, J. I., 2002. Study of the generation and stability of thorium(IV) colloids by LIBD combined with ultrafiltration. *Colloids and SurfacesA* **217**, 63-70.

Bolton, H., Girvin, D. C., Plymale, A. E., Harvey, S. D., and Workman, D. J., 1996. Degradation of metal-nitrilotriacetate complexes by *Chelatobacter heintzii*. *Environmental Science & Technology* **30**, 931-938.

Boukhalfa, H., Reilly, S. D., Smith, W. H., and Neu, M. P., 2004. EDTA and mixed-ligand complexes of tetravalent and trivalent plutonium. *Inorganic Chemistry* **43**, 5816-5823.

Brooks, S. C. and Carroll, S. L., 2003. Geochemical reactions governing the fate of Co-NTA in contact with natural subsurface materials. *Applied Geochemistry* **18**, 423-433.

Brooks, S. C., Taylor, D. L., and Jardine, P. M., 1996. Reactive transport of EDTA-complexed cobalt in the presence of ferrihydrite. *Geochimica et Cosmochimica Acta* **60**, 1899-1908.

Bryan, N. D., Jones, D. M., Appleton, M., Livens, F. R., Jones, M. N., Warwick, P., King, S., and Hall, A., 2000. A physicochemical model of metal-humate interactions. *Physical Chemistry Chemical Physics* **2**, 1291-1300.

Carey, G. H., Bogucki, R. F., and Martell, A. E., 1964. Mixed ligand chelates of thorium (IV). *Inorganic Chemistry* **3**, 1288-1295.

Carey, G. H., Martell, A. E., 1967. Mixed ligand chelates of uranium (IV)1,2. *J. Am. Chem. Soc.* **89**, 2859-2865.

Cartwright, A. J., May, C. C., Worsfold, P. J., and Keith-Roach, M. J., 2007. Characterisation of thorium-ethylenediaminetetraacetic acid and thorium-nitrilotriacetic acid species by electrospray ionisation mass spectrometry. *Analytica Chimica Acta* **590**, 125-131.

Champ, D. R., Young, J. L., Robertson, D. E., Abel, K. H., 1984. Chemical speciation of long-lived radionuclides in a shallow groundwater flow system. *Water Pollution Research Journal of Canada* **19**, 35-54.

Chen, C. L. and Wang, X. K., 2007. Sorption of Th (IV) to silica as a function of pH, humic/fulvic acid, ionic strength, electrolyte type. *Applied Radiation and Isotopes* **65**, 155-163.

Cleveland, J. M. and Rees, T. F., 1981. Characterization of plutonium in Maxey Flats radioactive trench leachates. *Science* **212**, 1506-1509.

Cocalia, V. A., Gutowski, K. E., and Rogers, R. D., 2006. The coordination chemistry of actinides in ionic liquids: A review of experiment and simulation. *Coordination Chemistry Reviews* **250**, 755-764.

Cole, R. B., 1997. *Electrospray Ionization Mass Spectrometry: Fundamentals, Instrumentation and Applications*. Wiley, New York.

Cotton, S., 2006. *Lanthanide and Actinide Chemistry*. Wiley Blackwell, Oxford.

DBERR, 2008. Meeting the energy challenge. A White Paper on nuclear power. Department for Business, Enterprise and Regulatory Reform. House of Commons.

De Stefano, C., Gianguzza, A., Milea, D., Pettignano, A., and Sammartano, S., 2006. Sequestering ability of polyaminopolycarboxylic ligands towards dioxouranium(VI) cation. *Journal of Alloys and Compounds* **424**, 93-104.

Delos, A., Walther, C., Schafer, T., and Buchner, S., 2008. Size dispersion and colloid mediated radionuclide transport in a synthetic porous media. *Journal of Colloid and Interface Science* **324**, 212-215.

Denecke, M. A., 2006. Actinide speciation using X-ray absorption fine structure spectroscopy. *Coordination Chemistry Reviews* **250**, 730-754.

Di Marco, V. B. and Bombi, G. G., 2006. Electrospray mass spectrometry (ESI-MS) in the study of metal-ligand solution equilibria. *Mass Spectrometry Reviews* **25**, 347-379.

Dimmock, P. W., Warwick, P., and Robbins, R. A., 1995. Approaches to predicting stability-constants. *Analyst* **120**, 2159-2170.

Dodi, A. and Monnier, V., 2004. Determination of ethylenediaminetetraacetic acid at very low concentrations by high-performance liquid chromatography coupled with electrospray mass spectrometry. *Journal of Chromatography A* **1032**, 87-92.

Dozol, M., Hagemann, R., Hoffman, D. C., Adloff, J. P., Vongunten, H. R., Foos, J., Kasprzak, K. S., Liu, Y. F., Zvara, I., Ache, H. J., Das, H. A., Hagemann, R. J. C., Herrmann, G., Karol, P., Maenhaut, W., Nakahara, H., Sakanoue, M., Tetlow, J. A., Baro, G. B., Fardy, J. J., Benes, P., Roessler, K., Roth, E., Burger, K., Steinnes, E., Kostanski, M. J., Peisach, M., Liljenzin, J. O., Aras, N. K., Myasoedov, B. F., and Holden, N. E., 1993. Radionuclide migration in groundwaters - review of the behavior of actinides - (technical report). *Pure and Applied Chemistry* **65**, 1081-1102.

Dzombak, D. A. and Morel, F. M. M., 1990. *Surface Complexation Modelling: Hydrous Ferric Oxide*. John Wiley and Sons, New York.

Ekberg, C., Albinsson, Y., Comarmond, M. J., and Brown, P. L., 2000. Studies on the complexation behavior of thorium(IV). 1. Hydrolysis equilibria. *Journal of Solution Chemistry* **29**, 63-86.

Elliott, H. A. and Denneny, C. M., 1982. Soil adsorption of cadmium from solutions containing organic-ligands. *Journal of Environmental Quality* **11**, 658-663.

Evans, N. D. M., Heath, T. G., 2004. The development of a strategy for the investigation of detriments to radionuclide sorption in the geosphere. *Serco Assurance Report SA/ENV-0611.*

Fetter, C. W., 1999. *Contaminant Hyrogeology.* Prentice-Hall Inc., Upper Saddle River.

Fox, P. M., Davis, J. A., and Zachara, J. M., 2006. The effect of calcium on aqueous uranium(VI) speciation and adsorption to ferrihydrite and quartz. *Geochimica et Cosmochimica Acta* **70**, 1379-1387.

Friedly, J. C., Kent, D. B., and Davis, J. A., 2002. Simulation of the mobility of metal-EDTA complexes in groundwater: The influence of contaminant metals. *Environmental Science & Technology* **36**, 355-363.

Gaillardet, J., Viers, J., and Dupre, B., 2003. Trace elements in river waters. In: Drever, I. (Ed), *Surface and Groun Water, Weathering, and Soils: Treatise on Geochemistry Vol. 5.* Elsevier, London

Geckeis, H., 2006. Research in actinide geochemistry: do we need speciation information at the molecular level? In: Van Iseghem, P. (Ed.),*Scientific basis for nuclear waste management XXIX.* Materials Research Society, Ghent, Belgium.

Gimbert, L. J., Andrew, K. N., Haygarth, P. M., and Worsfold, P. J., 2003. Environmental applications of flow field-flow fractionation (FIFFF). *Trac-Trends in Analytical Chemistry* **22**, 615-633.

Glaus, M. A., van Loon, L. R., Achatz, S., Chodura, A., and Fischer, K., 1999. Degradation of cellulosic materials under the alkaline conditions of a

cementitious repository for low and intermediate level radioactive waste Part I: Identification of degradation products. *Analytica Chimica Acta* **398**, 111-122.

Grubisic, S., Milicic, M. K., Radanovic, D. D., and Niketic, S. R., 2006. Conformational analysis of edta-type rhodium(III) complexes with mixed five- and six-membered chelate rings. Structural analysis of conformational flexibility in rhodium(III) complexes containing 1,3-propanediamine-N,N '-diacetate-N,N '-di-3-propionate ligand. *Journal of Molecular Structure* **794**, 125-132.

Gruning, C., Huber, G., Klopp, P., Kratz, J. V., Kunz, P., Passler, G., Trautmann, N., Waldek, A., and Wendt, K., 2004. Resonance ionization mass spectrometry for ultratrace analysis of plutonium with a new solid state laser system. *International Journal of Mass Spectrometry* **235**, 171-178.

Gu, B. H. and Ruan, C. M., 2007. Determination of technetium and its speciation by surface-enhanced Raman spectroscopy. *Analytical Chemistry* **79**, 2341-2345.

Guo, Z. J., Yu, X. M., Guo, F. H., and Tao, Z. Y., 2005. Th(IV) adsorption on alumina: Effects of contact time, pH, ionic strength and phosphate. *Journal of Colloid and Interface Science* **288**, 14-20.

Handley-Sidhu, S., Bryan, N. D., Worsfold, P. J., Vaughan, D. J, Livens, F. R., Keith-Roach, M. J., 2009. Corrosion and transport of depleted uranium in sand-rich environments. *Chemosphere* **In press**.

Hennig, C., Tutschku, J., Rossberg, A., Bernhard, G., and Scheinost, A. C., 2005. Comparative EXAFS investigation of uranium(VI) and -(IV) aquo chloro complexes in solution using a newly developed spectroelectrochemical cell. *Inorganic Chemistry* **44**, 6655-6661.

Hu, Q.-H., Weng, J.-Q., and Wang, J.-S., Sources of anthropogenic radionuclides in the environment: a review. *Journal of Environmental Radioactivity* **In Press, Corrected Proof**.

Hu, Q. H., Zavarin, M., and Rose, T. P., 2008. Effect of reducing groundwater on the retardation of redox-sensitive radionuclides. *Geochem. Trans.* **9**.

Jacopin, C., Sawicki, M., Plancque, G., Doizi, D., Taran, F., Ansoborlo, E., Amekraz, B., and Moulin, C., 2003. Investigation of the interaction between 1-hydroxyethane-1,1 '-diphosphonic acid (HEDP) and uranium(VI). *Inorganic Chemistry* **42**, 5015-5022.

Jardine, P. M., Mehlhorn, T. L., Larsen, I. L., Bailey, W. B., Brooks, S. C., Roh, Y., and Gwo, J. P., 2002. Influence of hydrological and geochemical processes on the transport of chelated metals and chromate in fractured shale bedrock. *Journal of Contaminant Hydrology* **55**, 137-159.

Jiang, J., Renshaw, J. C., Sarsfield, M. J., Livens, F. R., Collison, D., Charnock, J. M., and Eccles, H., 2003. Solution chemistry of uranyl ion with iminodiacetate and oxydiacetate: A combined NMR/EXAFS and potentiometry/calorimetry study. *Inorganic Chemistry* **42**, 1233-1240.

Katz, J. J., Seaborg, G. T., 1957. *The Chemistry of the Actinides*. John Wiley & Sons, Inc., New York.

Keith-Roach, M. J., Buratti, M. V., and Worsfold, P. J., 2005. Thorium complexation by hydroxamate siderophores in perturbed multicomponent systems using flow injection electrospray ionization mass spectrometry. *Analytical Chemistry* **77**, 7335-7341.

Kent, D. B., Davis, J. A., Anderson, L. C. D., Rea, B. A., and Coston, J. A., 2002. Effect of adsorbed metal ions on the transport of Zn- and Ni-EDTA complexes in a sand and gravel aquifer. *Geochimica et Cosmochimica Acta* **66**, 3017-3036.

Mackay, D. M., Roberts, P. V., and Cherry, J. A., 1985. Transport of organic contaminants in groundwater. *Environmental Science & Technology* **19**, 384-392.

Martell, A. E., Smith, R. M., , 1995. Critically selected stability constants of metal complexes database, Version 2.0., NIST Standard Reference Program, Gaithersburg, MD.

May, C. C., Worsfold, P. J., and Keith-Roach, M. J., 2008. Analytical techniques for speciation analysis of aqueous long-lived radionuclides in environmental matrices. *Trac-Trends in Analytical Chemistry* **27**, 160-168.

Mayes, M. A., Jardine, P. M., Larsen, I. L., Brooks, S. C., and Fendorf, S. E., 2000. Multispecies transport of metal-EDTA complexes and chromate through undisturbed columns of weathered fractured saprolite. *Journal of Contaminant Hydrology* **45**, 243-265.

McCarthy, J. F., Czerwinski, K. R., Sanford, W. E., Jardine, P. M., and Marsh, J. D., 1998. Mobilization of transuranic radionuclides from disposal trenches by natural organic matter. *Journal of Contaminant Hydrology* **30**, 49-77.

McCarthy, J. F. and Zachara, J. M., 1989. Subsurface transport of contaminants - mobile colloids in the subsurface environment may alter the transport of contaminants. *Environmental Science & Technology* **23**, 496-502.

Means, J. L., Kucak, T., and Crerar, D. A., 1980. Relative degradation rates of NTA, EDTA and DTPA and environmental implications. *Environmental Pollution Series B-Chemical and Physical* **1**, 45-60.

Means, J. L., Crerar, D. A., and Duguid, J. O., 1978. Migration of radioactive-wastes - radionuclide mobilization by complexing agents. *Science* **200**, 1477-1481.

Mibus, J., Sachs, S., Pfingsten, W., Nebelung, C., and Bernhard, G., 2007. Migration of uranium(IV)/(VI)in the presence of humic acids in quartz sand: A laboratory column study. *Journal of Contaminant Hydrology* **89**, 199-217.

Milic, N. B. and Suranji, T. M., 1982. Hydrolysis of the thorium(IV) ion in sodium-nitrate medium. *Canadian Journal of Chemistry-Revue Canadienne De Chimie* **60**, 1298-1303.

Milnes, A. G., 1985. *Geology and Radwaste*. Academic Press, London.

Monsallier, J. M., Artinger, R., Denecke, M. A., Scherbaum, F. J., Buckau, G., and Kim, J. I., 2003. Spectroscopic study (TRLFS and EXAFS) of the kinetics of An(III)/Ln(III) humate interaction. *Radiochimica Acta* **91**, 567-574.

Morris, K., Livens, F. R., Charnock, J. M., Burke, I. T., McBeth, J. M., Begg, J. D. C., Boothman, C., and Lloyd, J. R., 2008. An X-ray absorption study of the fate of technetium in reduced and reoxidised sediments and mineral phases. *Applied Geochemistry* **23**, 603-617.

Morris, D. E., 2002. Redox energetics and kinetics of uranyl coordination complexes in aqueous solution. *Inorganic Chemistry* **41**, 3542-3547.

Moulin, C., 2003. On the use of time-resolved laser-induced fluorescence (TRLIF) and electrospray mass spectrometry (ES-MS) for speciation studies. *Radiochimica Acta* **91**, 651-657.

Moulin, C., Amekraz, B., Steiner, V., Plancque, G., and Ansoborlo, E., 2003. Speciation studies on DTPA using the complementary nature of electrospray ionization mass spectrometry and time-resolved laser-induced fluorescence. *Applied Spectroscopy* **57**, 1151-1161.

Moulin, C., Amekraz, B., Hubert, S., and Moulin, V., 2001. Study of thorium hydrolysis species by electrospray-ionization mass spectrometry. *Analytica Chimica Acta* **441**, 269-279.

Moulin, C., Charron, N., Plancque, G., and Virelizier, H., 2000. Speciation of uranium by electrospray ionization mass spectrometry: Comparison with time-resolved laser-induced fluorescence. *Applied Spectroscopy* **54**, 843-848.

Moulin, C., Wei, J., Van Iseghem, P., Laszak, I., Plancque, G., and Moulin, V., 1999. Europium complexes investigations in natural waters by time-resolved laser-induced fluorescence. *Analytica Chimica Acta* **396**, 253-261.

Moulin, C., Laszak, I., Moulin, V., and Tondre, C., 1998. Time-resolved laser-induced fluorescence as a unique tool for low-level uranium speciation. *Applied Spectroscopy* **52**, 528-535.

Moulin, C., Decambox, P., Mauchien, P., Pouyat, D., and Couston, L., 1996. Direct uranium(VI) and nitrate determinations in nuclear reprocessing by time-resolved laser-induced fluorescence. *Analytical Chemistry* **68**, 3204-3209.

Moulin, V. and Moulin, C., 2001. Radionuclide speciation in the environment: a review. *Radiochimica Acta* **89**, 773-778.

Novikov, A. P., Kalmykov, S. N., Utsunomiya, S., Ewing, R. C., Horreard, F., Merkulov, A., Clark, S. B., Tkachev, V. V., and Myasoedov, B. F., 2006. Colloid transport of plutonium in the far-field of the Mayak Production Association, Russia. *Science* **314**, 638-641.

Nowack, B. and Sigg, L., 1996. Adsorption of EDTA and metal-EDTA Complexes onto Goethite. *Journal of Colloid and Interface Science* **177**, 106-121.

Nowack, B. and Sigg, L., 1997. Dissolution of Fe(III)(hydr)oxides by metal-EDTA complexes. *Geochimica et Cosmochimica Acta* **61**, 951-963.

Ogino, H., & Shimura, M., 1986. Kinetic studies on EDTA complexes of transition metals. *Advances in Inorganic and Bioinorganic Mechanisms* **4**, 107-135.

Olesik, J. W., Thaxton, K. K., and Olesik, S. V., 1997. Ion spray mass spectrometry for elemental speciation in aqueous samples: Preliminary investigation of experimental parameters, matrix effects and metal-ligand complexation. *Journal of Analytical Atomic Spectrometry* **12**, 507-515.

Osthols, E., 1995. Thorium sorption on amorphous silica. *Geochimica Et Cosmochimica Acta* **59**, 1235-1249.

Pace, M. N., Mayes, M. A., Jardine, P. M., McKay, L. D., Yin, X. L., Mehlhorn, T. L., Liu, Q., and Gürleyük, H., 2007. Transport of Sr^{2+} and $SrEDTA^{2-}$ in partially-saturated and heterogeneous sediments. *Journal of Contaminant Hydrology* **91**, 267-287.

Parkhurst, D. and Appelo, C., 1999. User's Guide to PHREEQC (v2) - a Computer Program for Speciation, Reaction-Path, 1D-Transport and Inverse Geochemical Calculations USGS.

Pasilis, S., Somogyi, A., Herrmann, K., and Pemberton, J. E., 2006. Ions generated from uranyl nitrate solutions by electrospray ionization (ESI) and detected with Fourier transform ion-cyclotron resonance (FT-ICR) mass spectrometry. *Journal of the American Society for Mass Spectrometry* **17**, 230-240.

Pasilis, S. P. and Pemberton, J. E., 2003. Speciation and coordination chemistry of uranyl(VI)-citrate complexes in aqueous solution. *Inorganic Chemistry* **42**, 6793-6800.

Pathak, P. N. and Choppin, G. R., 2007a. Kinetics and thermodynamics of uranium(VI) sorption on hydrous silica. *Radiochimica Acta* **95**, 507-512.

Pathak, P. N. and Choppin, G. R., 2007b. Sorption of uranyl ion on hydrous silica: Effects of ionic strength and ethylenediaminetetraacetic acid (EDTA). *Journal of Radioanalytical and Nuclear Chemistry* **272**, 37-43.

Payne, T. E. and Airey, P. L., 2006. Radionuclide migration at the Koongarra uranium deposit, Northern Australia - Lessons from the Alligator Rivers analogue project. *Physics and Chemistry of the Earth* **31**, 572-586.

Perfiliev, V. A., Mishchenko, V. T., and Poluektov, N. S., 1986. Different-ligand complex-compounds of uranium(iv) with ethylene diamine tetraacetic and ortho-phosphoric acids. *Ukr. Khim. Zh.* **52**, 493-497.

Prikryl, J. D., Jain, A., Turner, D. R., and Pabalan, R. T., 2001. UraniumVI sorption behavior on silicate mineral mixtures. *Journal of Contaminant Hydrology* **47**, 241-253.

Puigdomenech, I., 2006. http://www.kemi.kth.se/utbildning/gk/kemiskjmv/ last accessed 04/04/06

Quiles, F. and Burneau, A., 1998. Infrared and Raman spectroscopic study of uranyl complexes: hydroxide and acetate derivatives in aqueous solution. *Vibrational Spectroscopy* **18**, 61-75.

Rabung, T., Pierret, M. C., Bauer, A., Geckeis, H., Bradbury, M. H., and Baeyens, B., 2005. Sorption of Eu(III)/Cm(III) on Ca-montmorillonite and Na-illite. Part 1: Batch sorption and time-resolved laser fluorescence spectroscopy experiments. *Geochimica et Cosmochimica Acta* **69**, 5393-5402.

Rai, D., Moore, D. A., Rosso, K. M., Felmy, A. R., and Bolton, H., 2008. Environmental mobility of Pu(IV) in the presence of ethylenediaminetetraacetic acid: Myth or reality? *Journal of Solution Chemistry* **37**, 957-986.

Rao, L., Choppin, G. R., and Bergeron, R. J., 2000. Complexation of thorium(IV) with desmethyldesferrithiocin. *Radiochimica Acta* **88**, 851-856.

Read, D., Ross, D., and Sims, R. J., 1998. The migration of uranium through Clashach Sandstone: the role of low molecular weight organics in enhancing radionuclide transport. *Journal of Contaminant Hydrology* **35**, 235-248.

Reeve, P. and Eilbeck, K., 2007. Contaminated land and groundwater management at Sellafield, a large operational site with significant legacy and contaminated land

challenges. *11th International Conference on Environmental Remediation and Radioactive Waste Management*, Bruges, Brazil.

Reiller, P., Casanova, F., and Moulin, V., 2005. Influence of addition order and contact time on thorium(IV) retention by hematite in the presence of humic acids. *Environmental Science & Technology* **39**, 1641-1648.

Reinoso-Maset, E., Worsfold, P. J., and Keith-Roach, M. J., 2008. Radionuclides, organic complexing agents and solid phases: Exploring their interactions. *8th Annual V M Goldschmidt Conference*, Vancouver, CANADA.

Roth, P., Hollriegl, V., Li, W. B., Oeh, U., and Schramel, P., 2005. Validating an important aspect of the new ICRP biokinetic model of thorium. *Health Physics* **88**, 223-228.

Rydberg, J., Rydberg, B., 1952. Adsorption on glass and polythene from solutions of thorium and thorium complexes in tracer solutions. *Svensk Kemisk Tidskrift* **64**, 200-211.

Santschi, P. H., Roberts, K. A., and Guo, L. D., 2002. Organic nature of colloidal actinides transported in surface water environments. *Environmental Science & Technology* **36**, 3711-3719.

Schussler, W., Artinger, R., Kim, J. I., Bryan, N. D., and Griffin, D., 2001. Numerical modeling of humic colloid borne americium(III) migration in column experiments using the transport/speciation code K1D and the KICAM model. *Journal of Contaminant Hydrology* **47**, 311-322.

Serne, R. J., Cantrell, K. J., Lindenmeir, C. W., Owen, A. T., Kutnyakov, I. V., Orr, R. D., Felmy, A. R., 2002. Radionuclide-chelating agent complexes in low-level radioactive decontamination waste; stability, adsorbtion and transport potential. Pacific Northwest National Laboratory.

Siegel, M. D., and Bryan, C. R., 2005. Environmental geochemistry of radioactive contamination. In: Lollar, B. S. (Ed), *Environmental Geochemistry: Treatise on Geochemistry Vol. 9*. Elsevier, London.

Sillanpaa, M. and Sihvonen, M. L., 1997. Analysis of EDTA and DTPA. *Talanta* **44**, 1487-1497.

Sims, R., Lawless, T. A., Alexander, J. L., Bennett, D. G., and Read, D., 1996. Uranium migration through intact sandstone: Effect of pollutant concentration and the reversibility of uptake. *Journal of Contaminant Hydrology* **21**, 215-228.

Siripinyanond, A., Barnes, R. M., and Amarasiriwardena, D., 2002. Flow field-flow fractionation-inductively coupled plasma mass spectrometry for sediment bound trace metal characterization*Winter Conference on Plasma Spectrochemistry*, Scottsdale, Az.

Smith, P. A., Alexander, W. R., Kickmaier, W., Ota, K., Frieg, B., and McKinley, I. G., 2001. Development and testing of radionuclide transport models for fractured rock: examples from the Nagra/JNC Radionuclide Migration Programme in the Grimsel Test Site, Switzerland. *Journal of Contaminant Hydrology* **47**, 335-348.

Smith, R. M., Martell, A. E.,, 1989. *Critical Stability Constants: second supplement.* Kluwer Academic / Plenum Publishers, New York.

Stewart, II and Horlick, G., 1994. Electrospray mass-spectra of lanthanides. *Analytical Chemistry* **66**, 3983-3993.

Stumm, W. and Morgan, J. J., 1996. *Aquatic Chemistry - Chemical Equilibria and Rates in Natural Waters*. John Wiley and Sons, New York.

Sylwester, E. R., Allen, P. G., Dharmawardana, U. R., and Sutton, M., 2001. Structural studies of uranium and thorium complexes with 4,5-dihydroxy-3,5-benzenesdisulfonate (Tiron) at low and neutral pH by X-ray absorption spectroscopy. *Inorganic Chemistry* **40**, 2835-2841.

Szabo, Z., Toraishi, T., Vallet, V., and Grenthe, I., 2006. Solution coordination chemistry of actinides: Thermodynamics, structure and reaction mechanisms. *Coordination Chemistry Reviews* **250**, 784-815.

Toste, A. P., Lechner-Fish, T. J., Hedren, D. J., Scheele, R. D., Richmond, W. G., 1988. Analyses of organics in highly radioactive nuclear wastes. *Journal of Radioanalytical and Nuclear Chemistry* **123**, 149-166.

Toste, A. P., Osborn, B. C., Polach, K. J., Lechner-Fish, T.J., 1995. Organic analyses of an actual and simulated mixed waste: Hanford's organic complexant waste revisited. *Journal of Radioanalytical and Nuclear Chemistry* **194**, 25-34.

Vallet, V., Macak, P., Wahlgren, U., and Grenthe, I., 2006. Actinide chemistry in solution, quantum chemical methods and models. *Theoretical Chemistry Accounts* **115**, 145-160.

Vercammen, K., Glaus, M. A., and Van Loon, L. R., 1999. Evidence for the existence of complexes between Th(IV) and alpha-isosaccharinic acid under alkaline conditions. *Radiochimica Acta* **84**, 221-224.

Vercammen, K., Glaus, M. A., and Van Loon, L. R., 2001. Complexation of Th(IV) and Eu(III) by alpha-isosaccharinic acid under alkaline conditions. *Radiochimica Acta* **89**, 393-401.

Vercouter, T., Amekraz, B., Moulin, C., Giffaut, E., and Vitorge, P., 2005. Sulfate complexation of trivalent lanthanides probed by nanoelectrospray mass spectrometry and time-resolved laser-induced luminescence. *Inorganic Chemistry* **44**, 7570-7581.

VisualMinteq, 2006. http://www.lwr.kth.se/English/OurSoftware/vminteq/ last accessed 04/04/06

Walther, C., Rothe, J., Brendebach, B., Fuss, M., Altmaier, M., Marquardt, C. M., Buchner, S., Cho, H.-R., Yun, J.-I., Seibert, A., 2009. New insights in the formation process of Pu(IV) colloids. *Radiochim. Acta* **97**, 199-207.

Wang, H. J. and Agnes, G. R., 1999. Evaluation of electrospray mass spectrometry as a technique for quantitative analysis of kinetically labile solution species. *Analytical Chemistry* **71**, 3785-3792.

Warwick, P. W., Hall, A., Pashley, V., Bryan, N. D., and Griffin, D., 2000. Modelling the effect of humic substances on the transport of europium through porous media: a comparison of equilibrium and equilibrium/kinetic models. *Journal of Contaminant Hydrology* **42**, 19-34.

Whistler, R. L. and BeMiller, J. N., 1963. Reactions of Carbohydrates. In: Wolfrom, M. L. (Ed.), *Methods in Carbohydrate Chemistry*. Academic Press Inc., New York.

Xia, Y. X., Felmy, A. R., Rao, L. F., Wang, Z. M., and Hess, N. J., 2003. Thermodynamic model for the solubility of $ThO_{2(am)}$ in the aqueous Na^+-H^+-OH^--NO_3^--H_2O-EDTA system. *Radiochimica Acta* **91**, 751-760.

Xu, D., Chen, C. L., Tan, X. L., Hu, J., and Wang, X. K., 2007. Sorption of Th(IV) on Na-rectorite: Effect of HA, ionic strength, foreign ions and temperature. *Applied Geochemistry* **22**, 2892-2906.

Xue, H. B., Sigg, L., and Kari, F. G., 1995. Speciation of EDTA in natural-waters - exchange kinetics of Fe-EDTA in river water. *Environmental Science & Technology* **29**, 59-68.

Yun, J. I., Kim, M. A., Panak, P. J., Kim, J. I., and Fanghanel, T., 2006. Formation of aquatic Th(IV) colloids and stabilization by interaction with Cm(III)/Eu(III). *J. Phys. Chem. B* **110**, 5416-5422.

Zachara, J. M., Smith, S. C., and Kuzel, L. S., 1995. Adsorption and dissociation of Co-EDTA complexes in iron oxide-containing subsurface sands. *Geochimica et Cosmochimica Acta* **59**, 4825-4844.

Zhou, P. and Gu, B. H., 2005. Extraction of oxidized and reduced forms of uranium from contaminated soils: Effects of carbonate concentration and pH. *Environmental Science & Technology* **39**, 4435-4440.

www.environment-agency.gov.uk. last accessed 09/09/09, http://www.environment-agency.gov.uk/research/library/data/41337.aspx

www.nda.gov.uk. last accessed 09/09/09,

www.vae.lt. last accessed 09/09/09,

http://www.vae.lt/en/pages/management_of_long_lived_radioactive_waste